A Dissertation

for the Degree of Doctor of Philosophy

Development of poly(mannitol-co-PEI) gene transporter modified with rabies virus glycoprotein for brain targeted delivery of therapeutic siRNA

광견병 바이러스 당단백질로 수식된 뇌 표적 치료용 폴리만니톨계 siRNA 전달체의 개발

February, 2015

By

Tae Eun Park

Department of Agricultural Biotechnology

Graduate School

Seoul National University

Summary

Alzheimer's disease (AD) is the world's most common dementing illness, but no defensive treatments are available currently. A key reason is that AD drug development has been focused on symptomatic management without addressing basic cause of the disease. Hence, genetic intervention to suppress AD causative genes could represent an alternative to standard pharmacological approach. With the advent in therapeutic approach of RNA interference (RNAi), down-regulation of AD problematic genes including BACE1 has been extensively studied using viral vectors. Although viral vectors offered potential advantages for AD RNAi therapeutics, their clinical applications are limited by safety issue associated with viral-mediated carcinogenesis and immunogenicity, which led to the finding of nanotechnology-based non-viral vectors.

It is generally accepted that none of non-viral vectors is comparable to viral-vectors for delivery of genetic materials into host cells because non-viral vectors themselves are not equipped with modules for overcoming extracellular and intracellular barriers. Once delivered in body, therapeutic genes encounter extracellular barriers such as serum degradation, immune clearance, non-specific cell binding, and poor penetration of blood-brain barrier until they reach to target cells. After therapeutic genes are arrived in target cells, intracellular barriers inhibit RNAi activity which mainly includes cytotoxicity, poor endosomal escape and lysosomal degradation. The aim of the study is development of non-viral vector for AD RNAi therapeutics equipped with

modules to conquer the biological barriers, which is divided into three parts; i) study 1: development of non-viral vector to overcome intracellular barriers, ii) study 2: surface functionalization of the non-viral vector to overcome extracellular barriers, and iii) study 3: verification of AD RNAi therapeutic potential of the developed non-viral vector *in vivo*.

Study 1 mainly focused on an approach of controlling cellular uptake mechanism and consequent intracellular route of complexes to overcome the intracellular barriers. Since it became clear that uptake mechanism by which complexes are internalized determines their intracellular fates, caveolar endocytosis has emerged as an important endocytic target because it provides avoidance of lysosomal degradation. Caveolae vesicles are generally immobilized at the plasma membrane by the actin cytoskeleton, and internalized by certain stimulation via ligand-receptor interaction or osmotic stress. With a view to generating osmotically active gene carrier which facilitates caveolar endocytosis, degradable poly(mannitol-co-PEI) gene transporter (PMT) was generated by crosslinking low molecular weight PEI providing proton sponge effect and mannitol diacrylate as an osmolyte linker. PMT/DNA showed lower cytotoxicity compared to PEI/DNA complexes due to easily degradable ester groups and partially negatively charged mannitol backbone which can shield the remaining cationic charges of PEI. The proton sponge effect of PEI backbone partially contributed to gene delivery of PMT. More importantly, selective stimulation of caveolar endocytosis by mannitol backbone provided enhanced transfection efficiency via successful avoidance

of lysosomal degradation of cargo. The action mechanism of PMT/DNA complexes on stimulation of caveolae-mediated endocytosis was associated with the activation of Src-kinase by mannitol part of PMT.

In study 2, PMT was functionalized to overcome the extracellular barriers. Delivery of therapeutic siRNA to the brain is one of the biggest challenges for successful brain gene therapy because blood-brain barrier (BBB) permits selective entry of only few substances into the brain. In this study, 'Trojan horse strategy' was employed for ferrying PMT/siRNA complexes across the BBB. For this, PMT was conjugated with BBB-permeable rabies virus glycoprotein (RVG) via poly(ethylene glycol) (PEG) linker generating R-PEG-PMT. The PEG linker was expected to provide advantageous spatial arrangement of RVG peptide and stealth property on gene carrier. To determine the BBB penetration of complexes, *in vitro* BBB culture constructed by co-culture of bEnd.3 cells (mouse brain capillary endothelioma) and B23 cells (rat astrocytoma) on transwell system was utilized. The RVG ligand led to BBB penetration of PMT/siRNA complexes through receptor-mediated transcytosis via nicotinic acetylcholine receptors expressed on BBB. In mechanistic study, it was determined that improved BBB penetration of R-PEG-PMT/siRNA was achieved by stimulated receptor-mediated caveolar transcytosis. The enhanced accumulation in brain and biodistribution property of R-PEG-PMT/siRNA complexes was also demonstrated when systemically administrated.

In study 3, RNAi therapeutic potential of R-PEG-PMT/siBACE1 complexes

was examined *in vivo* using normal C57/BL6 mice. Intravenous administration of R-PEG-PMT/siBACE1 for three times within 2 weeks has shown brain-targeted suppression of BACE1 without significant systemic toxicity. Furthermore, decreased BACE1 led to inhibition of Aβ42 production, a marker of AD pathogenesis in hippocampus and cortex parts.

The overall results inferred that R-PEG-PMT is a promising tool for AD RNAi therapeutics. In aspect of overcoming intracellular barriers, i) degradable ester linkage of PMT reduced the cytotoxicity ii) PEI backbone of PMT has shown proton sponge effect, and iii) mannitol backbone provided the avoidance of lysosomal degradation via stimulation of caveolar endocytosis. In aspect of overcoming extracellular barriers, i) RVG offered neuronal cell targeting specificity, ii) stealth effect of PEG prevented the immune clearance *in vivo*, and iii) RVG directed the complexes across the BBB via receptor-mediated transcytosis and PMT facilitated trafficking of caveolae vesicle during transcytosis. The brain-targeted RNAi therapeutic effect of R-PEG-PMT/siBACE1 was demonstrated by suppression of BACE1 expression and Aβ42 production. Consequently, R-PEG-PMT is a powerful gene carrier which can conquer the biological barriers itself, and possess the potential to be widely applicable in neurodegenerative diseases as a safe and efficient brain-targeted gene carrier.

Key words: blood-brain barrier, RNA interference, polyethylenimine, mannitol, Alzheimer's disease, BACE1, caveolar endocytosis

Student number: 2011-21297

Contents

List of Tables and Figures

Tables

Figures

List of Abbreviations

Aβ: amyloid-beta

AD: Alzheimer's disease

ADA-SCID: adenosine deaminase deficiency

ALT: serum alanine transaminase

AP2: adaptor protein 2

APOE4: apolipoprotein E4

APP: amyloid precursor protein

AST: aspartate transaminase

BBB: blood-brain barrier

BCA: bicinchoninic acid

BUN: blood urea nitrogen

CD: cyclodextrin

CDPs: polycation containing CDs

CH: chloropromazine

CME: clathrin-mediated endocytosis

CNS: central nervous system

CPPs: cell penetrating peptides

CV: coefficient of variation

CvME: caveolae-mediated endocytosis

DLS: dynamic light scattering spectrophotometer

DMEM: dulbecco's modified Eagle's medium

DMF: dimethylformamide

DMSO: dimethylsulfoxide

DOGS: dioctadecylamidoglycylspermine

EF-TEM: energy-filtering transmission electron microscopy

ELISA: enzyme linked immunosorbent assay

FBS: fetal bovine serum

FDA: United State food and drug administration

FITC: fluorescein isothiocyanate

GABA: γ-aminobutyric acid

GAK: cyclin G-associated kinase

GDNF: glial cell line-derived neurotrophic factor

GE: genistein

GFP: green fluorescent protein

IDE: insulin-degrading enzyme

LMW: low molecular weight

LPL: lipoprotein lipase

LRP1: low density lipoprotein receptor-related protein 1

LRP2: low density lipoprotein receptor-related protein 2

MAPT: microtubule-associated protein tau

MEM alpha: minimum essential medium alpha

Mn: number averaged molecular weight

Mp: molecular weight at peak top

Mw: weight averaged molecular weight

M-β-CD: methyl-beta-cyclodextrin

nAchR: nicotinic acetylcholine receptor

NFTs: neurofibrillary tangles

NGF: nerve growth factor

NMDA: N-methyl-D-aspartate

NRTN: neurturin

OA: okadaic acid

PAMAM: polyamidoamine

PEI: polyethylenimine

PHFs: paired helical filaments

PMT: poly(mannitol-co-PEI)

PS1: presenilin-1

RLU: relative light units

RMT: receptor-mediated transcytosis

RNAi: RNA interference

R-PEG-PMT: PMT modified with RVG-PEG

RT: room temperature

RVG: rabies virus glycoprotein

SCID: severe combined immunodeficiency

SD: standard deviation

SDS: sodium dodecyl sulfate

siBACE1: siRNA targeting BACE1

siLUC: siRNA targeting luciferase

SLCs: solute carriers

SNALP: solid lipid-based system

TBE: tris-borate-EDTA

TEER: transendothelial electrical resistance

UBQLN1: ubiquilin-1

WO: wortmannin

Introduction

AD is the most common type of dementia in the elderly. In worldwide, approximately 26 million people suffer from AD and by the year 2050, the prevalence is expected to quadruple to 106.2 million, as a result of the aging of the world's population (Brookmeyer, R. *et al*., 2007). AD is caused by inherited genetic mutation or epigenetic changes that result in abnormal nervous system development, neurodegeneration, or impaired neuronal function. In situations in which none of the treatments is available or effective in slow or stop the malfunction in the brain, gene therapy is a particularly attractive approach. While pharmacological treatments aimed at increasing the amount of neurotransmitters acting downstream of the primary causative event, gene therapy is able to ultimately correct defective genes responsible for disease development (Ginn, S.L. *et al.*, 2013) providing solution to drawbacks of traditional approaches.

Since year 1993 when first clinical trial of gene therapy for brain diseases was conducted by Oldfield and Ram, a main stream of brain gene therapy was viral vector-mediated gene delivery due to its high transfection efficiency. Although development of viral vectors has attributed to the improvement in the field of gene therapy, important issues regarding their clinical use including ethical, regulatory authorities and acceptance by the general public limited the clinical uses. In recent, nanotechnology-based non-viral gene delivery has emerged as alternative to viral gene delivery. It is still far from clinical use

owing to its cytotoxicity and transfection efficacy, however, the advent of nanotechnology offers potential for overcoming those disadvantages.

To obtain the therapeutic effects of nucleic acid drugs, non-viral vectors need to overcome several extracellular and intracellular barriers. Once delivered in body, therapeutic genes encounter extracellular barriers such as serum degradation, immune clearance, non-specific cell binding, and poor penetration of blood-brain barrier until they reach to target cells. After therapeutic genes are arrived in target cells, intracellular barriers inhibit RNAi activity which mainly includes cytotoxicity, poor endosomal escape and lysosomal degradation. Therefore, maximal therapeutic benefit of gene therapy can be achieved by adequate design of gene carrier based on knowledge of extracellular and intracellular barriers and coping strategies. In this study, a polymeric gene carrier was developed reflecting on coping strategies dealing with the biological barriers for AD RNAi therapeutics (Table 1).

It became clear that endocytosis pathway determines the intracellular fates of cargo. In a virus imitation strategy, caveolae-mediated endocytosis used in SV40 entry bypassing lysosomal fusion has been shown to improve gene delivery efficiency. In the first approach, polyethylenimine (PEI), a golden standard of polymeric non-viral vector was modified to overcome intracellular barriers according to the strategies described in Table 1. Finally, a degradable PEI derivative, PMT was generated by low molecular weight PEI and mannitol diacrylate. PMT-mediated gene delivery has shown low cytotoxicity and

enhanced transfection efficiency by shifting of entry pathway into caveolar endocytosis. The mechanism by which PMT stimulate the trafficking of caveolae vesicle was determined to be associated with osmotic function of its mannitol part.

For nanoparticles to penetrate BBB, receptor-mediated transcytosis is an attractive strategy because of a few advantages: i) circumvention of Pgp efflux transporter in the BBB, ii) brain specificity and iii) unrestricted cargo size (Gan, C.W. and Feng, S.-S., 2010). There are several studies demonstrating that targeting caveolae-mediated transcytosis can enhance the drug delivery efficiency across the endothelium *in vivo* (McIntosh, D.P. *et al.*, 2002;Sukumaran, S.K. *et al.*, 2002). In the second approach, it was hypothesized that employment of brain targeting ligands and stimulation of caveolar endocytosis would synergistically improve BBB penetration efficiency. For this, PMT was conjugated with RVG ligand via PEG linker generating R-PME-PMT, expecting that the RVG ligand would direct the complexes across the BBB and stealth effect of PEG would prevent immune clearance and enhance accumulation in brain. The enhanced permeability of R-PEG-PMT/siRNA complexes and associated transcytotic mechanism were examined using *in vitro* BBB system.

In the third approach, siRNAs targeting BACE1, a causative gene of AD, was delivered *in vivo* to confirm the AD RNAi therapeutic potential of R-PEG-PMT. BACE1 (β-site APP cleaving enzyme) is a rate-limiting factor for

production of AD pathogenic Aβ42, and its level and activity increase in the onset of AD. Although BACE1 inhibitors are under development, their unsatisfactory selectivity, large size, poor brain permeability, and short half-life *in vivo* limit their clinical uses. Treatment of R-PEG-PMT/siBACE1 complexes *in vivo* has shown brain-targeted suppression of BACE1 without significant systemic toxicity and successful prevention of immune clearance. Furthermore, decreased BACE1 led to inhibition of Aβ42 production implying that R-PEG-PMT is a promising brain-targeted gene carrier for AD RNAi therapeutics.

Table 1. Challenges of brain-targeted non-viral gene delivery and coping strategies used at design of gene carrier

	Challenges	Strategies
	Intracellular barriers (Chapter 1)	
1	Cytotoxicity	1. Synthesis of degradable PEI derivatives using low molecular weight PEI and mannitol linker 2. Use of mannitol which quenches the remaining positive charges of the complexes
2	Endosomal escape	Intrinsic mechanism of "proton sponge effect" of PEI
3	Avoidance of lysosomal degradation	Selective stimulation of caveolar endocytosis which avoids lysosomal fusion of cargoes
	Extracellular barriers (Chapter 2)	
4	Brain targeting	Conjugation of rabies virus glycoprotein (RVG) ligand which specifically binds to neuronal cells
5	BBB penetration	1. Conjugation of brain targeting ligand, RVG for receptor-mediated transcytosis 2. Selective stimulation of caveolar endocytosis to avoid lysosomal fusion during transcytosis
6	Biodistribution	Conjugation of poly(ethylene glycol) (PEG) to prevent from opsonization and tissue off-target effect

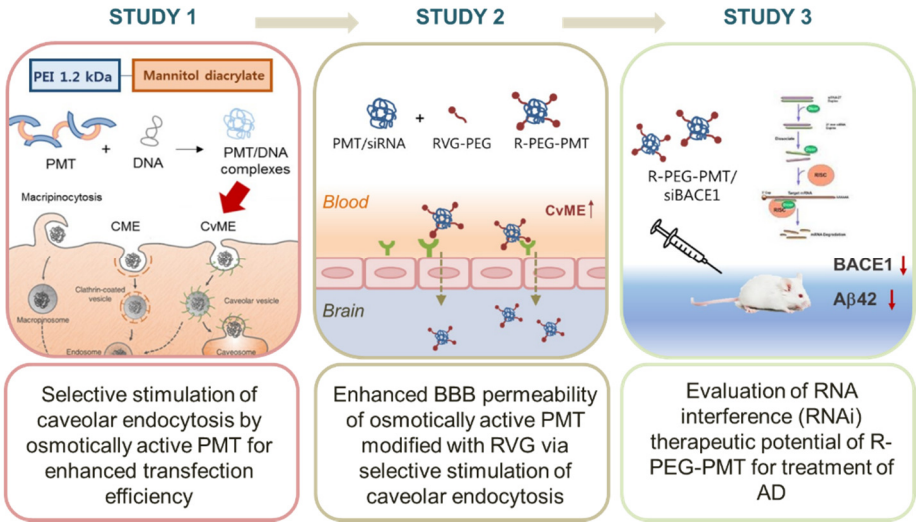

Figure 1. Schematic illustration of aim of the study

Review of Literature

1. Overview of gene therapy for neurological disorders

1) Historical evolution of gene therapy

The United State Food and Drug Administration (FDA) defines gene therapy as products "that mediate their effects by transcription and/or translation of transferred genetic material and/or by integrating into the host genome and that are administered as nucleic acids, viruses, or genetically engineered microorganism. The products may be used to modify cells *in vivo* or transferred to cells *ex vivo* prior to administration to the recipient." Since 1990 when FDA approved the first time a gene therapy trial in human (Blaese, R.M. *et al.*, 1995), 36 gene therapy clinical trials for neurological disease are ongoing or have been approved to date (Ginn, S.L. *et al.*, 2013).

The first step of gene therapy started from observation that chicken cells infected with Rous sarcoma virus stably mutated the gene through chromosomal insertion of foreign genetic materials implying that viruses can be used to deliver genes in host cells (Temin, H.M., 1961). Rogers and Pfuderer (1973) used Shope papilloma virus directly to human for treatment of urea cycle disorder by providing missing enzyme gene argininase. The outcome of the trial was negative because the virus did not encode argininase contrary to their expectation (Wirth, T. *et al.*, 2013).

Blaese and his colleagues were first to conduct a trial using a therapeutic

gene with FDA approval. They took white blood cells from two children suffering from adenosine deaminase deficiency (ADA-SCID) and inserted the normal gene. One of the patients who received the cells showed temporary responses (Blaese, R.M. *et al.*, 1995) although enzyme replacement therapy was conducted simultaneously.

In year 1993, first clinical trial of gene therapy in brain disease was conducted by Oldfield and Ram. They used retroviral vector containing the herpes simplex virus-thymidine kinase gene in 15 patients with progressive growth of recurrent malignant brain tumors. Antitumor activity was detected in five of the smaller tumors (1.4±0.5 ml). The results showed that high density of vector-producing cells are required for antitumor effect emphasizing importance for the development of delivery systems (Ram, Z. *et al.*, 1997).

The gene therapy strategy experienced boom, until Gelsinger suffered from a partial deficiency of ornithine transcarbamylase died during gene therapy clinical trial at the University of Pennsylvania in Philadelphia (Stolberg, S.G., 1999). Gelsinger's death was directly attributable to the administration of high dose of adenovirus vector. The systemic delivery of the vector triggered a massive inflammatory response that led to disseminated intravascular coagulation, acute respiratory distress and multi-organ failure (Thomas, C.E. *et al.*, 2003).

In year 2000, gene therapy entered new phase by the first report of successful clinical gene therapy trial against severe combined immunodeficiency (SCID)

by Fischer and Cavazzana-Calvo (2005). SCID is an X-linked inherited disorder by an early block in T and natural killer lymphocyte differentiation by mutation of the gene encoding the gamma cytokine receptor subunit of interleukin-2, -4, -7, -9, and -15 receptors. They utilized retroviral vector to deliver IL2RG gene into CD34+ cell taken from infant SCID patients. After a 10-month follow up period, transgene expressing T and NK cells were detected in two patients and function of the cells was found to be comparable to normal cells.

The first gene therapy product, Gendicine™ was approved for clinical use in China in 2003 (Ginn, S.L. *et al.*, 2013). Gendicine™ developed by SiBiono Gene Tech Co. is a non-replicative adenoviral vector encoding wild-type p53 gene for treatment of head and neck cancer. In 2005, China approved another gene therapy product, Oncorine™ developed by Sunway Biotech Co. Ltd for treatment of same diseases. Contrary to Gendicine™, Oncorine™ is replicative adenovirus with deletion in E1B 55K region in order to achieve tumor cell selectivity. Due to mutation, this product has preferential replication in cancer cells which is classified as oncolytic viral therapeutics (Campbell, R.N., 2008).

In 2007, phase 1 clinical trial of *in vivo* nerve growth factor (NGF) delivery by adeno associated viral vector for AD was reported by Arvanitakis et al. NGF is an endogenous neurotrophic-factor protein with the potential to restore function and to protect degenerating cholinergic neurons in AD. Bilateral stereotactic administration of adenoviral vector to nucleus basalis of Meynert

produced long-term and biologically active NGF expression for two years (Arvanitakis, Z. *et al.*, 2007;Rafii, M.S. *et al.*, 2014).

In year 2009, Bennett and his coworkers reported successful gene therapy for Leber's congenital amaurosis using AAV encoding the retinal pigment epithelium-specific 65 kDa protein. Leber's congenital amaurosis is degenerative disorder causing severe vision loss. Although eight-year boy obtained the greatest benefit, all participants whose age ranged from 8 to 44 gained some improvement in eyesight (Maguire, A.M. *et al.*, 2009).

A big step forward came in 2012, when the European Medicines Agency recommended for the first time a gene therapy product, Glybera for approval in the European Union and finally gave permission to sell its treatment. Glybera is an adeno-associated viral vector encoding lipoprotein lipase (LPL) for the treatment of severe lipoprotein lipase deficiency (Yla-Herttuala, S., 2012). The LPL gene, encoded by an AAV vector, is administered by means of multiple subcutaneous injections to the upper thighs during a single outpatient procedure.

Milestones of the history of gene therapy are described in Figure 2. Although many gene therapies have been tested around the world in hopes of curing various diseases, few governments have approved their sales. Sooner or later, gene therapy would be a part of the standard care for a variety of different diseases with advances in immunology, physiology, nanotechnology, virology and genetic technology. Many recently identified disease targets are considered 'undraggable' using small-molecule inhibitors. The potential of exogenous

nucleic acid may provide an avenue to translate our knowledge obtained from biomedical research into therapeutics.

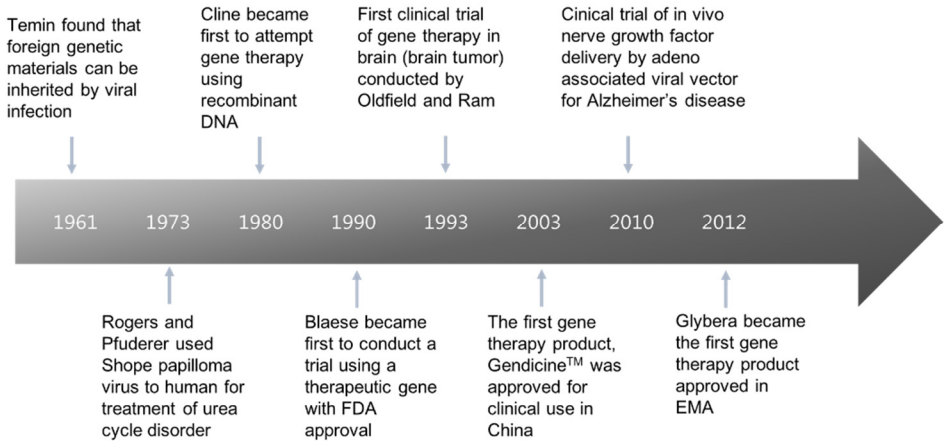

Figure 2. Timeline highlighting some important milestone of gene therapy

2) Progress and prospect of gene therapy for neurodegenerative disease

The nervous system is a complex and difficult organ system to study, and the brain is an organ where many of the most pervasive disease processes arise (Simonato, M. *et al.*, 2013). Despite the progress in research on neurodegenerative disease, successful drug and drug delivery strategy for overcoming BBB remains elusive (Di Stefano, A. *et al.*, 2011). Standard pharmacological and surgical interventions are either inadequate or unavailable for most neurodegenerative diseases. For example, at present, current management of AD patients involves drugs that provide only symptomatic therapy not its cause (Di Stefano, A. *et al.*, 2011). Hence, genetic interventions to supply gene products which permanently restore function or suppression of causative genes could represent an alternative to standard pharmacological

studies (Simonato, M. *et al.*, 2013) (Figure 3). On the basis of preclinical studies, early clinical trials have been carried out to test the safety and, in some case, efficacy of gene therapy (Table 2).

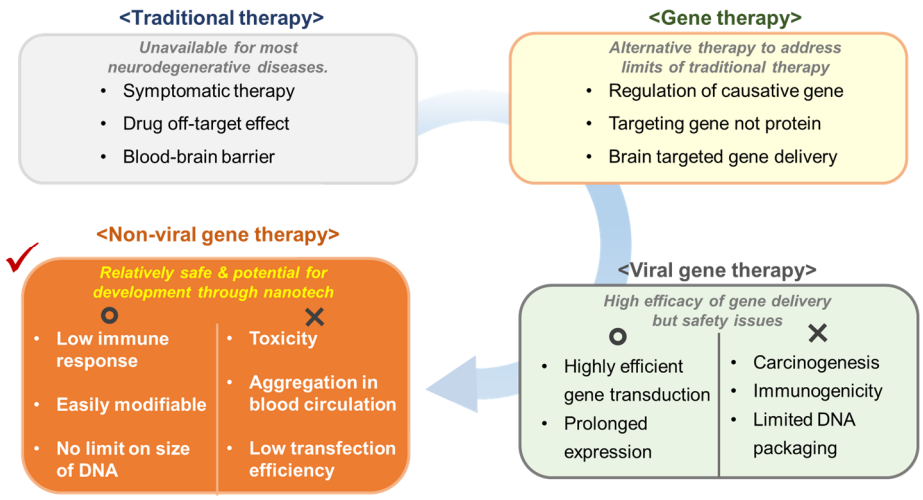

Figure 3. Progress and prospect of gene therapy for neurodegenerative diseases

Table 2. Clinical trials on gene therapy for the treatment of neurodegenerative diseases (Simonato, M. *et al.*, 2013)

Gene-delivery target	Clinical trial status	Viral vector	Therapeutic mechanism	Reference
Parkinson disease				
Stereotactic injection into putamen	Phase 1	AAV2	Aromatic acid decarboxylase (AADC) expression to convert levodopa to dopamine	(Christine, C.W. *et al.*, 2009)
Stereotactic injection into putamen	Phase 1	Equine infectious anaemia virus	AADA-mediated expression of tyrosine hydroxylase and GTP cyclohydrolase 1 to stimulate autonomous dopamine production from tyrosine	(Jarraya, B. *et al.*, 2009)
Stereotactic injection into putamen	Phase II	AAV2	Neurturin (NRTN) expression protects substantia nigra neurons, and promote nigrostriatal regeneration and upregulation of dopamine production	(Wirdefeldt, K. *et al.*, 2011)
Stereotactic injection into putamen	Phase 1-II	AAV2	Glial cell line-derived neurotrophic factor (GDNF) expression similar to NRTN	(Marks, W.J., Jr. *et al.*, 2010)
Stereotactic injection into substantia nigra and putamen	Phase II	AAV2	NRTN expression	(Kells, A.P. *et al.*, 2010)
Stereotactic injection into subthalamic nucleus	Phase II	AAV2	Glutamic acid decarboxylase gene expression converts glutamate to r-aminobutyric acid, thereby increasing synaptic inhibition in the subthalamic nucleus	(LeWitt, P.A. *et al.*, 2011)
Huntington disease				
Stereotactic injection	Preclinical	AAV2	NRTN expression provides neuroprotection	(McBride, J.L. *et al.*, 2011)

into striatum				
Injection of striatum or diffuse delivery	Preclinical	AAV	Expression of mutant Huntingtin siRNA (allele specific)	(Ramaswamy, S. *et al.*, 2009)
Alzhemier's disease				
Streotactic injection into nucleus of Meynert	Phase II	AAV2	Nerve growth factor gene expression enhances cholinergic neuron protection, axonal regeneration and upregulation of acetylcholine production	(Arvanitakis, Z. *et al.*, 2007)
Stereotactic injection into entorhinal cortex	Preclinical	AAV2	Expression of brain-derived neurotrophic factor enhances neuroprotection and axonal regeneration	(Nagahara, A.H. *et al.*, 2009)
Amytrophic lateral sclerosis				
Injection into spinal cord	Preclinical	Lentivirus-transduced neural progenitors	*Ex vivo* gene transfer of GDNF to human neural progenitor cells	(Suzuki, M. et al., 2007)
Ventral horn of spinal cord	Preclinical	AAV2	1GF1 expression	(Franz, C.K. et al., 2009)
Remote gene delivery by retrograde axonal transport; nerve or muscle injection	Preclinical	AAV2	IGF1 or GDNF	(Kaspar, B.K. et al., 2003)
Intrathecal injection	Phase1		Delivery of antisense oligonucleotides to target mutated SOD1	(Smith, R.A. et al., 2006)

2. Gene delivery system

Considering that over 1800 gene therapy clinical trials have been approved, the rate of success is terribly low owing to lack of safe, efficient and controllable methods for gene delivery. Indeed, viral vector system provided great advances in the field of gene therapy which accounts for almost 70% of clinical trials (Ginn, S.L. *et al.*, 2013) due to high efficiency of transduction and gene expression *in vivo* (Figure 4). However, they have severe limitations including carcinogenesis, immunogenicity, broad tropism, limited DNA packaging capacity and difficulty of vector production (Yin, H. *et al.*, 2014). Non-viral delivery systems have potential to address those disadvantages of viral vectors. Non-viral vectors are relatively free from safety issue related to viral antigenicity, which permit repetitive administration in clinical application and have ability to deliver larger cargoes. Nevertheless, they are yet far from clinical use owing to their low transfection efficiencies and limited duration of gene expression. None of these non-viral vectors are comparable to viral vectors which have evolved machinery for delivery of genetic materials into host cells (Yin, H. *et al.*, 2014). Given the potential of non-viral vectors as alternative tools for gene therapy, improvement of non-viral vector through the application of nanotechnology is urgently required. Figure 5 represents the classification of gene delivery systems for gene therapy.

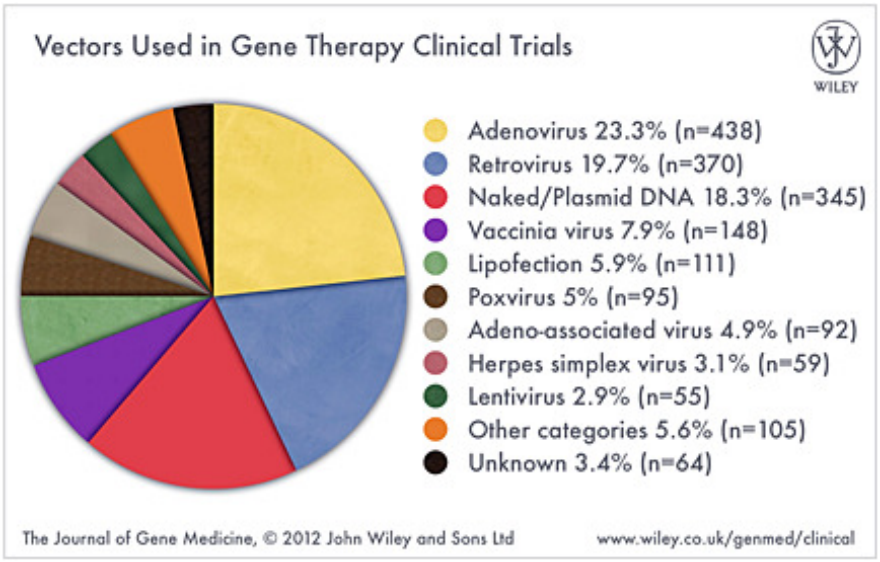

Figure 4. Gene delivery system for gene therapy in clinical trials (Ginn, S.L. *et al.*, 2013)

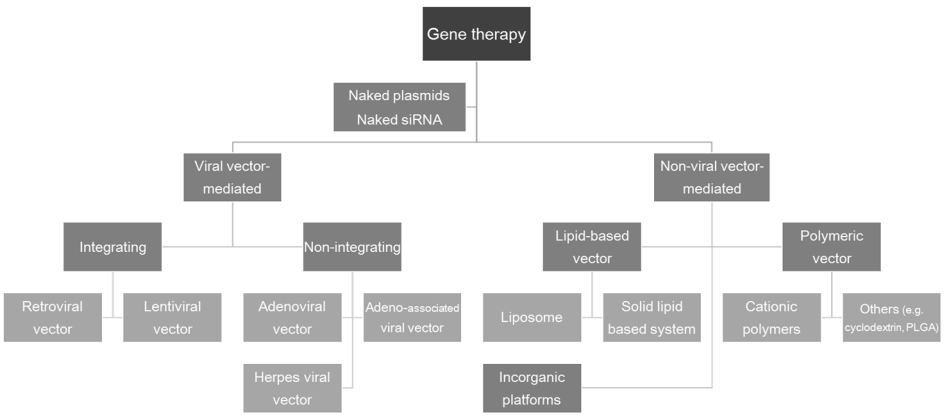

Figure 5. Classification of gene delivery system for gene therapy

1) Viral vectors

The key to development of viral vector for gene therapy is exploiting their capacity of transgene expression and eliminating viral replication after host transduction (Simonato, M. *et al.*, 2013). Great effort has gone into the development of viral vector suitable for clinical applications and the vectors vary in characteristics such as duration of expression, safety issues, target cells and so on (Table 3).

Table 3. Characteristics of viral vectors [modified from (Simonato, M. *et al.*, 2013))]

	Derived from pathogenic virus	Gene insert	Integration into host-genome	Achievable titer	Duration of expression	Target cells
Adenoviral vector	Y	7~8 kb	N	High	Transient	Dividing and non-dividing
Adeno-associated viral vector	N	~4.5 kb	N	High	Month to years	Dividing and non-dividing
Herpes viral vector	Y	~20-40 kb	N	High	Transient	Dividing and non-dividing
Lentiviral vector	Y	~8 kb	Y	Low	Month to years	Dividing and non-dividing

(1) Adenoviral vector

Adenoviral vector is non-enveloped virus with an icosahedral nucleocapsid containing a double stranded DNA genome (36 kb). It delivers relatively large sized transgene (~7.5 kb) into host cells with a high level of expression and without integration into host-cell genome. The introduced gene is left in the nucleus of the host cells and transcribed just like other gene, which provides short duration transgene expression (Simonato, M. *et al.*, 2013). Although treatment of adenovirus requires means of multiple administration in a growing cell population, it can avoid carcinogenesis caused by integration of transgene into host genome. As shown in Figure 2, adenoviral vector is mostly used in clinical trials which accounts for 23.3% in 2012. Immune responses occur

against the capsid, double-stranded DNA, viral protein by administration of adenovirus, which severely limits *in vivo* gene therapy (Nayak, S. and Herzog, R.W., 2010).

(2) Adeno-associated viral vector

Adeno-associated viral vector is derived from a non-pathogenic replication deficient parvovirus causing mild immune responses. The virtue of adeno-associated viral vector is safety, non-pathogenesis, and long-term gene expression. However, cloning capacity of adeno-associated virus is relatively low (~4.5 kb) owing to smallest genome size among the popular viral vectors (4.7 kb) (Simonato, M. *et al.*, 2013), which limits the clinical application. The adeno-associated viral vector is useful for brain gene therapy because it can infect non-dividing cells, such as neurons although high dose elicits brain immune responses where has been known as immune privileged site (Nayak, S. and Herzog, R.W., 2010).

(3) Herpes simplex viral vector

Herpes simplex viral vector is enveloped virus with an icosahedral nucleocapsid containing a double stranded and relatively large DNA genome (152 kb). The envelope covering the virus particle, when bound to specific receptors on the cell surface, will fuse with the host cell membrane and create an opening, or pore, through which the virus enters the host cells. A high transgene capacity allowing to carry long sequence of DNA (~20-40 kb) and efficient transduction of non-dividing cells made it amenable to gene therapy applications within the central nervous system (Zeier, Z. *et al.*, 2009). However,

it may cause toxicity and inflammation from leaky expression of viral genes and elicit immune responses, which limits the clinical application (Simonato, M. *et al.*, 2013).

(4) Lentiviral vectors

Lentiviral vector is a genus of the Retroviridae family. It transduces dividing and non-dividing cells and inserts gene of interest into host genome providing long-lasting transgene expression (Simonato, M. *et al.*, 2013). The introduced RNA molecules produce DNA copy via reverse transcription which are inserted into host genome by integrase. One of the problems of gene therapy using lentiviral vector is that integrase enzyme inserts the genetic material in any arbitrary position in the genome of the host cells posing a risk for insertional mutagenesis. Furthermore, if genetic materials is inserted in the middle of one of genes regulating cell division, uncontrolled cell division occurs (Thomas, C.E. *et al.*, 2003).

Numerous problems and risks associated with use of viral vector exist in clinical application. Viruses can infect healthy cells as well as target cells. Some viral vectors cause insertional mutagenesis or even cancer and transferred genes could be overexpressed causing adverse effect. Innate and adaptive immune responses elicited by some viral vectors leads to decreased efficiency of gene transfer or elimination of the transduced cells over time. Development of strategies to avoid viral vector associated risks via improvement of organ targeting specificity, inducible promoters, development of alternative viral serotypes, and the identification of new virus species would truly fulfil all of its

promises (Thomas, C.E. *et al.*, 2003) (Figure 6).

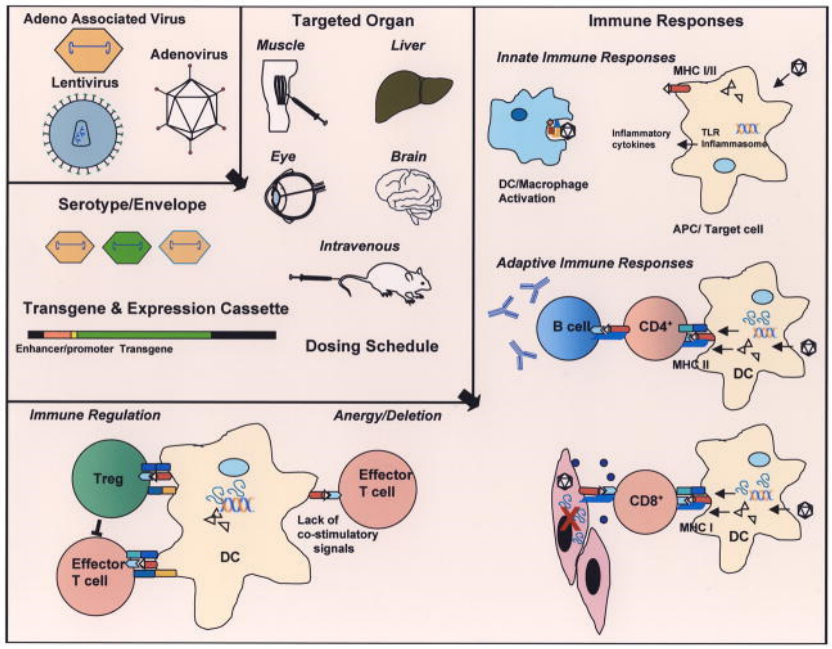

Figure 6. Overview of immune responses to viral vectors. Targeting specific organs, engineering viral envelopes, switching serotypes, modifying the transgene cassette, utilizing tissue-specific promoters, or immune modulation regimens can result in immune avoidance to the viral vector and transgene product, and in some cases even induce tolerance to the therapeutic gene product (Nayak, S. and Herzog, R.W., 2010).

2) Non-viral vectors

(1) Lipid-based non-viral vector

Hundreds of synthetic lipids have been developed for gene delivery since Fielgner et al. (Felgner, P.L. *et al.*, 1987) first synthesized cationic lipid *N*-[1-(2,3-dioleyloxy)propyl]-*N,N,N*-trimethylammonium chloride (DOTMA) to deliver plasmids into cells because they have many potential advantages such as ease of production, biodegradability, their ability to protect entrapped genes both from nuclease degradation and renal clearance, promotion of cellular uptake and endosomal escape (Zhi, D. *et al.*, 2010;Kanasty, R. *et al.*, 2013). As a consequence, several RNAi-based drugs using lipid systems also have been used for clinical trials. Anderson Cancer Center, for example, initiated a phase 1 clinical trial of siRNAs encapsulated by neutral liposome, 1,2-dioleoyl-sn-glycero-3-phosphatidylcholine (DOTC) for suppression of oncoprotein Eph2. Also, solid lipid-based system (SNALP)-mediated siRNA delivery targeting PLK1 protein has entered the phase 1 trials by Tekmira Pharmaceuticals Corporation. Although toxicities such as acute inflammation and pulmonary hypotension, tissue infiltration, decrease in white cell counts and tissue injury are reported, progress in nanotechnology would overcome challenges and push toward success in clinical application. This section emphasizes the nanoparticle-based delivery of siRNA for lung cancer therapy.

Liposome. Liposomes are small vesicles of unilamellar or multilamellar phospholipid/ lipid bilayers in an energetically favorable manner (Wong, H.L. *et al.*, 2012). Because liposomes have dynamic properties, low toxicity and are

relatively easy to manipulate, they are the most studied and wildly used gene carrier in clinical trials (Wong, H.L. *et al.*, 2012). On the other hand, disadvantages of liposomes including fat systemic elimination, quick metabolic degradation of the phospholipids, and stability issue after extended storages have limited the efficient gene delivery *in vivo* (Wong, H.L. *et al.*, 2012). To overcome those problems, the initial attempt at developing long-circulating liposomes involved mimicking red blood cell membranes by modifying the liposomal surface with glycosphingolipids (Ewert, K.K. *et al.*, 2010). Now, liposomes of new generation commonly employ peglyation strategy for extending circulation time to days (Ewert, K.K. *et al.*, 2010). Among the various types of liposomes, cationic liposomes having a positive charge through amines in the polar head group are typically used for gene delivery because cationic character facilitates the binding with anionic nucleic acids and plasma membrane (Patel, H.M. and Russell, N.J., 1988). Widely used commercial reagents for cationic lipid-mediated gene delivery include 1,2-bis(oleoyloxy)-3-(trimethylammonio)propane, 3β[*N*-(*N'*, *N'*-dimethylaminoethane)-carbamoyl]cholesterol, and dioctadecylamidoglycylspermine (Balazs, D.A. and Godbey, W., 2011). Anticipated Structure of simple liposomes and cationic liposomes are shown in Figure 7.

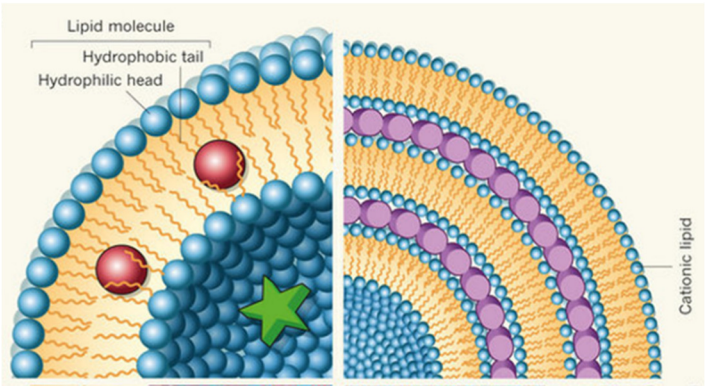

Figure 7. Structure of simple liposomes (left) and cationic liposomes (right) for gene delivery. Left: hydrophobic guest materials (red) are entrapped in hydrophobic within hydrophobic bilayer. Right: nucleic acids (purple) are sandwiched between cationic membranes [Modified by (Safinya, C.R. and Ewert, K.K., 2012)].

SLN. SLN referred as lipidoid are advanced lipid-based delivery systems as new class of safer and efficient gene delivery vectors. To overcome the disadvantages associated with the lipid state of oil droplet of liposome, liquid lipid was replaced by a solid lipid which forms micron colloid in aqueous surfactant solution (Figure 8). SLNs offer several advantages conferred by their colloidal dimensions including: i) improved physical stability; ii) controlled release; iii) improved biocompatibility; iv) potential for site specific drug delivery; vi) improved drug stability; vii) better formulation stability; viii) the ability to freeze dry and reconstitute; ix) high drug payload; x) controllable particle size; xi) the avoidance of carrier toxicity; xii) low production cost; and xiii) easy scale-up and manufacturing (Kaur, T. and Slavces, R., 2013). On the other hand, the disadvantages associated with SLNs relate mostly to their preparation involving high pressure and rapid temperature changes that can lead

to high pressure-induced drug degradation, lipid crystallization, gelation phenomena and the co-existence of several colloidal species.

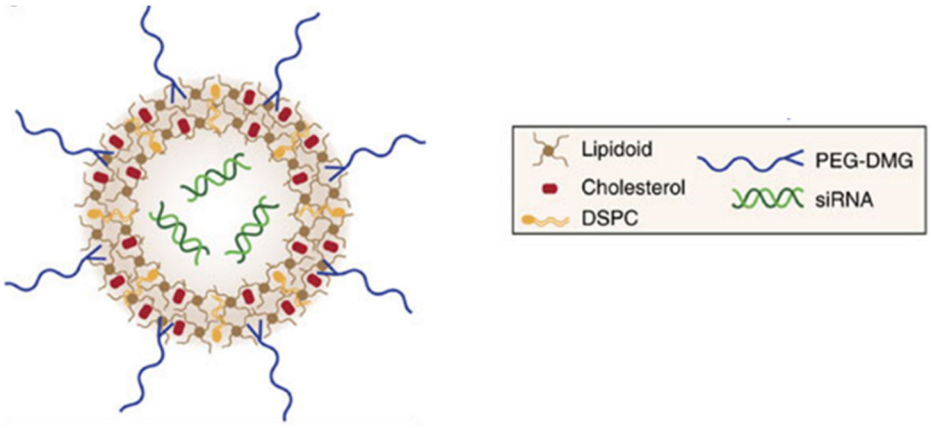

Figure 8. Schematics of SLN for gene therapy (Whitehead, K.A. *et al.*, 2014)

(2) Polymer-based non-viral vector

Recently, polymeric carrier have received significant attention in gene delivery because polymers have versatile nature with biocompatibility and provide a scope for diverse modifications to embrace desirable properties in polymeric carriers. Generally, cationic polymers are used as gene delivery vehicle because they readily form complexes with anionic nucleic acids and interact with plasma membrane enhancing adsorptive endocytosis. Also, polymer based non-viral vectors are more suitable at *in vivo* gene delivery because of higher stability compared to lipoplexes. Although polymeric carrier-mediated gene delivery is latecomer in the field of gene delivery, it has stepped forward clinical trials with enormous potential of development. In this section, most prevalent cationic polymers, PEI, polyamidoamine (PAMAM), chitosan, andcationic cyclodextrin (CD) will be explained.

PEI. Among polymeric carriers, PEI (Figure 9) has been used for gene delivery applications as a golden standard because it confers high gene delivery efficiency (Demeneix, B. and Behr, J.P., 2005). PEI has been successfully used for *in vivo* gene delivery to a variety of tissues including the central nervous system, kidney, lung, and tumors. However, growing concerns about high degree of cytotoxicity of PEI owing to cationic charge and non-degradability have accentuated the need for strategies to modify PEI. Although the presence of the high densities of primary amine forms the basis for this method of DNA packaging and a process of adsorptive endocytosis, it induces cell dysfunction and/or apoptosis by non-specific ionic interaction with plasma membrane, mitochondrial membrane, and cytosolic proteins (Moghimi, S.M. *et al.*, 2005).

One approach to solve the problem of cytotoxicity without reduction of transfection activity is crosslinking low molecular weight (LMW) PEI through biodegradable disulfide or ester bonds (Arote, R. *et al.*, 2007;Koo, H. *et al.*, 2010).

The relatively high gene-transfer activity of PEI has been believed to be due in large part to efficient escape from the endocytic pathway through the proton-sponge mechanism. In 1997, Behr proposed the "proton-sponge" hypothesis describing that unprotonated amines of PEI absorb protons in endolysosome where protons are continually pumped to lower pH, resulting in influx of more protons as well as more Cl^- ions and water (Figure 10). High osmotic pressure in endo-lysosome leads rupture of lysosomal membrane with release of its content. Without endosomal escape of nucleic acid cargo, therapeutic genes cannot reach to the target organelles and lysosomal degradation occur. In recent, as quantitative measurement of lysosomal pH becomes available, some studies suggest that PEI does not induce change in lysosomal pH and, thereby function of PEI is not related with proton sponge effect (Benjaminsen, R.V. *et al.*, 2013). These findings imply that further modification of PEI is required for higher gene delivery efficacy via conjugation of osmotically active moleculs and/or regulation of endocytic pathway directing avoids lysosome.

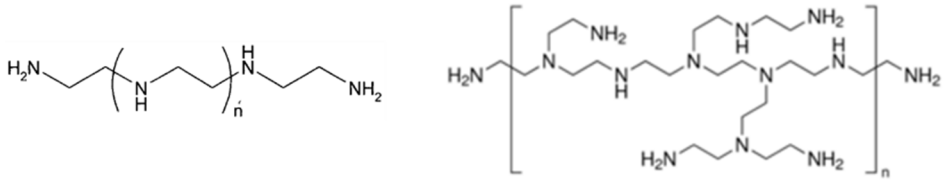

Figure 9. Chemical structure of linear and branched PEIs

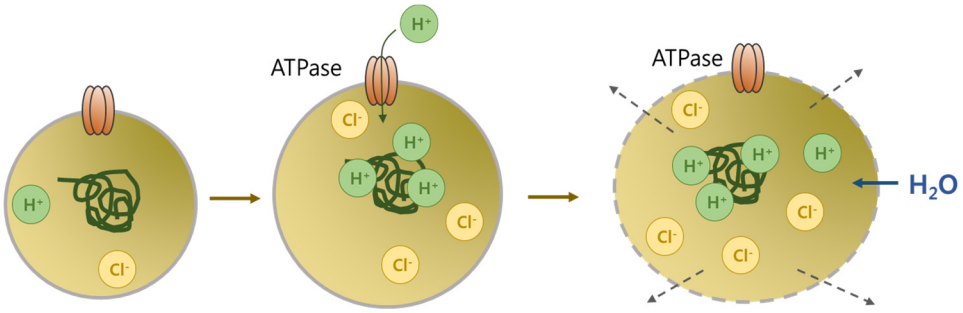

Figure 10. Schematic of proton sponge effect of PEI

PAMAM. PAMAM dendrimers are spheroidal, cascade polymers having a central core to which are connected several branched arms depending on the generation in the synthesis (Figure 11). Because of large number of secondary

and tertiary amine on the outer surface of PAMAM, it interacts with anionic charged nucleic acids and expected to have proton sponge effect. In general, PAMAM with higher generation number has higher transfection efficiency, however, is more cytotoxic compared to PAMAM with lower generation number. Haensler and Szoka found that sixth generation dendrimer was better than higher and lower generation emphasizing the optimization of generation number for safer and higher gene delivery efficiency (Haensler, J. and Szoka, F.C., Jr., 1993). Because of low density of cationic amine on the surface of PAMAM, the cytotoxicity of PAMAM is generally lower than that of PEI.

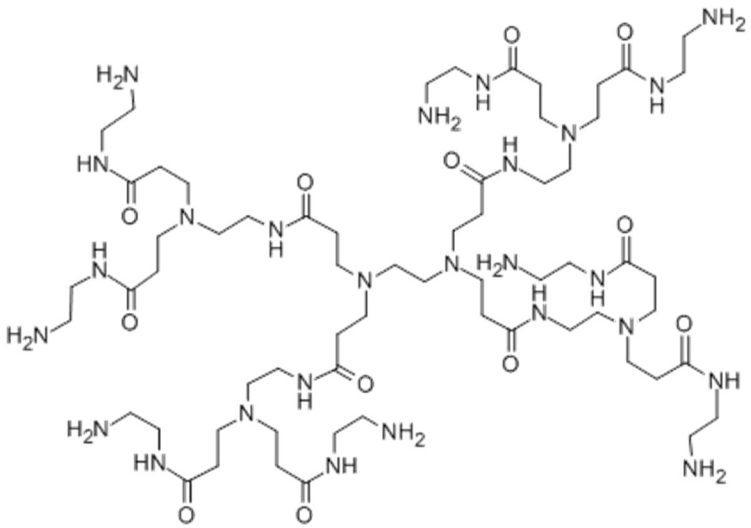

Figure 11. Chemical structure of G1 PAMAM

CD. Recently, CD-based polymers have attracted great attention for gene therapy because CD-based polymer system is the first representative of polymeric gene carriers that entered clinical trials for gene delivery less than a decade after its introduction. CDs are ring-shaped molecules comprising 6, 7 or 8 glucose units (Figure 12). The important character of CD is that the exterior of ring is hydrophilic and the interior is hydrophobic allowing encapsulation of both hydrophilic and hydrophobic drugs for forming inclusion complexes. CDs are biocompatible materials and are used in FDA-approved pharmaceutical formulations as solubilizing agents. Polycation containing CDs (CDPs) have been synthesized to impart the pharmaceutically attractive properties of CDs such as low toxicity and inclusion-complex formation with cationic polymers used for gene delivery. For example, Uekama and coworkers synthesized PAMAM dendrimer grafted CD and concluded that alpha-CD conjugation to G3 PAMAM (three generation) improved *in vitro* and *in vivo* gene delivery (Arima, H. *et al.*, 2001). PEI grafted CD also efficiently delivers genes *in vitro* and *in vivo* with lower toxicity than unmodified PEI (Forrest, M.L. *et al.*, 2004;Pun, S.H., 2004). Although CDP provide reduced toxicity than non-modified polycation, there is a tradeoff between reducing toxicity and decreasing efficacy of gene delivery, so optimization of relative ratio of each group is required.

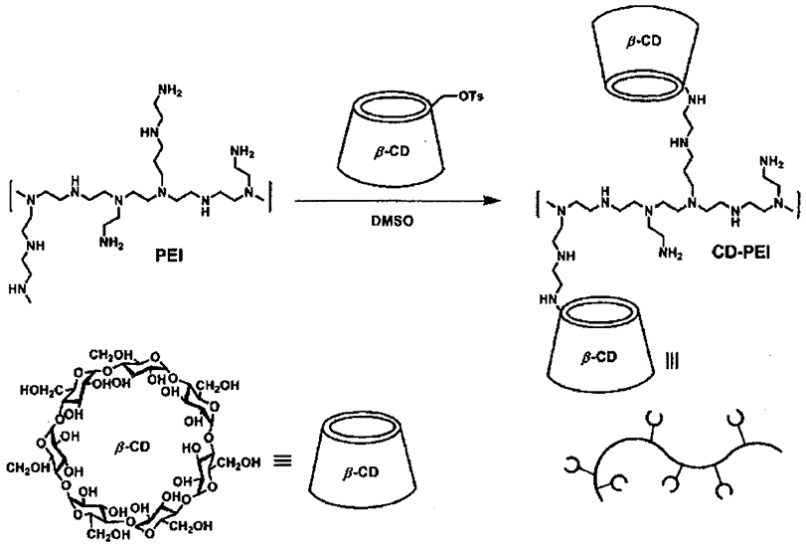

Figure 12. Scheme of synthesis of PEI grafted beta-CD (Tseng, H.R. *et al.*, 2010)

3. Extracellular barriers for brain-targeted non-viral gene delivery

For successful gene therapy for neurodegenerative disorders, non-viral vector need to overcome several extra- and intracellular barriers until they reach the site of action (Figure 13). Although non-viral delivery systems have potential to address disadvantages of viral vectors, their lack of ability to conquer the biological environment limited the clinical applications. Maximal therapeutic benefit of non-viral vector mediated gene therapy can be achieved by adequate design of vector based on knowledge of extra- and intracellular barriers with coping strategy. Generally, extracellular barriers of gene delivery include all biological, chemical and physical barriers encountered following administration of nanoparticles to reach the target cells including serum stability, inadequate cellular binding, rapid clearance, and poor uptake. In particular, BBB a highly regulative system separating brain from periphery is added to list of extracellular barriers for brain targeted gene delivery. Intracellular barriers include non-specific cellular uptake, poor endosomal escape and inadequate vector unpacking (Khalil, I.A. *et al.*, 2006). Non-viral vectors cannot readily cross over plasma membrane, instead, they are internalized by endocytosis. In the process of endocytosis, they are surrounded by plasma membrane which then bud off inside the cells to form trafficking vesicles. Depending on the uptake mechanisms, the vesicles tend to be fused with lysosomes or avoid it, which is closely related to transfection efficiency. Viruses evolutionary improved their machineries to escape or avail themselves of intracellular trafficking (Yin, H. *et al.*, 2014), therefore virus imitation strategy is helpful for rational design of non-viral vector. Given the potential of

non-viral vectors as alternative tools for gene therapy for neurodegenerative diseases, improvement of vector through the application of nanotechnology is urgently required. In this section, extra- and intracellular barriers in brain-targeted non-viral gene delivery and nanotechnology based coping strategies will be covered.

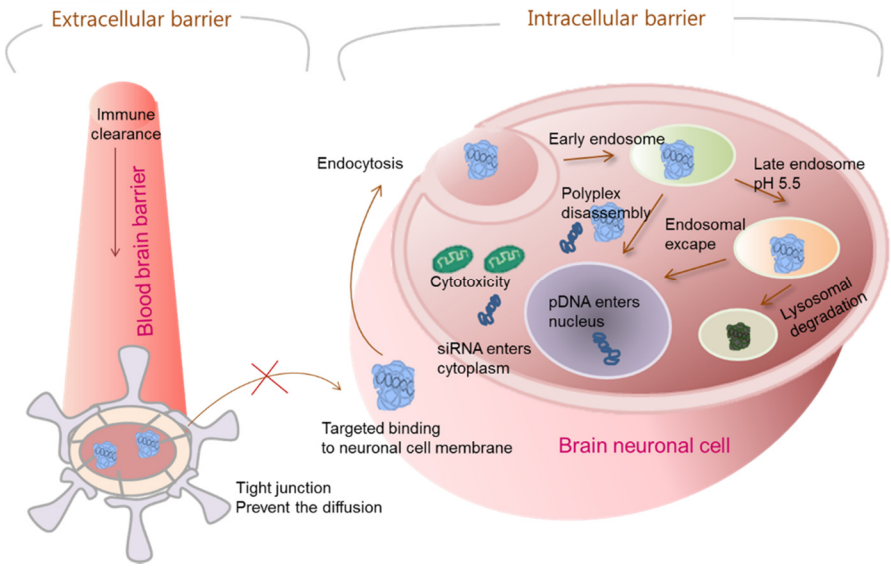

Figure 13. Scheme of extracellular and intracellular barriers in brain targeted non-viral gene delivery

1) BBB

(1) Characteristics of BBB

The BBB is a highly regulative diffusion barrier providing optimal chemical environment for central nervous system function (Figure 14). It is composed of complex of capillary endothelial cells, a basement membrane consisting of type IV collagen, pericytes which are embedded in the basement membrane, astrocyte surrounding basement membrane (Hawkins, R.A. *et al.*, 2006). The compact network of BBB confers to the endothelial layer with a transendothelial electrical resistance (TEER) over 1500 ohm·cm^2, which is one of the highest among the other endothelial district (Kanwar, J.R. *et al.*, 2012). The tightness of BBB is attributed by tight junction and adherent junction interconnecting brain vascular endothelial cells and support of surrounding cells. Adherens junction are protein complexes usually more basal than tight junctions which initiate cell-cell contacts and mediates the maturation and maintenance of the contact (Hartsock, A. and Nelson, W.J., 2008). Cadherin proteins, major transmembrane proteins of adherens junction span the intercellular cleft and linked into the cell cytoplasm via alpha, beta and gamma catenin. The tight junction provides regulation of the paracellular pathway which is composed of at least of 40 different protein complexes (Abbott, N.J. *et al.*, 2010). Although much protein types are present, the major types are the claudins and occludins which directly influence the barrier function spanning the intercellular cleft which are linked to cytoplasmic scaffolds via association with peripheral membrane proteins such as ZO-1 (Abbott, N.J. *et al.*, 2010). The tight junction prevents the passage of small molecules and ions between

cells, so that their passages are through diffusion and active transport (van Meer, G. and Simons, K., 1986). Furthermore, it prevents the movement of integral proteins between apical and basolateral membranes, which divides the membranes of endothelial cells into two distinct sides, thereby each of the surfaces preserves its peculiar function (Vaysse, L. *et al.*, 2000).

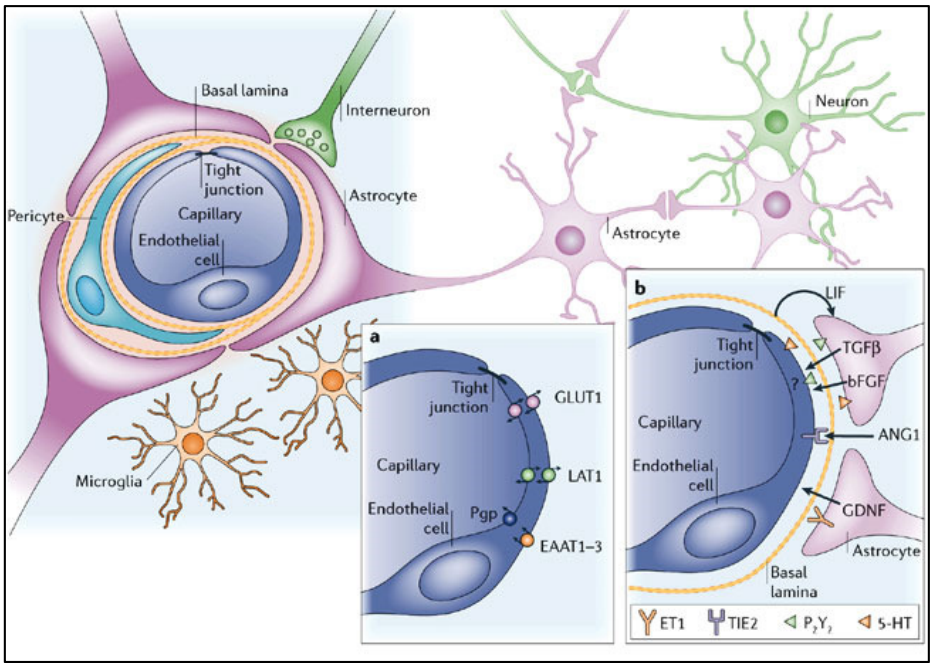

Figure 14. Cellular constituents of BBB (Abbott, N.J. *et al.*, 2006)

(2) Approaches to non-viral gene delivery across the BBB

Potential routes for transport across the BBB are paracellular pathway, passive diffusion, solute carriers, transcytosis and mononuclear cell migration (Abbott, N.J. *et al.*, 2010) (Figure 15).

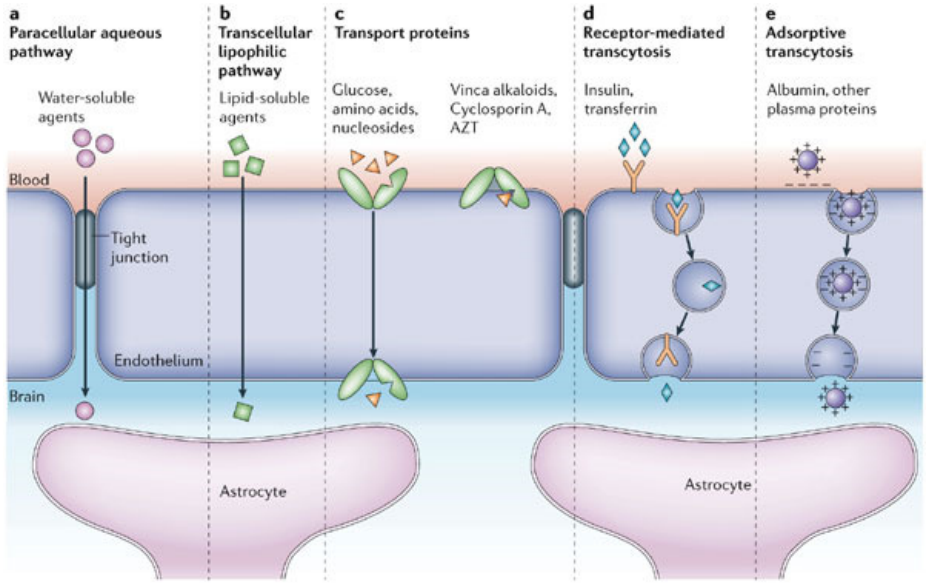

Figure 15. Main routes for molecular traffic across the BBB (Abbott, N.J. *et al.*, 2006). (a) Paracellular transport limited to small water soluble molecules. (b) Diffusion, driven by a concentration gradient, mainly involving small hydropholic molecules. (C) Solute transporter for transport of glucose, amino acids and nucleosides and some therapeutics such as vinca alkaloids, cyclosporine A, and AZT. (D) Receptor-mediated transcytosis for transport nutrient (iron and LDL) and peptidic signaling and regulatory molecules such as insulin, leptin and interleukins. (E) Adsorptive transcytosis mediated by ionic interaction between cationic cargoes and anionic cellular membrane.

Passive diffusion. Passive diffusion is a concentration-dependent

movement of molecules across the cellular membrane without aid of metabolic acid that is divided into paracellular and transcellular diffusion. For transcellular diffusion, factors which limit the transport of BBB are high polar surface area and formation of more than 6 hydrogen bonds which greatly increase the free-energy for movement from aqueous environment to lipid of cell membrane (Gleeson, M.P., 2008). Although passive diffusion of molecules is largely limited, some lipid soluble molecules smaller than 400 Da such as alcohol and can cross the BBB. Majority of non-viral vectors have higher molecular weight or have water solubility in that passive diffusion of non-viral vectors is virtually impossible (Pardridge, W.M., 2010). Even though non-viral vectors are designed to be hydrophobic and small, passive diffusion is not always available owing to ABC transporter which actively export the drugs.

Although paracellular diffusion does not occur easily due to strong tight junction, expansion of intercellular space by drugs or hypertonic solution allows transport of drugs between endothelial cells. Vasoactive agents including peptidase inhibitors, angiotensin II and bradykinins can transiently permeabilize the BBB by decreasing blood pressure (Qin, L.J. *et al.*, 2009). Administration of hypertonic solution including mannitol and urea provide osmosis thereby shrink the size of endothelial cells, which open the tight junction transiently. Such approaches provided the increased central nervous system (CNS) accumulation of drugs in animal model (Neuwelt, E.A. *et al.*, 1984;Salahuddin, T.S. *et al.*, 1988). Nevertheless, transient opening of BBB is associated with the risk of neurological damage because unexpected leakage of molecules, cells and chemicals brings imbalance in strictly controlled CNS

environment.

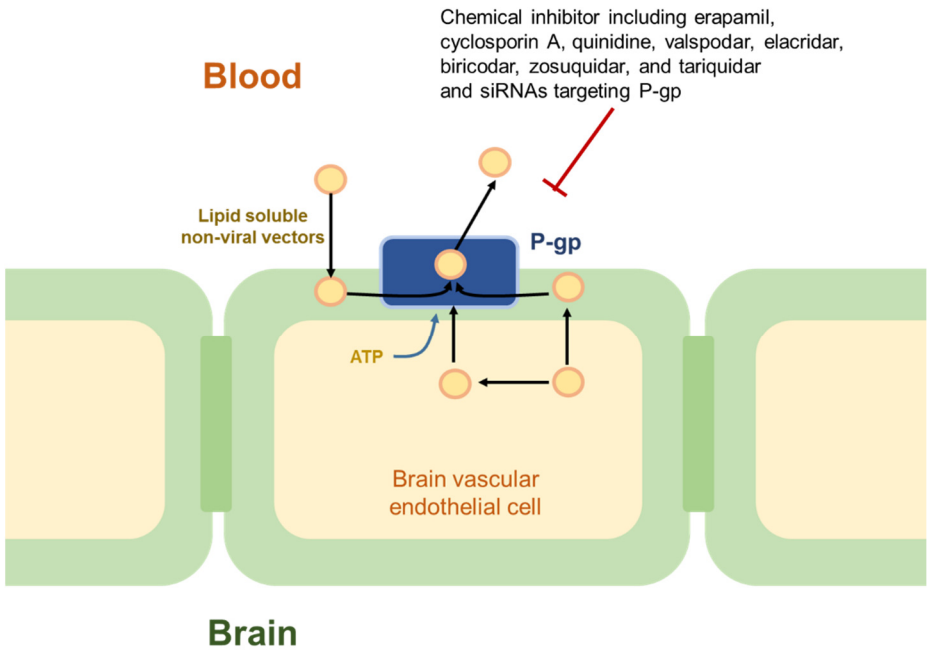

Figure 16. P-gp of brain capillary endothelial cells and pharmacological inhibitors

ABC transporter. Accumulation of lipid soluble drugs in brain is prevented by ABC transporters which has protective role with removal of potentially neurotoxic molecules (Figure 16). Therefore, the strategy of increasing the lipid solubility of drug may be counter-productive because the drugs can be substrates of ABC efflux transporter (Abbott, N.J. *et al.*, 2010). Among the ABC transporter, P-glycoprotein (Pgp, multidrug resistance protein 1) is of significance for efflux of drugs out of brain capillary endothelium in BBB. This drug efflux is circumvented by transporter inhibitor which can be co-delivered with therapeutic genes in nanoparticles. This strategy has been studied for chemotherapy resistant cancer cells and shown useful to overcome

multi-drug resistance (Wong, H.L. *et al.*, 2012). In that sense, transient inhibition of ABC transporter has a potential to be applied for brain drug delivery.

Solute carriers (SLCs). The influx and efflux of essential polar nutrients such as glucose and amino acids are strictly regulated by solute transporters. Most polar molecules are not readily permeate to cellular membrane and transported mainly through solute transporter expressed on the cellular membrane. Because BBB endothelial cells have polarity, location of SLCs determines the orientation of solute transport. For example, GLUT1, a transporter of glucose, is located in luminal and abluminal membrane and thus glucose is transported from blood to brain. On the other hand, SGLT1, sodium-dependent glucose transporter is on the abluminal site whose transport orientation is brain to endothelium (Abbott, N.J. *et al.*, 2010).

Specific BBB SLCs have also been targeted to deliver drugs across the BBB. Xie and coworkers modified liposomes with poly(ethylene glycol) (PEG)s which are covalently linked to cholesterol with glucose. The glucose on the surface of liposomes was recognized by the GLUT1 in the luminal membrane of BBB and successfully delivered the cargoes into CNSs (Xie, F.L. *et al.*, 2012).

Adsorptive transcytosis. Transcytosis provides the main route of macromolecules across the BBB. Although majority of drugs and endogenous molecules are prevented from entering the brain by BBB, some molecules with specific characters enter the brain via transcytosis. This type of transport is

described as movement of molecules uptaken via endocytosis from luminal cell side to the abluminal side where exocytosis occurs. The concept of adsorptive transcytosis was initiated from observation that cationic proteins can bind the endothelial cells and cross the BBB. Ionic interaction between molecules and luminal surface of endothelial cells allows adsorption of molecules to the clathrin-coated or caveolar vesicle membrane. And then clathrin-mediated and caveolar transcytosis provide the potential to mediate endocytosis and to function in transcellular movement of selective molecules.

The adsorptive transcytosis can be easily targeted when designing non-viral vectors. A first possibility is a choosing start material bearing positive charges at physiological pH such as PEI and PAMAM. Most polymeric non-viral vectors are positively charged to form complexes with negatively charged nucleic acids. Although they can facilitate the adsorptive transcytosis across the BBB, non-functionalized cationic non-viral vectors can be easily opsonized during blood circulation and removed by immune cells. As decrease of drug concentration at the luminal surface of BBB allows lesser opportunity to enter the brain, optimization of surface charge is necessary for maximized cellular uptake.

Second possibility is modification of non-viral vectors or nucleic acids with polycationic cell penetrating peptides (CPPs) (Figure 17). CPPs typically have an amino acid composition that either contains a high relative abundance of positively charged amino acids such as lysine or arginine. CPPs covalently or non-covalently coupled to nucleic acids leads them to cross over BBB via adsorptive transcytosis. Gatti and coworkers modified antisense

oligonucleotides with arginine rich CPPs (RXRRBR; R=L-arginine, X=6-aminohexanoic acid, B=beta-alanine) for treatment of neurological disorder, ataxia-telangiecatasia (Du, L. *et al.*, 2011). The antisense oligonucleotides specifically targeted the ATM splicing mutations for restoration of ATM protein close to normal levels. Conjugation of CPPs to antisense oligonucleotides dramatically improved the brain uptake efficiency and ATM splicing correction rates. Not only CPP conjugated nucleic acids, non-viral vectors with CPP modification have potential to cross the BBB and translocate to the nucleus of neuron with protecting the nucleic acids. For example, Qin and coworkers found that the conjugation of liposome with TAT peptide enhanced its brain delivery *in vitro* and *in vivo* via absorptive endocytosis. The majority of TAT-modified liposome accumulated in brain in 24 h after intravenous injection implying that TAT-mediated transport is clinically applicable strategy for brain-targeted gene delivery (Qin, Y. *et al.*, 2011). For bringing the CPP in the field of gene therapy, detailed mechanism of adsorptive transcytosis needs to be identified. Which anionic components are involved in the binding of CPP modified vectors and their intracellular fates during transcytotic trafficking remained unclear. Also, development of brain targeted CPP is urgently required to decrease the dose necessary to obtain therapeutic effect.

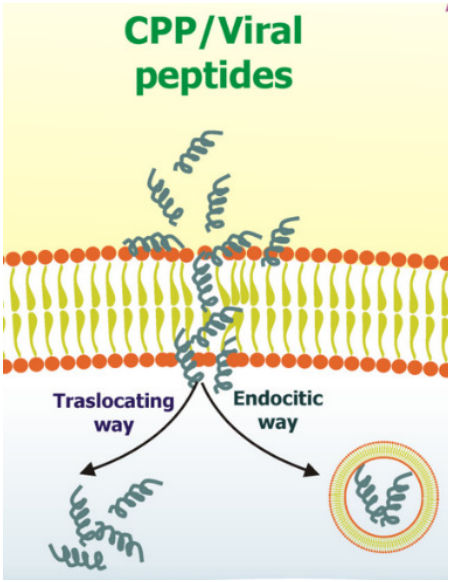

Fig 17. Penetration of CPP via translocating and endocytic way.

Receptor-mediated transcytosis. Receptor-mediated transport is an attractive strategy because of a few advantages: i) circumvention of Pgp efflux transporter in the BBB, brain specificity, unrestricted cargo size (Gan, C.W. and Feng, S.-S., 2010). Receptor-mediated transcytosis is distinct from adsorptive transcytosis at initiation of activation. Receptor-mediated transcytosis is activated by ligand-binding to luminal side receptors distinct from adsorptive transcytosis which is largely dependent on non-specific ionic interaction. The transcytosis starts with uptake either through clathrin-mediated or caveolar endocytosis (Figure 18). Detailed information will be covered in section of intracellular barriers.

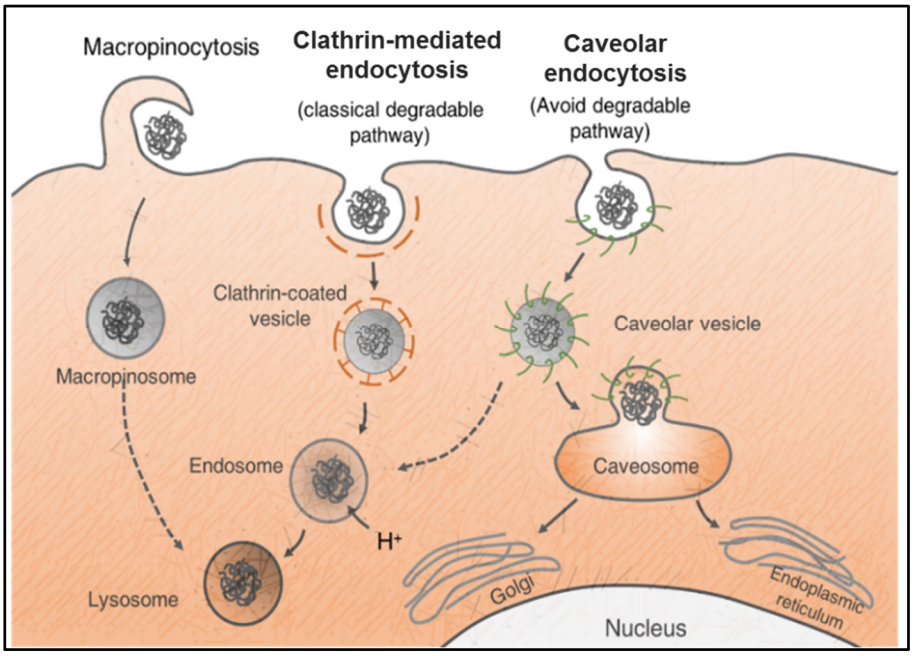

Figure 18. Schematic illustration of endocytosis pathway

Clathrin-mediated internalization is started from binding of a ligand to specific receptor in specialized regions of the plasma membrane, called clathrin-coated pits. Ligand-receptor clusters opsonized by clathrin-coated vesicles form curvature, and pinch off from the plasma membrane. On reaching early endosome, some of receptors are recycled to the membrane and internalized cargos experience drop in pH and further fuse with lysosomes (Hillaireau, H. and Couvreur, P., 2009).

Many pathogens including SV40 internalize the cells using caveolar endocytosis and were delivered to the caveosome of neutral pH in which SV40 can safely move into endoplasmic reticulum or Golgi apparatus. In contrast to the dynamic nature of endosome, caveolae are highly immobile in membrane

and are only slowly internalized when stimulated. With time, some vesicles converge with endosomes and eventually lysosomes like a clathrin-mediated endocytosis pathway and others are delivered to endoplasmic reticulum or Golgi system via a non-degradative pathway. The major difference of caveolar endocytosis with classical clathrin-mediated endocytosis is that some part of cargoes in caveolar vesicles do not experience a drop in pH and follow the nonacidic and nondegradative routes, which determines drug delivery efficiency (Kiss, A.L. and Botos, E., 2009).

Targeting caveolar transcytosis can enhance the drug delivery efficiency across the endothelium *in vivo*. A monoclonal antibody specific to lung-endothelial caveolae directed rapid transcytosis within 10 min (McIntosh, D.P. *et al.*, 2002), implying that targeting caveolar transcytosis has potential overcoming endothelium barrier including BBB.

Identification of properties of drug delivery vehicles that direct their intracellular processing in BBB is important for rationale design of non-viral vector. Georgieva and coworkers demonstrated the surface modification of nanoparticles affected their mode of internalization by brain endothelial cells (Georgieva, J.V. *et al.*, 2011). They investigated intracellular processing of 500 nm gold particles, particles functionalized with PEI or prion protein in an *in vitro* BBB model using metabolic inhibitors. The results suggested that adsorptive endocytosis of nanoparticles modified with PEI and receptor-mediated endocytosis of particles decorated with prion protein were via distinct pathway. Interestingly, they showed that transcytotic potential is higher for the receptor-mediated and caveolar pathways than adsorptive endocytosis. Hence,

exploiting the strategy for rationale design non-viral vector leading receptor-mediated and caveolar pathway is required for enhanced penetration of BBB.

Among the receptors of BBB, the transferrin, insulin receptor and low-density lipoprotein are the most widely studied for brain targeted drug delivery. Transferrin receptor is a transmembrane glycoprotein and highly expressed on immature erythroid cells, rapidly dividing cells, hepatocytes and endothelial cells of the BBB. The role of transferrin receptor is transporting iron into the brain which is bound to transferrin. Although controversy, some studies have reported that most of the transferrin were able to cross over BBB without undergoing intraendothelial degradation. As a result, various transferrin-conjugated nanoparticles of liposome (Visser, C.C. *et al.*, 2005), poly(lactic acid) (Gan, C.W. and Feng, S.-S., 2010;Ren, W.-h. *et al.*, 2010), polyamidoamine dendrimer (Huang, R.-Q. *et al.*, 2007) and human serum albumin (Ulbrich, K. *et al.*, 2009) were suggested as brain targeted drug delivery system. Huang et al. conjugated the transferrin to PAMAM via bifunctional PEG for non-viral gene delivery to the brain. This vector showed 2.25-fold higher brain uptake efficiency and ~2-fold higher transfection efficiency compared to unmodified PAMAM and PAMAM-PEG *in vivo* (Huang, R.-Q. *et al.*, 2007). Although some study suggests that transferrin receptors are almost saturated in physiological condition (de Boer, A.G. and Gaillard, P.J., 2007), transferrin seems to be performant in directing nanoparticles to cross over BBB.

Apolipoprotein is a 34 kDa protein of high-density lipoprotein and very low-density lipoprotein which transport cholesterol in the plasma and CNS.

Lipoprotein receptors expressed on BBB recognize the apolipoprotein and uptake them into endothelial cells. Taking into consideration that low density lipoprotein receptor-related protein 1 (LRP1) and 2 (LRP2) are able to cross over BBB, they have been utilized for brain targeted drug delivery. For example, Ke and coworkers functionalized PEG-PAMAM dendrimers with LRP1 as ligand for brain-targeting gene delivery. They were observed to be internalized by brain capillary endothelial cells *in vitro* through clathrin- and caveolae-mediated endocyotosis and highly accumulated in brain than unmodified one (Ke, W. *et al.*, 2009). Carbon nanotube conjugated with LRP2 also showed ability to reach glioma cells *in vivo* (Xie, F.L. *et al.*, 2012). Nanoparticles coated with polysorbate 80 had been successfully used for brain delivery of drugs *in vivo*. Afterward it was found that polysorbate 80 coated nanoparticles adsorb apolipoproteins in the bloodstream and undergo receptor-mediated transcytosis via interaction with lipoprotein receptors (Kreuter, J. *et al.*, 2002).

Recently, rabies virus glycoprotein (RVG), 29-amino acids derived from RVG peptide of rabies virus is widely utilized as BBB transporting and neuronal cell targeting ligand (Figure 19). The receptor of RVG was suggested as nicotinic acetylcholine receptor (AchR) and other components of the cell membrane such as gangliosides. Kumar and colleages synthesized a chimaeric peptide by adding nonamer arginine residues at C-terminal of RVG peptide (RVG-9R) to enable siRNA binding (Kumar, P. *et al.*, 2007). Intravenous administration of RVG-9R efficiently delivered siRNAs protecting against fatal viral encephalitis in mice. Also they confirmed that repeated administration did not induce the inflammatory cytokines or antibodies. RVG conjugated to PEG-

PAMAM (Liu, Y. *et al.*, 2009), PEI (Son, S. *et al.*, 2011), Pluronic-based nanocarrier (Kim, J.Y. *et al.*, 2013) and exosomes (Alvarez-Erviti, L. *et al.*, 2011) showed enhanced accumulation of therapeutic genes *in vivo*. Although infection route of rabies virus is well recognized, BBB penetration mechanism of RVG peptide remain unanswered. Further research on transcytosis mechanism of RVG peptide is urgently needed for improved modification of non-viral vector.

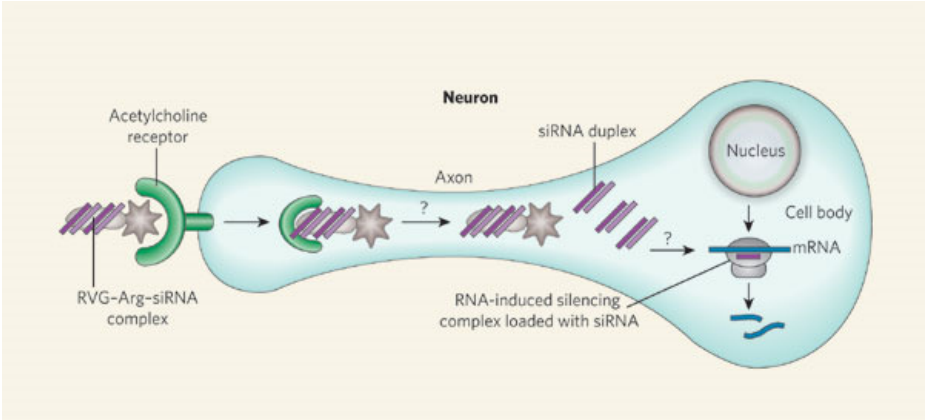

Figure 19. Binding and uptake of RVG peptide-conjugated siRNA by neuronal cells (Cantin, E.M. and Rossi, J.J., 2007)

2) Reticuloendothelial system (RES) recognition

In other to condense anionic nucleic acids, most non-viral vectors have positive charge. The cationic charges of vectors not only aid penetration of BBB via adsorptive transcytosis and entering the target cells but also promote the non-specific interaction with anionic serum protein. The process of opsonization is one of the most important biological barriers, making it more visible to phagocytic cells (Nie, S., 2010). After opsonization by serum proteins, nanoparticles are recognized as foreign materials and captured by phagocytic cells. The engulfed nanoparticles are eventually disrupted and removed from bloodstream. Furthermore, binding sites of ligands which are shielded by serum protein cannot be recognized by specific receptor inhibiting receptor-mediated transcytosis. The opsonization rates of nanoparticles largely depend on their surface properties such as charge and hydrophobicity. In that sense, surface modification by PEG or hydroxyl group is an important strategy to increase colloidal stability of nanoparticles by blocking nonspecific interaction with serum protein (Nie, S., 2010).

Although PEGylation is one of the most effective strategy for enhancing biodistribution of non-viral vector, it may reduce the potential of cellular uptake by shielding surface charge. To solve the PEG dilemma, enzyme-sensitive or pH-sensitive linkers can be applied to conjugate PEG, which regulates the PEG shedding upon reaching the target cells (Guo, X. and Szoka, F.C., Jr., 2001;Walker, G.F. *et al.*, 2005). However, difficulty in control of PEG shedding rate limits the application of the strategy in brain gene therapy owing to absence of considerable change in pH and enzyme in BBB environment. As an

alternative, targeting ligands can be introduced on the nanoparticle surface to enhance the cellular uptake of PEG-conjugated carriers. For example, Son et al. conjugated RVG29 ligand to bioreducible PEI using bi-functional PEG to deliver DNA in the brain, which showed higher serum stability as well as brain targeted gene delivery efficiency (Son, S. *et al.*, 2011).

4. Intracellular barriers for brain-targeted gene delivery

The sites in which nucleic acids can activate are intracellular organelles - nucleus for DNA and cytoplasm for small interference RNA. Thus, non-viral vectors must cross over the plasma membrane and nucleic acids should be released from vectors and then safely reach the target sites. Intracellular barriers includes cytosolic degradation, non-specific cellular uptake, poor endosomal escape and inadequate vector unpacking (Khalil, I.A. *et al.*, 2006). Most of nanoparticles cannot readily cross over plasma membrane due to their size and hence they are internalized by endocytosis. In the process of endocytosis, nanoparticles are surrounded by plasma membrane and bud off to the inside cells to form trafficking vesicles (Ziello, J.E. *et al.*, 2010). Depending on the uptake mechanisms, the vesicles tend to fuse with lysosomes or avoid it, which determine the gene delivery efficiency. Recently, targeting of specific endocytosis pathway is becoming a promising strategy on the concept of regulating intracellular fate of therapeutic genes. Therefore, rationale design of non-viral vector requires understanding of both intracellular trafficking mechanism and characteristics of vector material.

1) Protection and release of genes in cytosol

It has been shown that naked DNAs delivered by microinjection into cytoplasm become degraded by cytosolic nuclease. This result implies that direct delivery of nucleic acids is not adequate because they are exposed to harsh environment in cytosol. Although non-viral vectors protect nucleic acid degradation by cytosolic nuclease for a while, inadequate release of genes from

non-viral vector is another problem. Thus, optimization of release of nucleic acids from non-viral vector is able to maximize the gene delivery efficiency.

2) Intracellular trafficking in endocytosis pathways

Cells uptake large molecules that otherwise would be impermeable to cellular membrane through 'endocytosis'. Endocytosis pathways important in gene delivery fall into three categories: clathrin-mediated endocytosis, macropinocytosis, and caveolae-mediated endocytosis (Hillaireau, H. and Couvreur, P., 2009) (Figure 20).

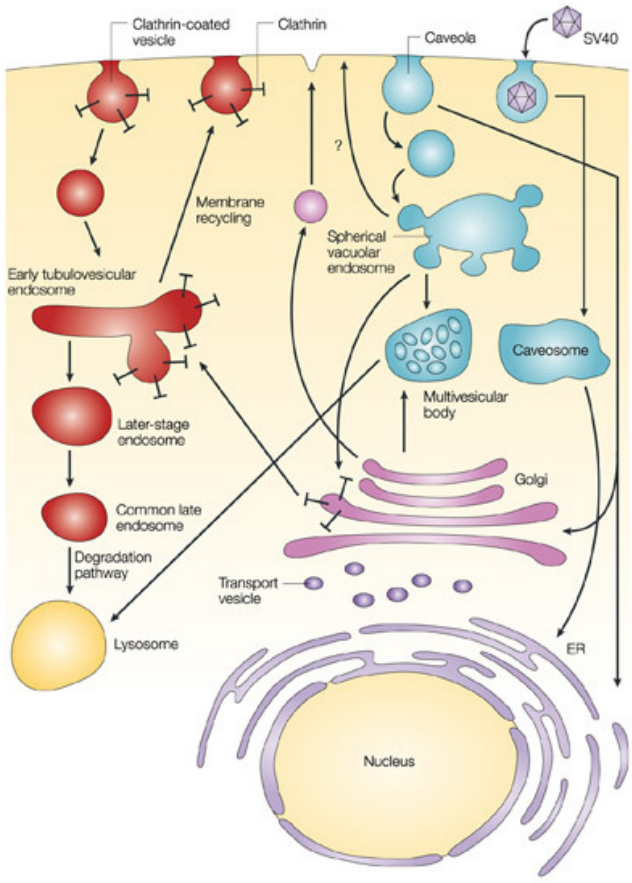

Figure 20. Intracellular trafficking of clathrin-mediated and caveolar endocytosis.

Clathrin-mediated endocytosis delivers cargo into lysosome without endosomal escape. Alternatively, molecules can be internalized by caveolae vesicles. Viruses such as SV40 are internalized by caveolae using a slower mechanism (2–3 h) to caveosomes, then are subsequently transported to the ER. It is also possible that caveolae could traffic directly to the ER or Golgi (Carver, L.A. and Schnitzer, J.E., 2003).

(1) Endocytosis pathways

Clathrin-mediated endocytosis. The first step of clathrin-mediated endocytosis is strong binding of ligand to specific receptor concentrated in specialized regions of the plasma membrane, called clathrin-coated pits. It was shown that formation of clathrin-coated pits is initiated through the nucleation of FCHo proteins which bind phosphatidylinositol-4,5-bisphosphate rich zones, various scaffold proteins and intersectin which promote cell membrane curvature, followed by recruitment of adaptor protein 2 (AP2). AP2 recruits several receptors to promote the clathrin coat assembly in hexagons and pentagons. The GTPase dynamine recruited at the neck of vesicles induces the membrane scission with aid of the polymerization of actin machinery. Finally, Auxilin or cyclin G-associated kinase (GAK) recruits the heat shock cognate 70, which diassembles clathrin pit and produces an endocytic vesicles containing the cargo molecules (Figure 21).

After they enter the early endosome, they are either recycled back or are degraded in late endocome/lysosome. On reaching early endosomes, some of receptors are recycled to the membrane and internalized genes experience drop in pH and enzymatic degradation following classical endocytic pathway. Therefore, endosomal escape became a big challenge as most of cationic

polymers follows the adsorptive and clathrin-mediated endocytosis.

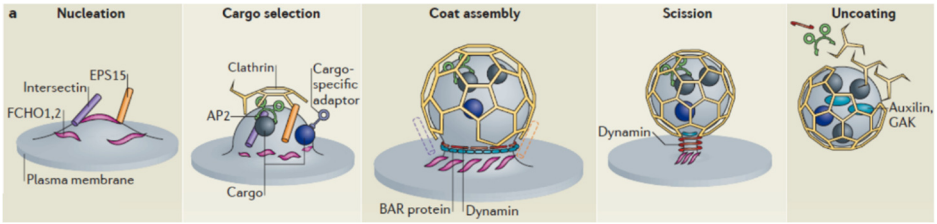

Figure 21. The clathrin-coated vesicle cycle (McMahon, H.T. and Boucrot, E., 2011)

Caveolar endocytosis. Distinct from the classical clathrin-mediated endocytosis, non-clathrin-mediated endocytosis have been identified. For example, the uptake of SV 40, cholera-toxin B subunit, interleukin-2 receptor beta is not inhibited by removal of clathrin-coated fit but sensitive to cholesterol depletion (Figure 22). Caveolae are morphologically identified as flask like invagination on plasma membrane containing sphingolipid, cholesterol and caveolin proteins which play important role in these pathway, forming distinct intracellular vesicles. The caveolae endocytosis is compared with the clathrin-coated vesicle pathway in their delivery of molecular cargo to the Golgi, endoplasmic reticulum and lysosomes (Figure 20). Caveolar endocytosis is initiated from formation of invagination followed by the fission at the neck of the invagination. Caveolae vesicles are formed in lipid-rafts through ATP-, GTP-, and Mg^{2+} dependent polymerization of caveolin-1 and 2 (Schnitzer, J.E., 2001). Although non-viral vectors bind to the membrane, some factors triggering signal transduction cascade are required to lead local protein tyrosine phosphorylation and de-polymerization of cortical actin cytoskeleton. Actin monomers are recruited to the caveolae following dynamin recruitment to neck

of caveolae vesicles. Dynamin pinches off the vesicles from the membrane into the cytosol (Kiss, A.L., 2012).

The major difference of caveolar endocytosis with classical clathrin-mediated endocytosis is that some part of cargoes in caveolar vesicles do not experience a drop in pH and follow the nonacidic and nondegradative routes, which determines drug delivery efficiency (Kiss, A.L. and Botos, E., 2009). Rejman and coworkers investigated the effect of uptake pathway on transfection efficiency and found that non-viral vectors uptaken by clathrin-mediated endocytosis are targeted to lysosomal compartment, while vectors taken up by caveolar endocytosis largely avoid lysosomal fusion permitting efficient transfection (Rejman, J. *et al.*, 2005). These results imply that strategy of targeting caveolae is promising to achieve better transfection efficiency.

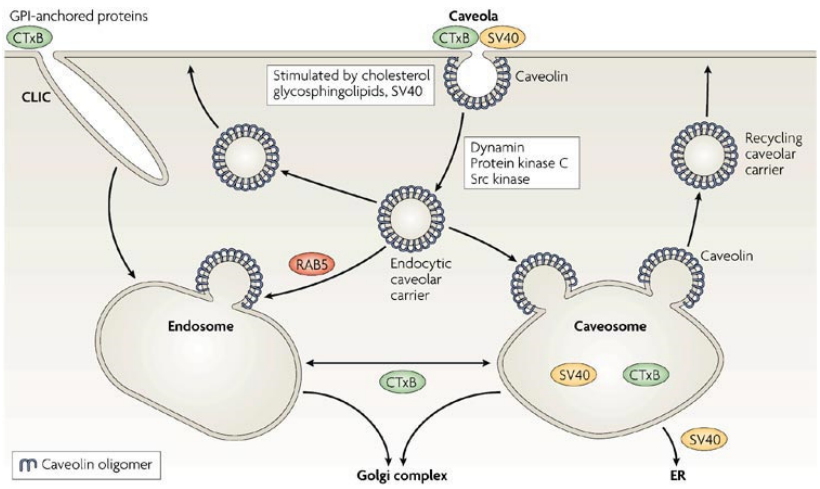

Figure 22. Cellular trafficking of caveolar endocytosis (Parton, R.G. and Simons, K., 2007)

Macripinocytosis. Macropinocytosis is actin-dependent fluid phase process which uptakes relatively solutes or large materials in close proximity to the cell membrane (Yeo, Y., 2013). In general, relatively large macromolecules enter cells through macropinocytosis, whereas smaller molecules are taken up by clathrin- or caveolar endocytosis. After actin filament-driven ruffling of plasma membrane uptake molecules, it is folded and pinched off of irregular sized vesicle, macropinosome. This process is largely dependent on on PI3K and Rho GTPase activities which regulate actin reorganization (Medina-Kauwe, L.K. *et al.*, 2005). Macropinosome undergos a process of maturation by increasing expression of Rab7 and fused with lysosomes where the contents are degraded (Yeo, Y., 2013).

(2) Factors affecting the regulation of cellular uptake by polymeric gene carriers

The development of an ideal polymeric gene carrier that is able to overcome intra- and extracellular barriers will be very challenging without the careful consideration and modification of physical, geometrical, chemical and biological properties of the carriers. Structural modification should be used in order to add such functional properties to polymeric gene vectors. To apply this concept to polymeric carrier design, this section investigates various potential systems which regulate uptake and intracellular pathways by providing physical, geometrical, chemical or biological signaling to cells (Figure 23).

Physical cues. Physical cues are physical stimuli provided by gene carriers

which trigger the regulation of cellular uptake. Osmotic activity is one of the most essential factors in regulating and improving cellular uptake. Cho and coworkers synthesized the poly(sorbitol-co-PEI) by crosslinking of LMW PEI with non-ionic osmolytes such as sorbitol to confer the osmotic activity in non-viral vector. They confirmed that osmotically active non-viral vector selectively stimulated cavaeolae endocytic pathway, which played important role in high transfection efficiency (Luu, Q.P. *et al.*, 2012). Also, they found that induction of regulatory molecules such as COX-2 (a molecular factor that augments cellular uptake process) in response to hyperosmotic activity (Islam, M.A. *et al.*, 2011). Hence, establishment of optimum osmotic potential can be a worthwhile subject for employment of 'physical cue' strategy in design of successful gene carriers.

Geometrical cues. The cellular membranes and endocytic machineries have well defined flexibilities and geometries which regulate or restrict the cellular uptake depending on the geometrical characteristics of gene carriers. Therefore, investigation into finding a suitable particle size and shape could be very useful for effectively regulating uptake pathways and achieving high transfection efficacy. It is widely known that the particles in the range of 500 nm in diameter are trafficked slowly via a non-digestive caveolar endocytosis whereas smaller particles are easily taken up by clathrin-mediated endocytosis (Rejman, J. *et al.*, 2004). Some recent studies also have found that particle shape is an important factor to control cellular uptake depending on time and the complexity of actin structure that form the curvature to uptake them. Non-spherical shaped nanoparticles such as rod-, worm- and UFO-like particles have

shown accelerated internalization depending on cell types (Karaman, D.S. *et al.*, 2012). Elucidating the mechanism of controlled-shape nanoparticles on cellular uptake and interdependent role of the size, shape and other factors will allow more elaborate control of uptake routes relying on geometrical cues.

Chemical cues. The manipulation of chemical cues such as specific ligands, CPP and the amphipathicity of gene carriers can also regulate the endocytic pathway. Surface modification with specific ligands, known as receptor-mediated endocytosis, has been regarded as an important way to guide the internalization of a gene carrier via defined endocytosis pathways. The conjugation of CPPs onto gene carriers enables efficient cellular delivery by both direct penetration and endocytosis pathways independently to membrane receptors and cell types (Madani, F. *et al.*, 2011). The uptake mechanism of gene carriers can be controlled with the physiochemical features of the CPPs. Beyond the traditional methods for providing chemical cues as described above, controlling the surface amphipathicity of gene carrier represents a new strategy allowing the gene carrier to slip inside without membrane disruption (Fernandez-Carneado, J. *et al.*, 2004).

Biological cues. Biological cues such as microenvironments, types of targeted cells, cell cycles and cellular polarization are key points to consider for designing polymeric gene carriers (Kong, H.J. *et al.*, 2005;Mennesson, E. *et al.*, 2005;Dhaliwal, A. *et al.*, 2010). Although biological cues largely affect the cellular uptake mechanism, it is quite difficult to control and manage to bring them in clinical application. Instead, knowledge of the biological cues could be an effective tool for controlled gene delivery. Since the stimulation of cellular

uptake is also relying on the interaction between specific extracellular matrix (ECM) and cells, consideration of the microenvironment of target cells will be useful in the design of suitable gene carriers (Kong, H.J. *et al.*, 2005). By applying this stimulation into cellular uptake machineries (depending on cell types, cell cycles and cellular polarization), a well-developed uptake mechanism could be deliberately targeted for the purpose of effective gene transfer.

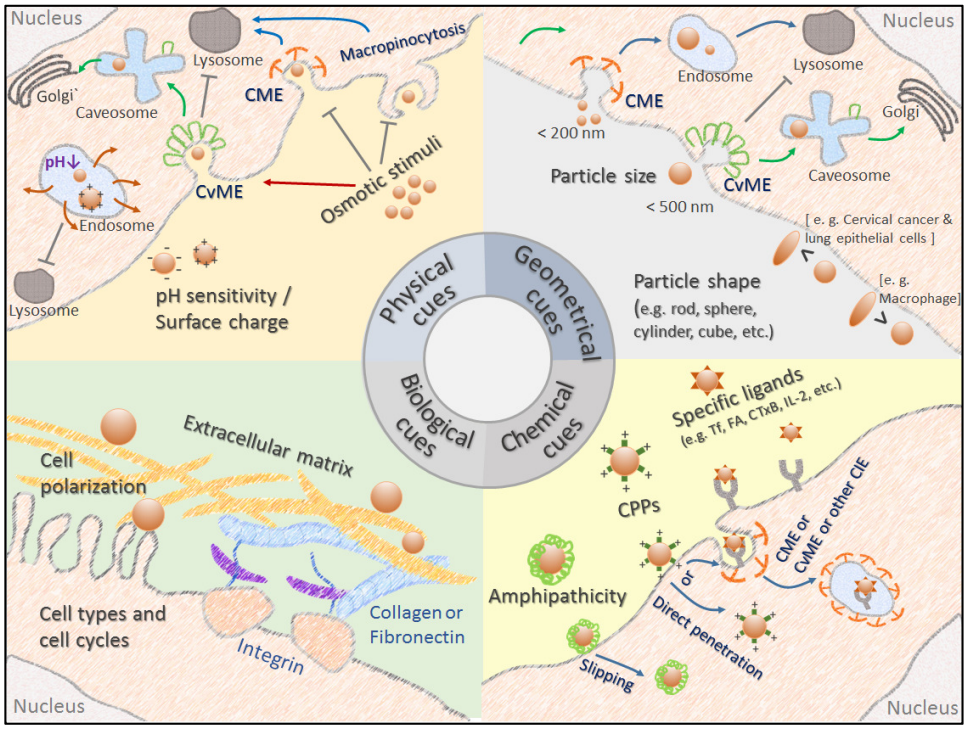

Figure 23. Schematic illustration on factors affecting the regulation of cellular uptake and endocytic trafficking by polymeric gene carriers. CME: clathrin-mediated endocytosis; CvME: caveolae-mediated endocytosis.

5. AD: pathogenesis and neuropathology

AD is the most common form of dementia. In 2009, 36 million cases were recorded worldwide and the number of cases will be more than doubled by 2050 reflecting an aging population (Minati, L. *et al.*, 2009). There is no cure for the disease, which worsens as it progresses, and eventually leads to death. Since AD brings not only the impact on the lives of patient, but also psychological and economical burden on caregiver, it became the greatest health care challenge of modern history (Minati, L. *et al.*, 2009).

The hall marks of brain of patient with AD are amyloid-beta (Aβ) plaque and neurofibrillary tangles (NFTs) composed of abnormally phosphorylated tau protein. The progression of Aβ plaque and NFT throughout the brain are closely correlated with AD progression and loss of synapses (Querfurth, H.W. and LaFerla, F.M., 2010). AD exists in familial form which accounts for 5% of cases and sporadic form as majority of AD cases. Mutation on two genes encoding amyloid precursor protein (APP), presenilin-1 (PS1) or PS2 and one gene tau-encoding microtubule-associated protein tau (MAPT) (Ittner, L.M. and Gotz, J., 2011) causes familial forms of AD. Sporadic AD is associated with polymorphisms of apolipoprotein E4 (APOE4), insulin-degrading enzyme (IDE) which is active in the degradation of Aβ or ubiquilin-1 (UBQLN1) which affects intracellular APP trafficking.

The amyloid cascade model formed the current understanding of pathogenesis of AD. The step-wise cleavage of cell surface receptor APP results in formation of 39-42 amino acid peptide Aβ. As shown in Figure 23, APP is

cleaved by both α-secretase and β-secretase releasing soluble extracellulr fragments. Cleavage by β-secretase leaves β-CTF which produces Aβ through subsequent cleavage by γ-secretase while α-secretase cleavages takes place within the Aβ region, preventing Aβ production. Both pathways occur in normal metabolism, however, the increased β-secretase activity and decreased α-secretase are observed in sporadic AD. Aβ40 and Aβ42 are common product of β-secretase and γ-secretase. Aβ42 is prone to aggregation, giving rise to toxic species of oligomers and fibrils affecting synapse function while Aβ40 is less neurotoxic. An imbalance between production and clearance causing fast accumulation of Aβ42 is regarded as initiating factor of AD. Oligomer Aβ disrupts the release of presynaptic neurotransmitters and postsynaptic glutamate receptor ion current by facilitating endocytosis of *N*-methyl-D-aspartate surface receptor and α-amino-3-hydroxy-5-methyl-4-isoxazole propionic acid surface receptor, which results in impairment of synaptic plasticity by altering the balance between long-term potentiation and long-term depression and reduction of dendrite spine. Clinical trials of β-secretase and/or γ-secretase inhibitor, aggregation blocker, vaccination of Aβ, and antibodies against epitope are in progress.

Neurofibrillary tangles aggregates of insoluble hyperphosphorylated tau proteins (Figure 25). In normal condition, tau in axons promotes the assembly and stability of microtubules and vesicle transport. It is generally believed that altered ionic homeostasis and oxidative stress following accumulation of Aβ cause the imbalance between phophatase and kinase regulating phosphorylation

of tau protein (Querfurth, H.W. and LaFerla, F.M., 2010). Although mechanism of tau neurotoxicity is unclear, evidences have shown that tau is essential for NMDA dependent postsynaptic dysfunction by Aβ (Ittner, L.M. *et al.*, 2010). Also, the accumulation of hyperphophorylated tau unbinds from the microtubules and accumulates in perykaria and dendrites, leading to neurodegeneration (Minati, L. *et al.*, 2009). Although counteracting these changes are not available, inhibitors of Aβ and tau aggregation are under way.

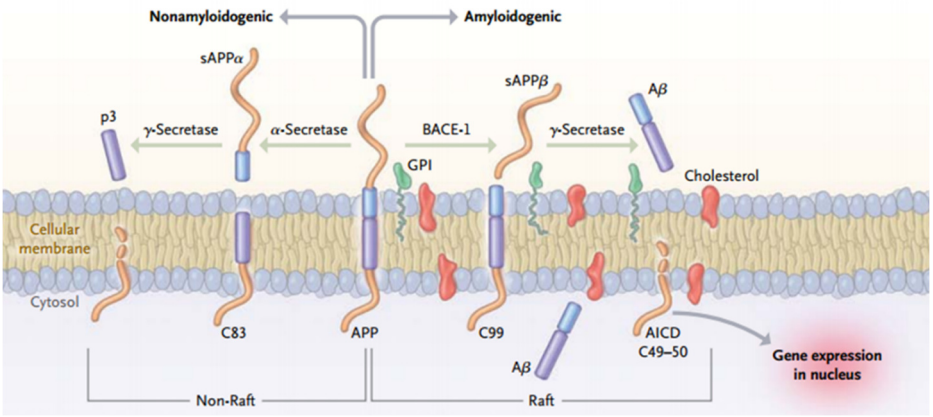

Figure 24. Processing of amyloid precursor protein. Cleavage by α-secretase initiates nonamyloidogenic processing. sAPPa ectodomain is released leaving an 83-residue C-terminal fragment which is subsequently cleaved by γ-secretase releasing non-toxic protein p3. Cleavage by β-secretase initiates the amyloidogenic processing. Retained C99 is cleaved by γ-secretase generating Aβ and AICD. AICD is released into cytoplasm and activates signal transcription. Aβ prone to aggregate forming Aβ plaques. Reproduced with permission from (Querfurth, H.W. and LaFerla, F.M., 2010), Copyright Massachusetts Medical Society.

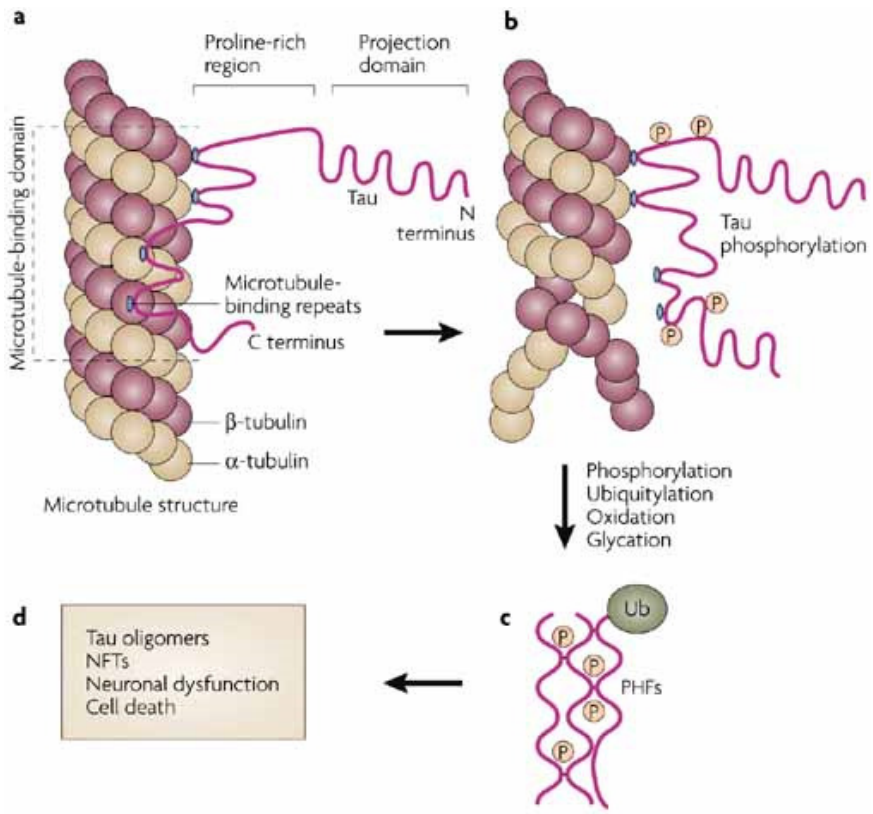

Figure 25. Tau structure and phosphorylation. (a) Six tau isoforms exist in human brain tissue. Among them, three have three binding repeats and the other three have four binding repeats separated by flexible linkers stabilizing microtubule structure. (b) Hyperphosphorylation by certain affinity-regulating kinases, including GSK3beta, CDK5 and ERK2 tends to flank the microtubule-binding repeats, which results in destabilization of microtubules. (c) Tangles are formed by aggregation of hyperphosphorylated and accumulated in paired helical filaments (PHFs). (d) Proteolytic processing leads to the formation of tau oligomers and insoluble aggregates called NFTs (Mazanetz, M.P. and Fischer, P.M., 2007).

Chapter 1. Selective stimulation of caveolae-mediated endocytosis by an osmotically active poly(mannitol-co-PEI) gene transporter

1. Introduction

Gene therapy is a promising therapeutic strategy that addresses a medical problem at its source. Successful gene therapy relies on the development of a safe vector that efficiently delivers genes into cells (Edelstein, M.L. *et al.*, 2007). Given the immunological and potential mutational disadvantages of viral vectors, research on non-viral vector systems has become important in gene delivery. Among the non-viral vectors, PEI, a cationic polymer, is widely used in gene delivery as a golden standard. The positive surface charges of PEI condense DNA into small particles, bind to negatively charged receptors of the cell membrane, and are internalized by endocytosis. PEI also has the capacity to escape from endosomes through a unique “proton sponge mechanism” to avoid lysosomal degradation of the DNA (Thomas, M. and Klibanov, A.M., 2003).

However, PEI is still far from being clinically ideal because of its cytotoxicity and low-transfection efficiency compared to viral vectors (Li, S. and Huang, L., 2000). PEI has been extensively modified in an effort to improve those disadvantages. One approach to improve the cytotoxicity without reduction of transfection activity is crosslinking LMW PEI through biodegradable disulfide or ester bonds (Arote, R.B. *et al.*, 2008;Koo, H. *et al.*, 2010;Li, S. *et al.*, 2011). Also, to improve transfection efficiency, several

biological barriers must be overcome. For effective traverse of the plasma membrane, introduction of ligands such as folic acid or cell-penetrating peptides have been successfully used (Nguyen, J. *et al.*, 2008). Beyond the endothelial barrier, using hypertonic osmolytes such as sucrose, sorbitol and mannitol have been described (Doran, S.E. *et al.*, 1995;McCarty, D.M. *et al.*, 2009). Recently, targeting certain uptake pathways has become a promising strategy for increasing the efficiency of non-viral vectors since it is becoming apparent that the intracellular fate of nanoparticles is closely linked to their pathway of entry into cells (Khalil, I.A. *et al.*, 2006;Rejman, J. *et al.*, 2006).

The endocytosis mechanism of nanoparticles falls into two broad categories: the well-characterized clathrin-mediated pathway and non-clathrin-mediated endocytosis (Le Roy, C. and Wrana, J.L., 2005). The clathrin-mediated pathway follows the classical endocytic route, which carries nanoparticles into the endosome, which fuses with the lysosome followed by enzymatic degradation. In contrast, in the non-clathrin-mediated pathway, caveolae-mediated endocytosis leads internalized molecules to nonacidic and nondigestive routes (Ferrari, A. *et al.*, 2003). Also recently, particles taken up by caveolae-dependent pathway were shown to be delivered to caveosomes with a neutral pH or the early endosome, which does not fuse with the lysosome (Pelkmans, L. and Helenius, A., 2002). As one of the critical goals for non-viral vectors is efficient delivery of transgenes to nucleus or cytoplasm, targeting caveolae-mediated uptake was described as advantageous.(Dokka, S. and Rojanasakul, Y., 2000;Rejman, J. *et al.*, 2005;Chung, Y.C. *et al.*, 2011) Caveolae, a special type of lipid raft, are generally immobilized at the plasma membrane by the

actin cytoskeleton. However, internalization can be stimulated by certain ligands (Kiss, A.L. and Botos, E., 2009) or cellular stress (Kang, Y.S. *et al.*, 2000). Stimulation of caveolae trafficking is mainly described as occurring by ligand-receptor binding. For, PEI modification with ligands such as folic acid and the Tat peptide have been used (Moulton, H.M. *et al.*, 2003;Kurosaki, T. *et al.*, 2011).

Interestingly, according to a recent report, hypertonic exposure of alveolar cells caused down-regulation of clathrin and fluid-phase endocytosis while stimulating caveolar endocytosis (Wang, S. *et al.*, 2011). These endocytic responses are supported by a previous report that cellular osmotic stress induces phosphorylation of caveolin-1 protein by Src-kinase activity, which is essential for budding and pinching off from the membrane. Hypertonic solutes were used as non-ionic osmolytes with multi-hydroxyl groups such as sorbitol and mannitol that did not penetrate the plasma membrane (Volonte, D. *et al.*, 2001). Non-penetrating osmolytes tend to draw water from the intracellular space through an osmotic gradient, cause cell hypertonic stress accompanied by cell shrinkage. As endocytic transport and signal transduction for homeostasis are tightly coupled in caveolae (Kiss, A.L. and Botos, E., 2009). This implies that gene delivery through the use of hypertonic stress might be a new strategy. Based on this, I hypothesized that polyol-based gene transporter can stimulate and target caveolae endocytic pathway for efficient gene delivery. Among the polyol osmolytes, mannitol, which has long been used in routine medical applications (Nilsson, H. *et al.*, 2007;Hinson, H.E. *et al.*, 2011), was employed as backbone of a new gene transporter.

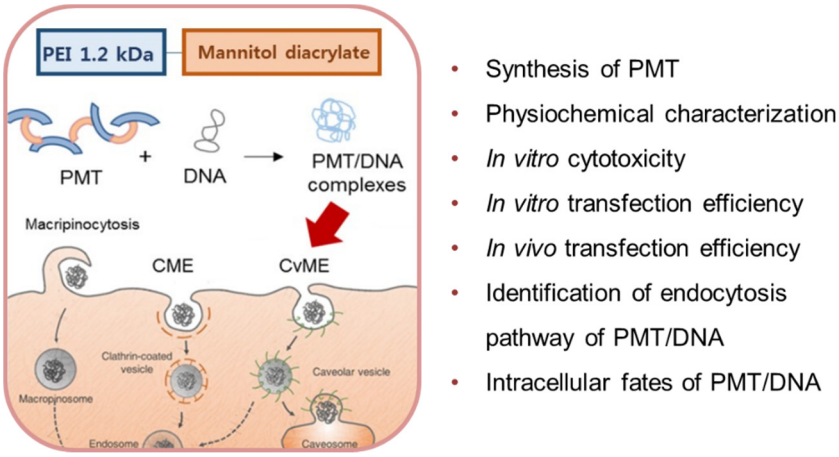

Figure 26. Experimental flow of the study 1

2 Materials and methods

1) Materials

Branched PEI (BPEI) (Mn: 1200 Da and 25 kDa), dimethylsulfoxide (DMSO), D-mannitol, tetrazolium (MTT) reagent, dimethylformamide (DMF), pyridine, bafilomycin A1, chloropromazine (CH), genestine (GE), methyl-beta-cyclodextrin (M-β-CD), wortmannin (WO) were purchased from Sigma (St. Louis, Mo, USA). Luciferase reporter assay for *in vitro* transfection study and pGL3-control vector with SV-40 promoter, and enhancer encoding firefly (*Photonus pyralis*) luciferase and PureYield plasmid maxiprep System for plasmid purification were purchased from Promega (Madison, WI, USA). tGFP (turbo GFP) which has the green fluorescent protein (GFP) gene were from Origene (CA, U.S.A.). A competent *Escherichia coli* strain, JM109, was used for amplification of plasmids. The concentration of purified DNA was determined at 260 nm UV absorbance. Roswell Park Memorial Institute (RPMI)-1640 culture medium, Dulbecco's modified Eagle's medium (DMEM), fetal bovine serum (FBS) and penicillin/ streptomycin were from HyClone (Logan, Utah). Minimum essential medium alpha (MEM alpha) medium was from GibcoBRL (Merelbeke, Belgium). Phospho-caveolin-1 (Tyr14) IgG (rabbit polyclonal antibody) was from Cell Signaling Technology (Danvers, MA, U.S.A.). Actin IgG (rabbit polyclonal Antibody) and goat anti-rabbit IgG-HRP were from Santa Cruz Biotechnology (U.S.A).

2) Synthesis of mannitol diacrylate and PMT

Mannitol diacrylate (MDA) was prepared by reaction of mannitol and

acryoyl chloride. Briefly, 1 g of anhydrous mannitol was dissolved in 30 ml DMF in the presence of 10 ml pyridine solution. After stirring for 30 min, acryloyl chloride dissolved in 7.5 ml DMF was added drop wise. The reaction was done for 24 h at 4 C. After precipitation with diethyl ether, MDA was dried overnight at room temperature. Poly(mannitol-co-PEI) (PMT) was synthesized with mannitol diacrylate and BPEI (1200kDa) by Michael addition reaction. MDA (Mn: 290) dissolved in anhydrous DMSO was dropped into the BPEI DMSO solution at a molar ratio of 1 : 1. For the Michael addition reaction, the stirring was continued at 80 C for 24 h with N_2 bubbling. The reaction mixture was dialyzed using dialysis membrane (MW cut off 3,500) at 4 C for 24 h. The dialyzed polymer solution was lyophilized for 3 days.

3) Characterization of PMT

PMT was characterized by ^{1}H high resolution NMR Spectrometer (AVANCE 600, Germany, Bruker - 600mHz) to estimate the composition of PEI in PMT. Molecular weight of PMT was measured using a gel permeation chromatography column (GPC) with TSKgel G5000PWxl-TSKgel • G3000PWxl-C. The Column temperature was kept at 35 C with a flow rate of 1.0 ml/min and 0.1 M $NaNO_3$ was used as the mobile phase.

4) Measurement of particle sizes and zeta-potential

Particle size and zeta-potential of nanoparticles were measured using a dynamic light scattering spectrophotometer (DLS) (Otsuka Electronics DLS-7000). To measure nanoparticle sizes, PMT/DNA complexes were made at various N/P ratios (5, 10, 15 and 20) with 80 μg pGL3 for each in 2 ml of total

volume. The particle sizes of the complexes were examined in the presence of serum percentages (0, 10, 20 and 30%) at an N/P ratio of (5, 10, 15 or 20). The surface charge of the complexes of PMT/DNA complexes was measured with a 20 degree scattering angle at 25 C.

5) Gel retardation assay

Gel retardation assay was carried out with a common gel electrophoretic technique. Agarose gels were casted with 1% agarose dissolved in Tris-acetate-EDTA (TAE) buffer. Polymer and pGL3 plasmids (0.1 μg) were complexed at various N/P ratios at room temperature for 30 min. After adding 6X dye, complexes were loaded in gels and electric current (100 V) applied for 30 min. Gels were illuminated by the ultraviolet lamp and analyzed.

6) Observation of morphology of PMT/pGL3 complexes

The morphologies of PMT/pGL3 complexes prepared at an N/P ratio of 10 were observed by energy-filtering transmission electron microscopy (EF-TEM) (LIBRA 120, Carl Zeiss, Germany).

7) DNA protection and release assay

DNA protection in a DNase1 environment and release of DNA from complexes was assayed using a gel electrophoretic technique. PMT and pGL3 plasmids (0.2 μg) were complexed at an N/P ratio of 10 for 30 min at room temperature. Two units of DNase1 and 1X DNase/Mg^{2+} digestion buffer were added to complexes and free pGL3 and incubated for 30 min at 37C in the incubation shaker. After incubation, 4 μl of 250 mM EDTA dissolved in 5N

NaOH was added to each sample and left for 30 min for DNase 1 inactivation. Then, 5 μl of 1% sodium dodecyl sulfate (SDS) was added to each sample and incubated for 2 h. After adding 6X dye, samples were loaded into 0.1% agarose gels with electric current (50 V) for 1 h. Gels were illuminated by the UV lamp.

8) Cell lines and cell culture

A549 cells (human lung adenocarcinoma epithelial cells; ATCC number CCL-185) were maintained in RPMI-1640 culture medium and HeLa cells (human cervix epithelial carcinoma cells; ATCC number CCL-2) were cultured in DMEM culture medium. Neuro2a cells (mouse neuroblastoma cells ; ATCC number CCL-131) were cultured in alpha-MEM. Culture media contained 10% heat-inactivated FBS with 1% penicillin/streptomycin. All cells were grown at 37 C in a humidified atmosphere containing 5% CO_2.

9) *In vitro* cell viability assay

Cell viability of three different cell lines (A549, HeLa and Neuro2a) was measured with MTT assay. Cells were seeded at density of 10×10^4 cells/ml and grown to 80~90% confluence in 24-well plates. PMT (or PEI) and DNA were complexed with different N/P ratios in the 500 μl serum free media. Complexes were added to the each well and incubated for 24 h. After incubation, MTT reagent was added to the each well and incubated for an additional 4 h for reduction to purple formazan. Medium was aspirated carefully and DMSO was added to each well to dissolve purple formazan. Colored solutions were transferred to 96-well plates and optical density was measured at 540 nm using a VERSAmax tunable microplate reader (Sunnyvale, USA)

10) *In vitro* transfection efficiency

In vitro transfection efficiency in three different cell lines (A549, HeLa and Neuro2a) was measured by luciferase assay. Cells were seeded at density of 10×10^4 cells/ml and grown to 80~90% confluence in 24-well plates as above. Purified pGL3 plasmids (1 μg) were complexed with PMT or PEI at various N/P ratios. Serum-free media containing complexes were added to each well and incubated for 4 h. Media were replaced with the complete media (10% FBS) and incubated for additional 24 h. After removing all media, 100 μl of passive lysis buffer was added. Luciferase assay was carried out according to the manufacture's protocol (luciferase assay system protocol-Promega). Cells were scraped in the presence of lysis buffer followed by one cycle of freeze-thaw and moved into a 1.5 ml tube. After centrifuge at 14,000 rpm and 4 C for 15 min, cell lysates were moved into a new 1.5 ml tube kept on ice. Chemiluminometer (Autolumat, LB953; EG&G Berthold, Germany) was used to measure relative light units. Relative light units (RLU) were normalized by total proteins measured by a BCA assay. *In vitro* cell transfection in the presence of different serum concentrations (0, 10, 20 and 30%) was also performed for A549 cells at an N/P ratio of 20. The experiment was performed in triplicate and the transfection activity was evaluated as RLU/mg of protein.

11) *In vivo* transfection efficiency

To evaluate the efficiency of transfection of PMT *in vivo*, aerosol administration of PMT/tGFP complexes was performed in mice lungs. Six-week-old C57BL/6 (4 mice/group) were used following the policy and

regulations for the care and use of laboratory animals (Laboratory Animal Center, Seoul National University, Korea). Mice were kept in the laboratory animal facility with temperature and relative humidity maintained at 23 ± 2 C and 50 ± 20%, and a 12 h light/dark cycle. All experimental protocols were reviewed and approved by the Animal Care and Use Committee at Seoul National University (SNU-120112-2). We used aerosol delivery system as previously described (Islam, M.A. *et al.*, 2011). For this study, 1 mg of tGFP was complexed with PMT or PEI at an N/P ratio of 20. After 24 h of gene delivery, mice were sacrificed and lungs were perfused with 4% paraformaldehyde, and fixed in 4% paraformaldehyde overnight and stored in 30% sucrose for 48 h at 4 C. Lungs were embedded in Tissue-TekOCT (Sakura, Torrance, CA, USA) at below 20 C. Lungs were sectioned at 20 um and mounted on slides for analysis. Lung sectioned on slides were observed for tGFP signal using a ZeissLSM510 confocal microscope (Carl Zeiss, Inc.).

12) Effect of bafilomycin A1 on transfection efficiency

Cells were seeded at 10×10^4 cells/ml and grown to 80~90% confluence in 24-well plates. Bafilomycin A1, an inhibitor of vacuolar-type H+-ATPase, was dissolved in DMSO and mixed with serum-free media at 200 nM. Bafilomycin A1 was added to cells for 15 min before transfection with complexes (N/P 10). Luciferase activity was measured according to the method above.

13) Effect of cellular uptake inhibitors on transfection efficiency

Cells were seeded at 10×10^4 cells/ml and grown to 80~90% confluence in 24-well plate. Cellular uptake inhibitors CH, M-β-CD, GE and WO dissolved

in DMSO were mixed at serum free media with various concentrations. Inhibitors were added to the cells and incubated for 1 h at 37 C in a humidified atmosphere of 5%. CO_2. PMT/DNA and PEI/DNA complexes (N/P 10) were treated and incubated for 4 h without removing inhibitors. The luciferase assay was conducted as described in supplementary information.

14) Western blot analysis of caveolin-1 (pY 14)

Cells were transfected with PMT/pGL3 complexes for 30 min or genistein was treated before transfection. Cells were also treated with 600 mM mannitol for 10 min for hypertonic conditions as a positive control. On ice, cells were washed with ice cold PBS and protein was collected by radio immunoprecipitation assay RIPA buffer supplemented with protease inhibitor and phosphatase inhibitor. Collected protein was incubated for 30 min on the ice and mildly stirred for 5 min and then centrifuged in 14,000 rpm at 4 C for 25 min. Lysate was removed into a new tube on ice. Protein concentration was measured by bicinchoninic acid (BCA) assay as described in supplementary information. Equal amounts of protein mixed with 5X sample buffer containing dithiothreitol were boiled for 5 min. Samples were loaded on SDS-PAGE gels (15%) and run in the cold. Protein was transferred to the nitrocellulose membranes using a semi-dry method on 10 V for 60 min and pre-blocked with 5% bovine serum albumin in Tris-buffered saline Tween 20 solution overnight at 4 C with agitation, and incubated with phospho-caveolin-1 (Tyr14) IgG (rabbit polyclonal antibody) or actin IgG (rabbit polyclonal antibody) overnight at 4 C. After washing three times for 15 min, goat anti-rabbit IgG-HRP was treated and incubated for 1 h with agitation. Bands of interest were visualized

using a luminescence image analyzer LAS-3000 (Fujifilm, Tokyo, Japan)

15) Observation of confocal microscopy

PMT and PEI were fluorescently labeled with FITC dissolved in pH 8 bicarbonate buffer at room temperature for 12 h. After labeling, the mixture was dialyzed with dialysis membrane (MW cut-off 3500) at 4 C for 24 h and lyophilized for 3 days. Cells were seeded in cover glass-bottom culture dishes (35 mm) and grown to 80% of confluence. Cells were incubated for 12 h in 50 μg/ml of Alexa-dextran 594 prior to transfection with FITC-PMT/pGL3 or FITC-PEI/pGL3 complexes for 3 h. Colocalization of complexes in lysosomes was observed using Image Restoration Microscopy (DeltaVision RT, AppliedPrecision, USA)

3. Results and discussions

1) Synthesis and characterization of a PMT

For the Michael addition reaction, MDA as a crosslinking agent was prepared by reaction of mannitol and acryolyl chloride in the presence of pyridine at 4 C for 24 h. By adjusting the ratio of 2 mol acryoyl chloride to 1 mol mannitol, diacrylate can be introduced to only 1 and 6 positions of the hydroxyl groups of mannitol because these positions of primary alcohols are more reactive than the hydroxyl groups of secondary alcohols. PMT was successfully prepared from MDA and LMW BPEI (MW: 1200 Da) in anhydrous DMF at 80 C for 24 h.

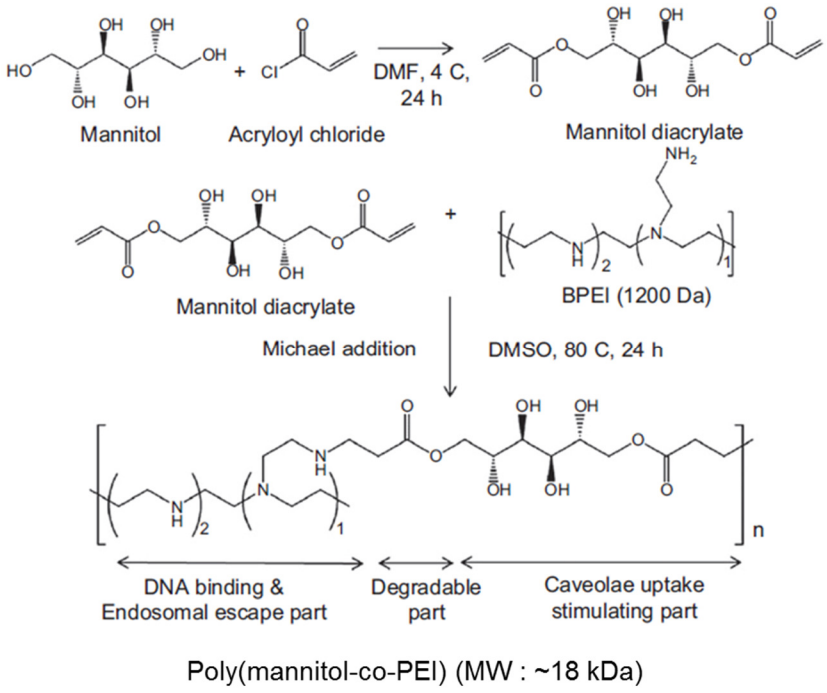

Figure 27. Schematic illustration of PMT synthesis.

The nucleophilic diacrylate terminal of MDA was reacted with amine groups of BPEI through the Michael addition reaction. The proposed reaction scheme of the synthesis is in Figure 27. Each part in the structure suggests the different functions of the PMT as indicated. The composition of the prepared PMT was estimated by ^{1}H NMR spectroscopy (Figure 28) and the final molecular weight was measured by GPC (Table 4). PMT was completely water soluble, possibly because of the hydrophilic property of the mannitol backbone, although the molecular weight distribution of the PMT was broad. Also, the synthesized PMT was susceptible to hydrolysis in physiological conditions forming acid and alcohol, and producing LMW non-toxic products because this PMT has ester linkages, which suggest the degradability of the PMT.

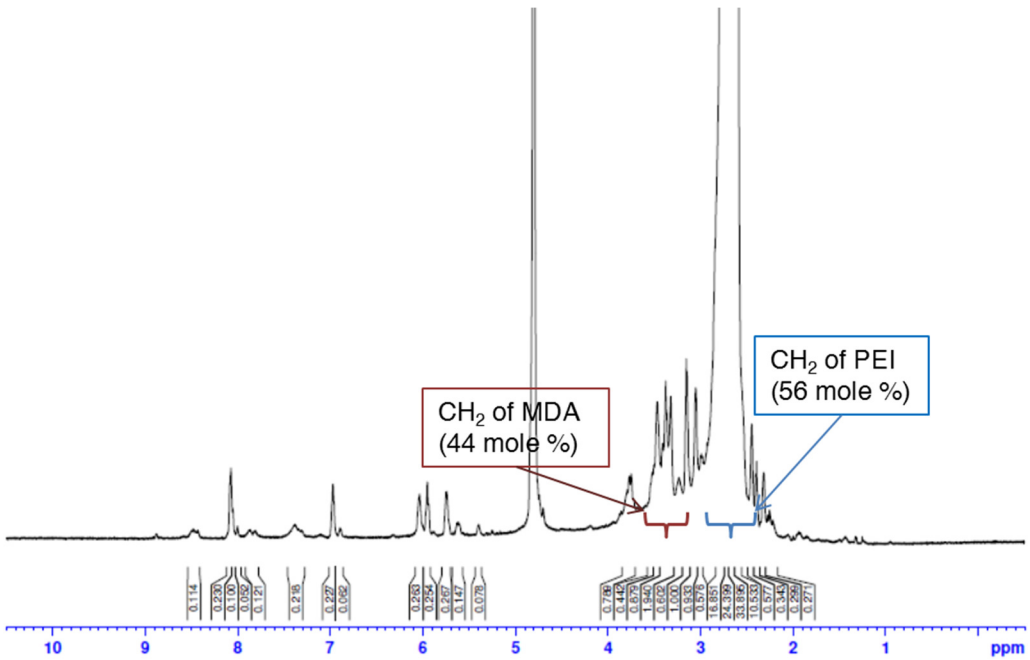

Figure 28. ^{1}H-NMR spectra of PMT in D_2O

Table 4. Characterization of PMT measured using GPC.

Test	Mn	Mw	Mp	Mw/Mn
RUN1	8942	17449	13831	1.96
RUN2	8942	17441	13831	1.95
SD	0.00	41.01	0.00	
CV	0.00	0.23	0.00	
Average	8942	17470	13831	1.95

Mn (number averaged mol weight); Mw (weight averaged mol weight); Mp (mol weight at peak top); SD (standard deviation); CV (coefficient of variation)

2) Physiochemical characterization of PMT/DNA complexes

The particle size and zeta-potential of complexes are important factors in non-viral vector systems because they determine the *in vivo* distribution, biological fate and toxicity (Barreto, J.A. *et al.*, 2011). The particle sizes of PMT/DNA complexes slowly increased with the increase of N/P ratios to 279 nm at N/P 30, unlike PEI/DNA complexes, which is due to sterically bulky hydroxyl groups of mannitol inducing repulsive force. In case of PEI/DNA complexes, the particle sizes of PEI/DNA decreased as N/P ratios increased because of net electrostatic repulsive forces among the highly positive charges of the complexes (Table 5). The particle sizes of PMT/DNA complexes at N/P ratio of 20 observed by TEM were smaller than them measured by DLS (Figure 29). A zeta potential above ± 30 mV is reported to be stable in suspension as the surface charge prevents flocculation (Barreto, J.A. *et al.*, 2011). The zeta potential of PMT/DNA complexes tended to be little lower than the PEI at each N/P, which is because that partial negative charges on the hydroxyl groups of mannitol shielded surface charges, as described previously (Islam, M.A. *et al.*, 2011).

Table 5. Size and zeta potential of PMT/DNA complexes

N/P ratios	Size (nm)		Zeta potential (mV)	
	PMT/DNA	PEI/DNA	PMT/DNA	PEI/DNA
5	173.5±4.5	177.9±1.8	2.67±0.1	13.0±1.0
10	228.7±9.6	166.9±6.2	17.8±1.6	32.0±2.1
20	239.5±4.1	168.6±5.1	40.7±4.5	42.9±4.7
30	279.1±7.8	154.5±1.6	31.6±6.7	40.1±1.7

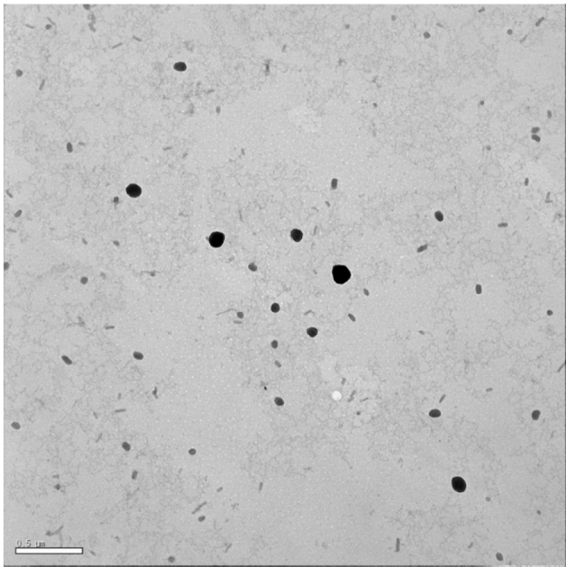

Figure 29. TEM image of PMT/DNA complexes (N/P 20). Scale bar represents 0.5 μm

Gel retardation assays confirmed the DNA complexing with PMT. PEI, with high cationic charge density, ionically interact with negatively charged DNA; this electrostatic self-assembly is a major characteristic of cationic polymers as non-viral vector systems. From an N/P ratio 1, no DNA was observed by perfect neutralization and condensation (Figure 30) A DNA protection assay was also carried out to determine if condensed DNA was protected from nuclease degradation. Compared with DNA directly exposed to DNase 1 (Figure 30B for lane 2), DNA preserved by PMT was unchanged (Figure 30B for lane 4), indicating that DNA can be protected and released from PMT/DNA complexes.

The maintenance of osmolyte activity is critical for the selective pathway of PMT. Osmolarity of PMT/DNA complexe was measured by osmometer (Gallay Medical & Scientific, Osmomat 010) by varying the concentration of mannitol. Like mannitol, the osmolarity of PMT/DNA increased with increase in mannitol content of the PMT in the solution (Table 6). The data revealed that the osmotic strength as well as PMT/DNA complex was maintai ned as the concentration of mannitol increased.

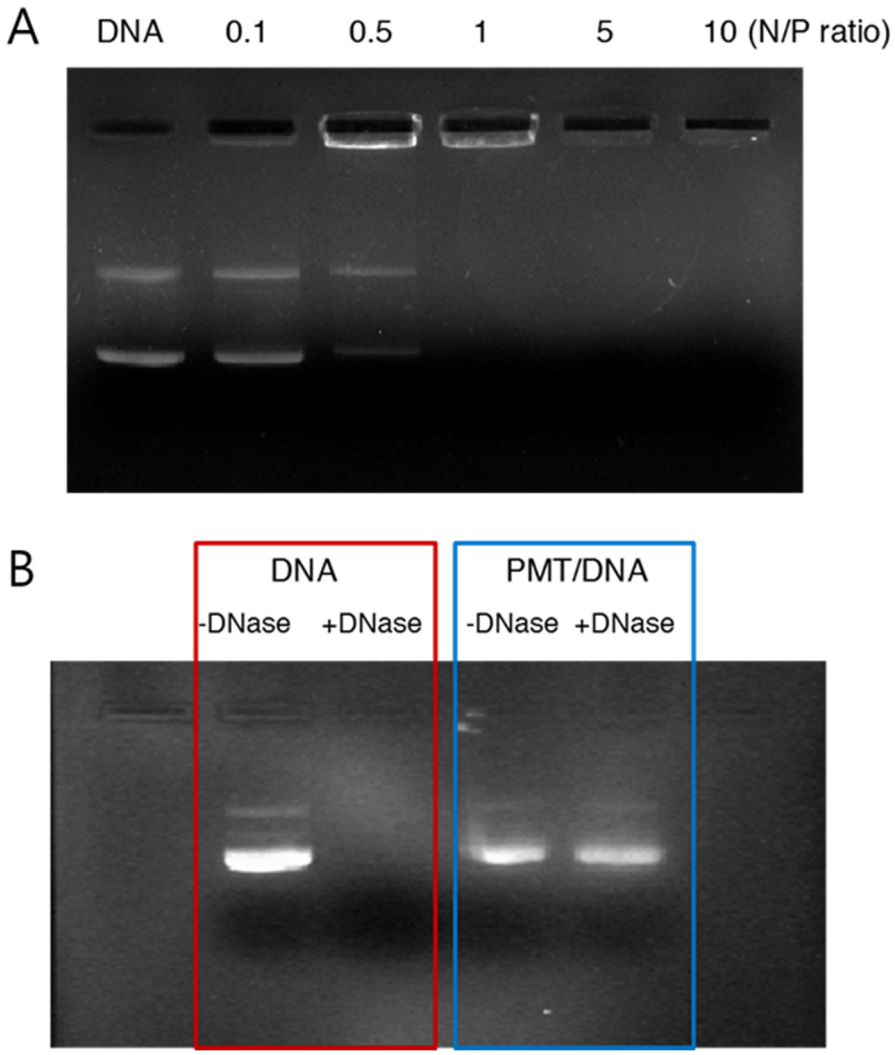

Figure 30. Gel retardation and DNA protection assay. (A) gel electrophoresis of PMT/DNA (0.1 μg of pGL3) complexes at various N/P ratios. (B) DNA (0.2 μg of pGL3) was released by addition of 1% SDS. (lane 1: DNA without DNase, lane 2:DNA treated with DNase, lane 3: PMT/DNA complex with PMT without DNase, lane 4: PMT/DNA complex with DNase)

Table 6. Osmolarity of PMT/DNA complexes

		Osmolarity [mOsm]
RPMI + 10 % FBS		276
Mannitol	1 %	348
	3 %	441
	5 %	531
PMT/DNA (N/P 20)	1 % mannitol (wt. %)	297
	3 % mannitol (wt. %)	395
	5 % mannitol (wt. %)	421

3) *In vitro* cytotoxicity of PMT/DNA complexes

An *in vitro* cytotoxicity study was undertaken using A549, Neuro2a and HeLa cell lines using a MTT assay method. Although PEI was proven to be effective gene delivery vehicle, high cytotoxicity of PEI limited medical applications. Some studies showed that a high N/P ratio of PEI/DNA complexes induced cell dysfunction with high densities of primary amine and this was highly dependent on the molecular weight of PEI (Moghimi, S.M. *et al.*, 2005). To minimize side effects while maintaining the gene transfer efficiency, crosslinking LMW PEI has been used (Park, T.G. *et al.*, 2006;Werth, S. *et al.*, 2006). Therefore, ester groups was employed in PMT that could be easily degradable and removed physiologically. Partial neutral charges on hydroxyl groups in mannitol was also employed to quench the remaining positive charges of the complexes. The results showed that the PMT/DNA complexes were less cytotoxic in three different cell lines (A549, Neuro2a and HeLa) than high molecular weight (HMW) PEI (25 kDa), particularly with transfection at high N/P ratios (Figure 31).

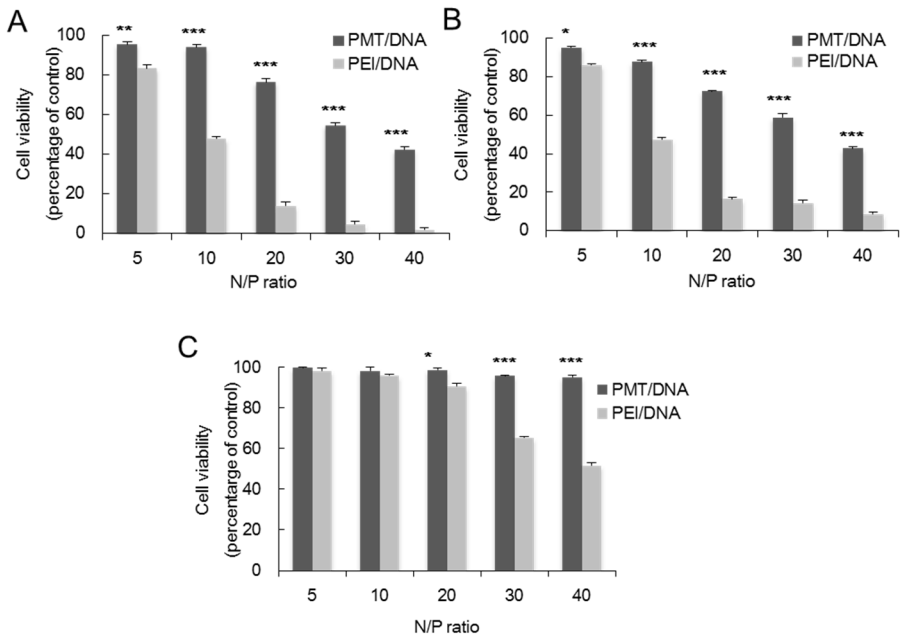

Figure 31. Cytotoxicity of PMT/DNA complexes. cytotoxicity of PMT and PEI/DNA complexes was measured using MTT assay and given as percentage of control in A549 cells (A) Neuro2a cells (B) and HeLa cells (C). (n=3, error bar represents standard deviation, *p<0.05, **p<0.01, ***p<0.005, one-way ANOVA).

4) *In vitro* transfection efficiency of PMT/DNA complexes with or without serum

The molecular weight of carriers and N/P ratios of complexes are reported to be important factors of transfection efficiency. Many studies found that LMW PEI requires higher N/P ratios for optimal transfection efficiency compared to HMW PEI because of the particle sizes and charges of complexes (Werth, S. *et al.*, 2006). We delivered pGL3 luciferase reporter plasmids using kinds of non-viral vectors: PMT, PEI, and Lipofectamine 2000, in three different cell lines and performed luciferase assay. As shown in Figure 32, the transfection efficiency of PMT/DNA complexes was higher for PEI/DNA complexes at the same N/P ratios in all cell lines despite the many hydroxyl groups in PMT because the introduction of PEG in the gene carrier reduced transfection efficiency *in vitro* . Especially in the A549 and HeLa cells, a more significant difference in transfection efficiency between PMT and Lipofectamine 2000 was obtained. To study the serum effect on transfection efficiency, PMT/DNA and PEI/DNA complexes were transfected to the A549 cells in serum-containing media. Serum protein adsorption is critical for the outcomes of these materials. As shown in Figure 32D, the transfection efficiency of PMT/DNA complexes was less affected by serum proteins while the transfection efficiency of PEI/DNA decreased with increasing of serum. The extent of the serum effect was determined by competition between attractive forces including electrostatic attraction and non-specific repulsion forces including hydration forces. The hydrophilic mannitol of the PMT surface is associated with water molecules,

which induces repulsive hydration against serum protein since the energy obtained by adsorption does not exceed the energy required for water displacement of water (Morra, M., 2001;Hughes, A.B., 2009). With these chemical interactions, the repulsive hydration between mannitol and serum proteins seemed to protect PMT from losing its transfection function (Figure 32).

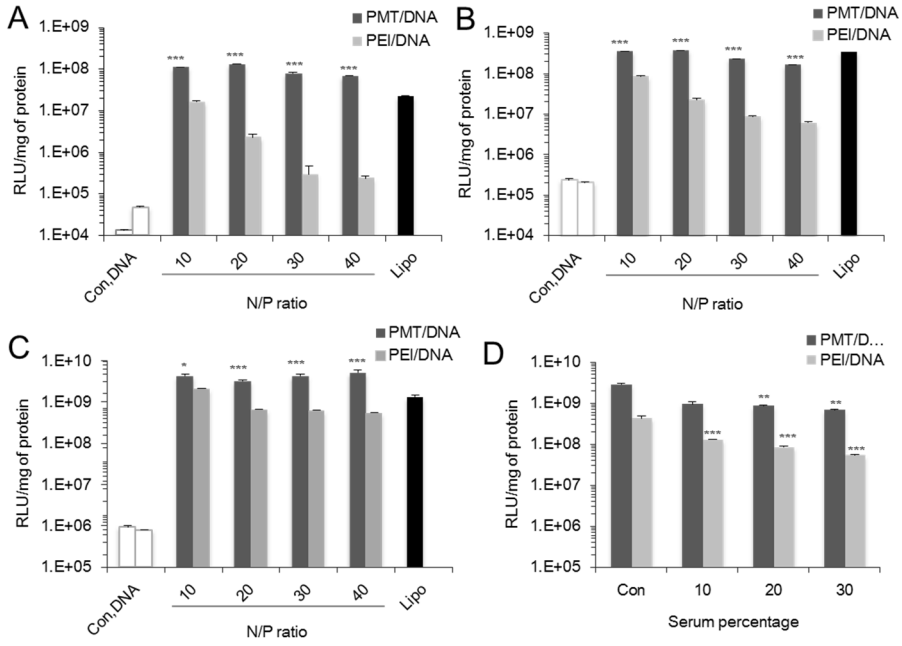

Figure 32. Transfection efficiency of PMT/DNA complexes with or without serum *in vitro* . The same amount of pGL3 plasmids were complexed with PMT, PEI and Lipofectamine 2000 and delivered to (A) A549 cells, (B) Neuro2a cells, (C) HeLa cells without serum. (D) The PMT and PEI/pGL3 complexes were transfected in A549 cells in presence of various amount of serum. Luminescence was measured 24 h after transfection and normalized with the amount of protein. (n = 3, error bar represents standard deviation; *p<0.1, **p<0.05, ***p<0.01, one-way ANOVA compared to that of PEI/DNA complexes (A-C) and control (D)).

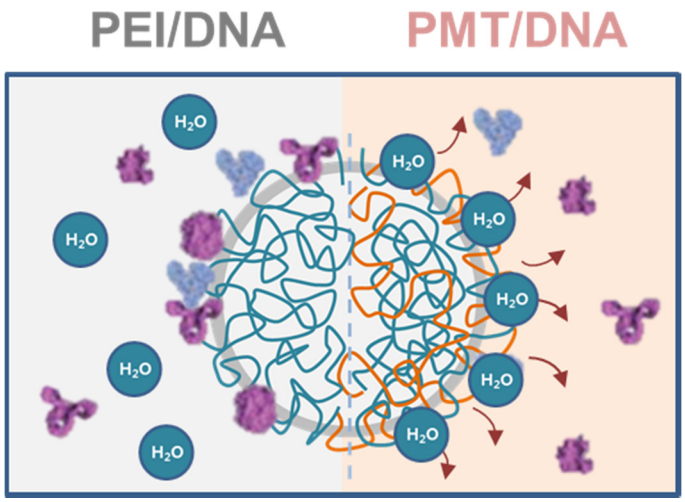

Figure 33. Schematic illustration of repulsive hydration of PMT/DNA complexes

4) *In vivo* transfection efficiency of PMT/DNA complexes

To confirm the *in vitro* results of transfection efficiency of PMT *in vivo*, we performed aerosol administration. To evaluate the transfection efficiency of PMT in lungs, expression of green fluorescent protein was analyzed after aerosol delivery of PMT/tGFP complexes to mice (C57BL/6; n=4) lungs using nose-only exposure chamber. After 24 h, lungs were collected and flushed with 0.01 M Phosphate buffered saline through the trachea to minimize the background GFP signals from red blood cells. As shown in fluorescent microscopic images, control groups showed minimum background GFP signals and PMT/tGFP groups showed enhanced tGFP expression that was even higher than PEI/tGFP complexes, consistent with the results of the *in vitro* transfection efficiency (Figure 34).

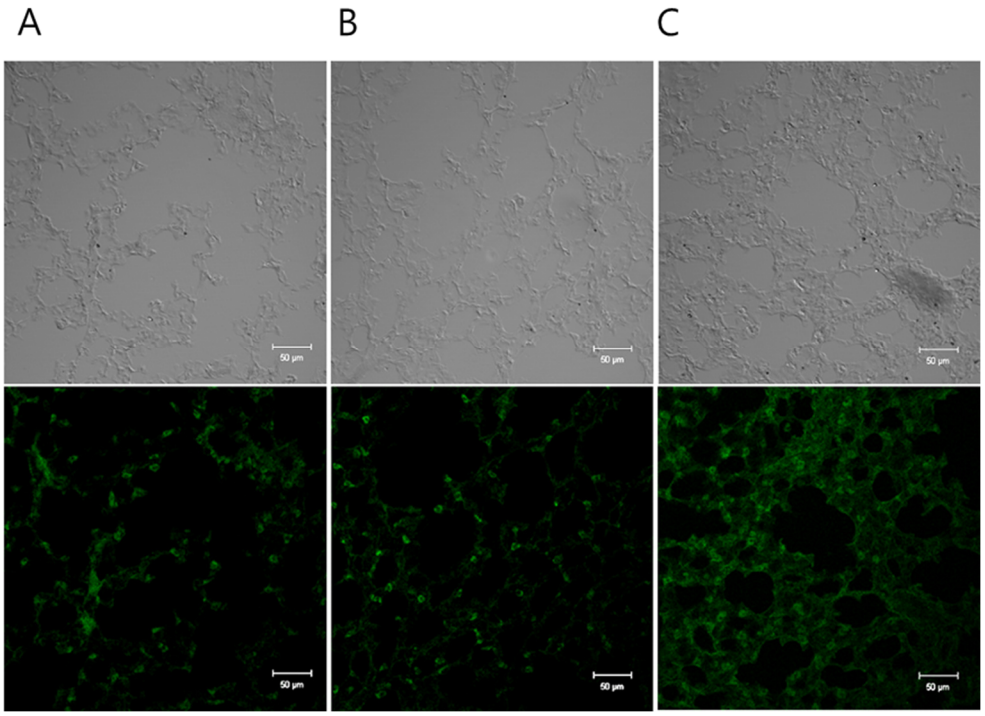

Figure 34. Fluorescent microscopic images of tGFP expression in mice lungs. Mouse was inhaled with PEI and PMT/tGFP complexes in aerosol form for 30 min. Mice lungs were extracted after 24 h of transfection and green fluorescence was observed with confocal laser scanning microscopy. Scale bar represents 5 µm.

5) Mechanism of gene delivery of PMT

(1) Proton sponge effect of PEI backbone of PMT

The relatively high transfection efficiency of PEI has been postulated to be due to its intrinsic ability to escape the endosome by the proton sponge effect. This hypothesis suggests that buffering of PEI during the acidification of the endosome triggers influx of Cl^- with protons that leads to osmotic swelling and rupture of endosomes (Boussif, O. *et al.*, 1995). To investigate the proton sponge effect of PMT/DNA complexes, transfections were conducted in the presence of bafilomycin A1, a proton pump inhibitor. Treatment with bailomycin A1 inhibits the protonation of PEI inside endosomes and, therefore, prevents endosomal escape (Akinc, A. *et al.*, 2005). Figure 35 shows that the use of 200 nM bafilomycin A1 decreased the transfection efficiency of PEI/DNA complexes by 5.6×10^3 and PMT/DNA complexes by 1.1×10^2. This result strongly suggested that endosomal escape of PMT/DNA complexes was based on the proton sponge effect of PEI. However, another mechanistic explanation was needed for the higher transfection efficiency of PMT/DNA complexes in that PMT was less dependent on endosomal escape for transfection compared to PEI. Among the various factors explaining high transfection efficiency *in vitro* and *in vivo*, my study focused on the effects of osmolyte mannitol on the endocytic pathway.

(2) Endocytosis pathway of PMT/DNA

To compare the two complexes in the endocytosis pathway, four cellular

uptake inhibitors were used before transfection. The concentration of the inhibitors were optimized after checking cell viability because the inhibitors induce cytotoxicity at high concentrations. Figure 35B-E shows the change in transfection efficiency of PMT/DNA and PEI/DNA complexes in the presence of cellular uptake inhibitors CH as an inhibitor of clathrin endocytosis, GE and M-β-CD as inhibitors of caveolae endocytosis, and WO as an inhibitor of fluid-phase endocytosis. Treatment of A549 cells with GE and M-β-CD drastically decreased PMT-mediated transfection, indicating that transfection of PMT/DNA complexes occurred through a selective caveolae endocytic pathway although 56 mole percent of PEI exists in PMT. In contrast, the transfection efficiency of the PMT/DNA complexes changed little in the endocytic pathway with treatment with CH or WO, an indication of a decreased relationship of transfection with clathrin or fluid-phase endocytic pathway. In contrast to PMT/DNA complexes, treatment of CH, GE, M-β-CD, and WO reduced the transfection of PEI/DNA complexes, suggesting the non-selective endocytic pathway. This result indicated that PMT shifted the endocytosis pathway to caveolae-mediated endocytosis because of the osmotically active mannitol. How the mannitol backbone of PMT shifted the uptake pathway is not clear. It was assumed that mannitol induced hyperosmotic stress (as shown in Table 6) to cope with cellular stress, resulting in a change of the endocytic response because, as described by many studies osmotic stress stimulated caveolae endocytosis with transient down-regulation of clathrin and fluid-phase endocytosis. This is consistent with my result (Wang, S. *et al.*, 2011).

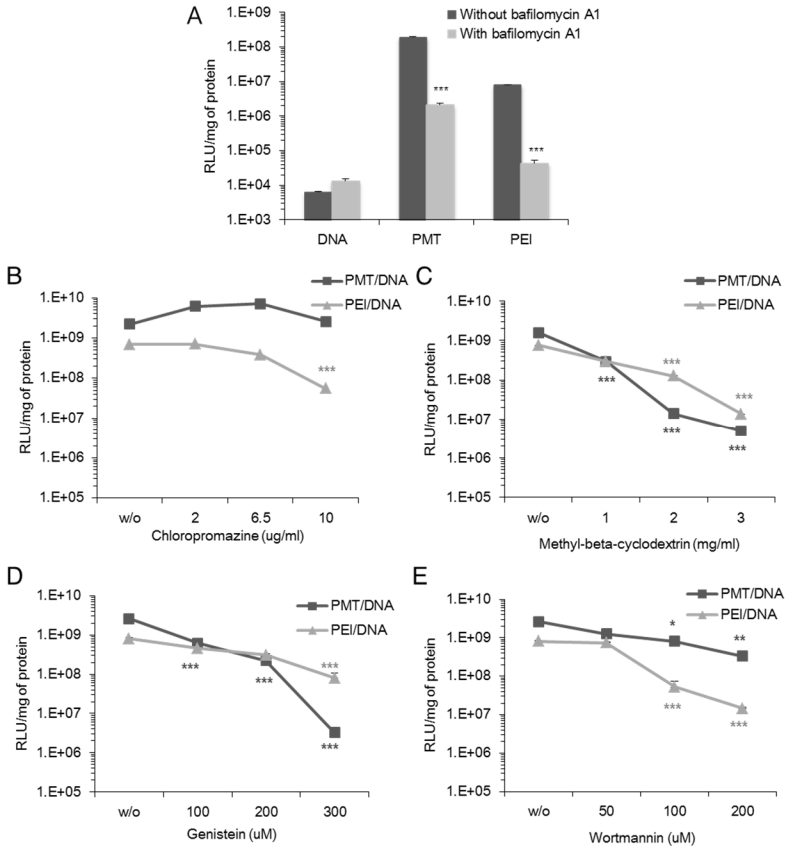

Figure 35. Effect of Bafilomycin A1 and endocytosis inhibitors on transfection efficiency of PMT/DNA complexes. (A) Cells pre-incubated with 200 nM of bafilomycin A1 were transfected with PMT and PEI/pGL3 complexes (N/P 10) and screened for luciferase expression. B-E, Cells pre-incubated with various amount of (B) chloropromazine, (C) methyl-beta-cyclodextrin, (D) genistein, and (E) wortmannin were transfected with PMT and PEI/pGL3 complexes (N/P 10) and luciferase assay was conducted. (n = 3, error bar represents standard deviation; *p<0.1, **p<0.05, ***p<0.01, one-way ANOVA compared to that of control without inhibitor).

(3) Mannitol part of PMT as a caveolae-mediated endocytosis stimulant

The endocytosis of caveolae is observed to be stimulated by certain ligands or cellular stress, which differs from efficient constitutive endocytosis (Chidlow, J.H., Jr. and Sessa, W.C., 2010). Despite the differences in stimulants, common mechanisms are involved in these internalization pathways with a crucial role for Src-kinase, dynamin, and actin recruitment (Parton, R.G. and Simons, K., 2007). As essential steps, Src-kinase-mediated phosphorylation of caveolin-1 is required for caveolae budding and phosphorylation of dynamin is necessary to pinch caveolae from the plasma membrane. Also Src-mediated phosphorylation regulates the actin cytoskeleton for caveolae vesicle formation and release (Sverdlov, M. *et al.*, 2007).

To examine the above mechanism, phosphorylation of caveolin-1 as an essential requirement of stimulated endocytosis was evaluated by western blot. A549 cells treated with PEI/DNA and PMT/DNA complexes (N/P 20 and 30 min) or hypertonic mannitol were used as positive controls reported (600 mM and 10 min) (Volonte, D. *et al.*, 2001). Cells were lysed and western blots were conducted using phospho-caveolin-1 antibody. As shown in Figure 36, phosphorylation of caveolin-1 was induced transiently by PMT/DNA complex treatment and the positive control (lane 3 and 5) while this was not detectable with PEI/DNA complex treatment or the negative control (lane 1 and 2). To determine if phosphorylation of caveolin-1 is mediated by Src kinase, cells were pre-incubated with an inhibitor of Src tyrosine kinase inhibitor (Akiyama, T. and Ogawara, H., 1991) before treatment of PMT/DNA complexes. Then, the cell lysate was observed to have no phosphorylated caveolin-1, indicating

that activation of Src tyrosine occurred. Therefore, PMT was a caveolae stimulant for endocytosis and substantially affected uptake mechanism. Some reports have described that plasma membrane tension by osmotic pressure has a significant impact on exocytosis and endocytosis for homeostasis by adding or removing plasma membrane (Apodaca, G., 2002), although how tension regulates endocytosis is not clear. According to recent reports, sensing signaling is tightly coupled to the endocytic response of caveolae, and caveolae are described as membrane-mediated sensors and regulators of the plasma membrane tension (Kapus, A. *et al.*, 1999;Apodaca, G., 2002;Sens, P. and Turner, M.S., 2006). This is consistent with previous results, suggesting that cellular stress induced phosphorylation of caveolin-1 through Src-kinase and translocation of caveolin-1 to cytosol following cellular shrinkage in NIH3T3 cells (Volonte, D. *et al.*, 2001). Based on previous reports and my results, I postulate the mechanism of uptake of PMT/DNA complexes is that the mannitol of PMT transiently induced activation of Src-kinase and successfully stimulated caveolae endocytosis (Figure 36).

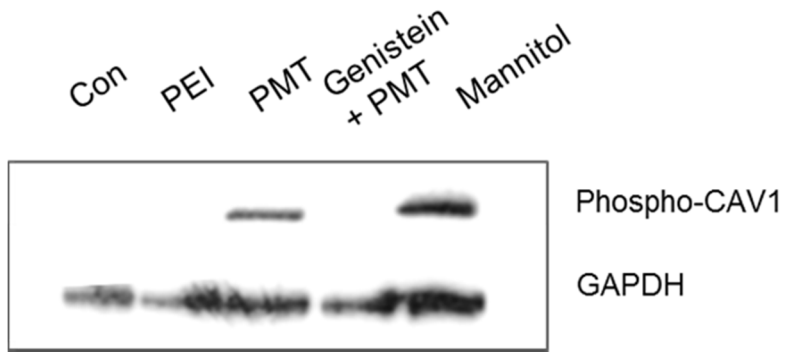

Figure 36. Phosphorylation of caveolin-1 on tyrosine 14 induced by PMT/DNA complexes. A 549 cells were untreated (lane 1) or treated with PEI/DNA (lane 2), PMT/DNA complexes (lane 3) (N/P 20) for 10 min and mannitol (600 mM) for 10 min (lane 5). To inhibit Src tyrosine kinase, genistein was treated before transfection with PMT/DNA complexes (lane 4).

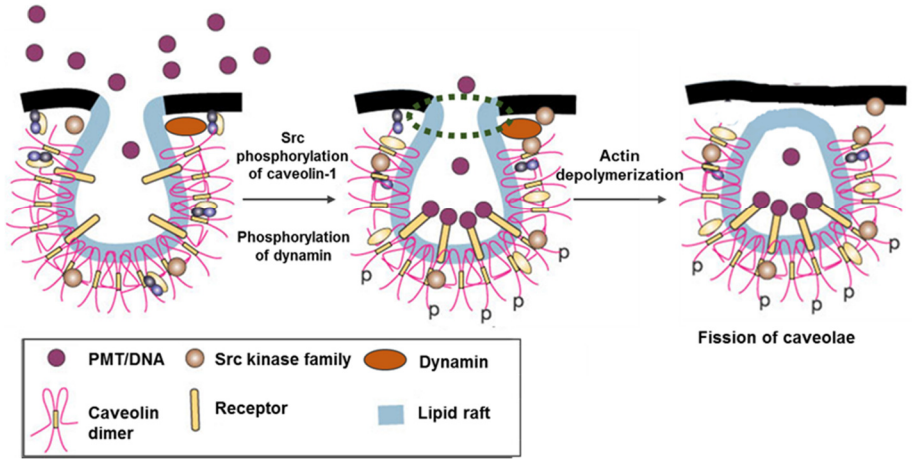

Figure 37. Suggested mechanism of stimulation of caveolar endocytosis by PMT/DNA complexes.

(4) Intracellular fate of PMT/DNA

To obtain insight into the intracellular fates of PMT and PEI/DNA complexes depending on their endocytosis pathway, A549 cells were incubated with a lysosomal marker (Dextran, AlexaFluor 594) and subsequently with FITC conjugated PMT or FITC conjugated PEI/DNA complexes for 3 h (Rejman, J. *et al.*, 2006). The colocalization of the two complexes and lysosomes were observed in living cells by image restoration confocal microscopy (Figure 38). Although both PMT and PEI/DNA complexes (green) were partially found in lysosomes stained with lysosomal marker (red), the percentage of colocalization (yellow) was different between the two complexes. Approximately 70% of PEI/DNA complexes were localized in the lysosome whereas only 20% of PMT/DNA complexes were localized in the lysosome, and followed by translocation into nucleus (Figure 38). This suggested that shifting endocytosis pathway affected the intracellular fate of PMT/DNA complexes to effectively avoid lysosomes (Figure 39).

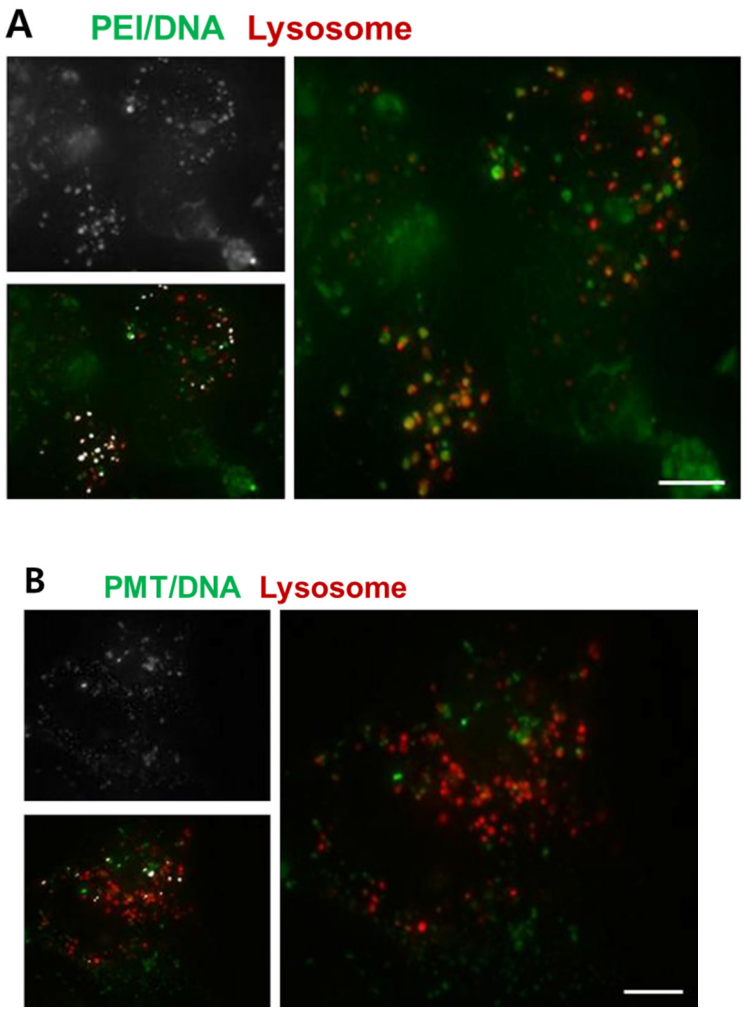

Figure 38. Co-localization study of PMT/DNA complexes with lysosome. A-B**:** A 549 cells were pre-incubated with fluorescent dextran for lysosome staining (red) and transfected with (A) FITC-PEI/DNA (green) or (B) FITC-PMT/DNA complexes (green) for 3 h and then, colocalization of lysosomes and polyplexes was observed with fluorescent microscopy. Upper left images represent complexes detected with FITC and lower left images represent colocalization spot analyzed by ImageJ program. The overlay of polyplexes and lysosome appeared in yellow is shown in the right image. Scale bar represents 5 µm.

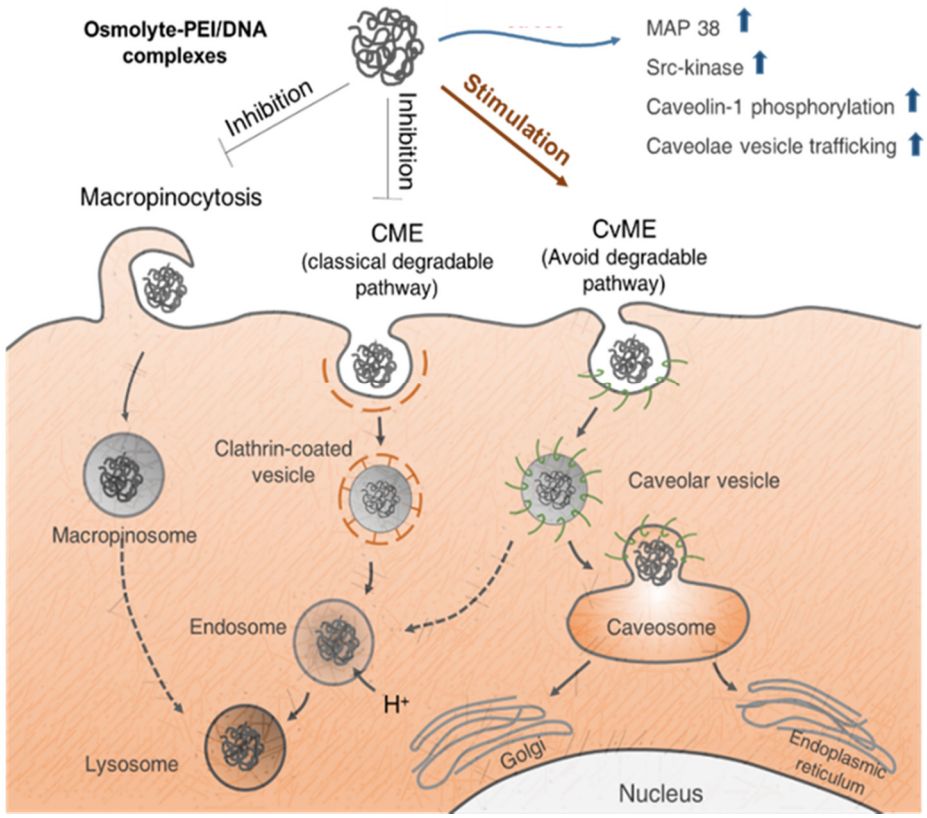

Figure 39. Concept of targeting caveolae-mediated endocytosis by PMT/DNA complexes

4. Conclusion

In summary, we designed a new non-viral vector PMT composed of PEI and mannitol with highly improved gene delivery function and cytotoxicity through regulation of the endocytosis pathway by osmotically active mannitol. The mannitol backbone of PMT was chosen to shift the uptake route into caveolae-mediated endocytosis by hyperosmotic activity. This led PMT/DNA complexes to efficiently avoid lysosomal degradation, suggesting that controlling the intracellular fate of nanoparticles is a promising strategy for gene delivery. In mechanistic studies, we determined that the osmotic activity of mannitol activated Src-kinase and stimulated caveolae-mediated endocytosis. Knowledge of the mechanism will allow the non-viral vector to be targeted to the intended endocytosis pathway.

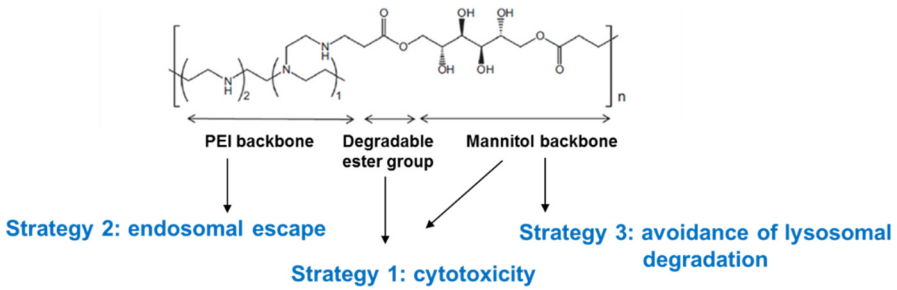

Figure 40. Three functional part of PMT

Chapter 2. Enhanced BBB permeability of poly(mannitol-co-PEI) gene transporter modified with rabies virus glycoprotein via selective stimulation of caveolar endocytosis

1. Introduction

The prevalence of neurodegenerative diseases is rapidly escalated, although treatments to prevent the progression of symptoms have not been identified (Brookmeyer, R. *et al.*, 2007). As an alternative to the chemical-based treatment, RNAi therapeutic holds one of promising tools by directly and specifically turning off the causative genes (Chen, S. *et al.*, 2013). For successful clinical application of RNAi of great potential, development of safe and efficient siRNA delivery systems is an essential task. The initial strategies to deliver therapeutic genes to brain have relied on the use of viral vectors, however, some of severe limitations such as safety concerns and induction of immune responses opened new vistas in non-viral gene therapy (Kanasty, R. *et al.*, 2013). In particular, multiple studies have focused on the development of cationic polymers which can condense nucleic acid with ionic interaction and efficiently deliver genes by escaping from endosome using proton buffering capacity (Thomas, M. and Klibanov, A.M., 2003). Among the cationic polymer, PEI widely used in gene delivery has been reengineered for successful RNAi therapeutics (Jere, D. *et al.*, 2008;Jere, D. *et al.*, 2009;Islam, M.A. *et al.*, 2012;Islam, M.A. *et al.*, 2014).

Despite the great potentials of non-viral RNAi therapeutics for

neurodegenerative diseases, brain targeted-siRNA delivery remains underdeveloped due to extra- and intracellular barriers. The administrated drugs do not reach their target sites during circulation because brain is protected by BBB (Stamatovic, S.M. *et al.*, 2008). The BBB is a homeostatic defense mechanism characterized by low and selective permeability to molecules by tight junction and less developed vesicle system (Stamatovic, S.M. *et al.*, 2008). To overcome the BBB associated problems, many strategies have been investigated including i) neurosurgical strategy, ii) chemical based-delivery by increasing lipid solubility, and iii) biological approaches in order to access endogenous BBB transporter or receptors (Pardridge, W.M., 2006). Among them, biological approach using Trojan horse is a promising strategy considering the invasiveness of neurosurgical strategy and difficulties of chemical modifications of drugs with maintenance of drug characters. The surface modification of nanoparticles by endogenous, virus-mediated or phage-displayed peptides allows therapeutic genes to gain access to brain via receptor-mediated transcytosis (RMT) across the brain endothelial cells (Liu, Y. *et al.*, 2010;Hwang do, W. *et al.*, 2011;Li, J. *et al.*, 2011). Recently, rabies virus glycoprotein (RVG) fragment peptide, a rabies virus mediated ligands, has been widely used as Trojan horse that delivers genes to brain neuronal cells since it possesses a high brain penetration capability. Although controversial, the cellular uptake of RVG was determined to be clathrin- and caveolae- mediated endocytosis and related to γ-aminobutyric acid (GABA) receptor or/and nAChRs (Liu, Y. *et al.*, 2009). RVG-decorated non-viral vectors such as disulfide linked PEI (Hwang do, W. *et al.*, 2011;Son, S. *et al.*, 2011), dendrimer

(Liu, Y. *et al.*, 2009), exosome (Alvarez-Erviti, L. *et al.*, 2011) showed enhanced brain targeted gene delivery efficiency both *in vitro* and *in vivo* although the efficacies of them are still in question to provide the therapeutic effects *in vivo*.

Transcytosis of molecules in the brain endothelial cells mostly relies on clathrin- and caveolae-mediated endocytosis at first step (Polo, S. and Di Fiore, P.P., 2006). It became clear that uptake mechanisms are decisive factors in subcellular trafficking and intracellular fates of delivered genes in most cell types including brain capillary endothelial cells (Georgieva, J.V. *et al.*, 2011). The strong evidences suggest that caveolae-mediated endocytosis does not lead to degradative pathways of their cargoes while molecules uptaken by clathrin-mediated endocytosis are destined to lysosomal degradation unless there is a step of endosomal escape (Rejman, J. *et al.*, 2005). Most commonly, uptakes of unfunctionalized cationic polymers occur by adsorptive-mediated transcytosis via electrostatic interaction with the luminal surface of BBB although surface modification of such a nanoparticles shifts the mode of internalization and thereby enhances the transcytotic potentials (Broadwell, R.D., 1989).

PMT composed of branched PEI and mannitol with highly improved gene delivery function through stimulation of caveolae-mediated endocytosis was suggested in previous chapter. Given that cellular osmotic stress induces phosphorylation of caveolin-1 protein by Src-kinase activity which is essential step for budding and pinching off of cavolae vesicles from the membrane, it was mechanistically determined that osmotically active mannitol of PMT

regulated the uptake pathway and thereby enhanced efficacy of gene delivery. In this study, PMT providing well-modulated caveolae-mediated endocytosis was modified with RVG peptide (R-PEG-PMT) to cross the BBB and target the neuronal cells. Beta-secretase 1 (BACE1) which plays an early role in amyloid plaque generation (Kobayashi, D. *et al.*, 2008) was targeted to evaluate the AD therapeutic potential of thestrategy. R-PEG-PMT was validated as brain targeted non-viral vector by its capability of CNS targeting specificity and siRNA delivery efficiency *in vitro* and *in vivo*. The regulated transcytotic mechanism of BBB permeable R-PEG-PMT was also verified using *in vitro* BBB model.

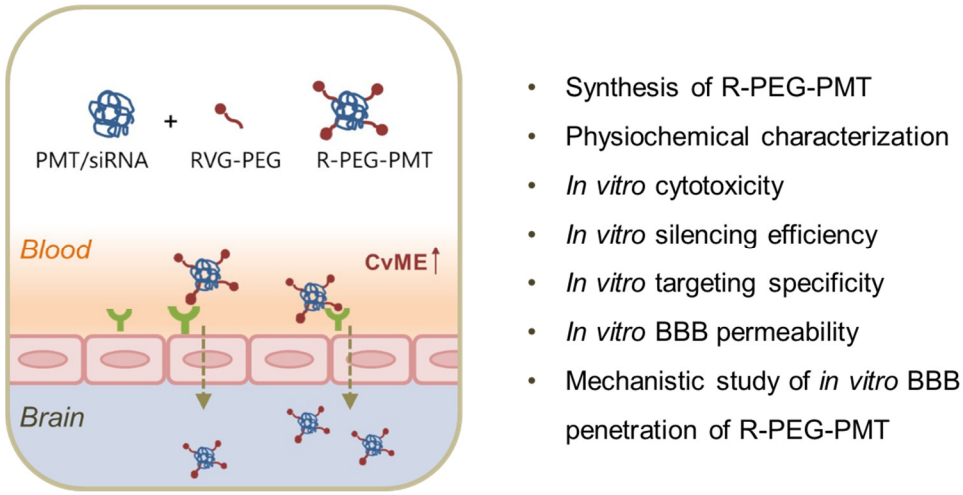

Figure 41. Experimental flow of the study

2. Materials and methods

1) Materials

Branched PEI (BPEI) (Mn: 1200 Da and 25 kDa), dimethylsulfoxice (DMSO), D-mannitol, tetrazolium (MTT) reagent, dimethylformamide (DMF), pyridine, chloropromazine (CH), genistein (GE), methyl-beta-cyclodextrin (M-β-CD), wortmannin (WO), okadaic acid (OA), fluorescein isothiocyanate (FITC) and gapdh IgG (rabbit polyclonal antibody) were purchased from Sigma (MO, USA). pGL3 control vector and luciferase assay system were purchased from Promega (Madison, WI, USA). Roswell Park Memorial Institute (RPMI)-1640 culture medium, Dulbecco's modified Eagle's medium (DMEM), fetal bovine serum (FBS) and penicillin/streptomycin were from HyClone (USA). Minimum essential medium alpha (MEM alpha) medium was from GibcoBRL (Belgium). Cell culture insert (24 well, 1.0 μm pore size) was from BD Bioscience (CA, USA). Caveolin-1 IgG (rabbit polyclonal antibody) was from Abcam (MA, USA) and goat anti-rabbit IgG-HRP was from Santa Cruz Biotechnlogy (CA, USA). RVG polypeptide (YTIWMPENPRPGTPCDIFTNSRGKRASNG) was synthesized from Anygen (Changsung, South Korea). siRNAs were purchased from Bioneer (Seoul, South Korea). MAL-PEG5K-NHS was from NOF Corporation (Tokyo, Japan) and methoxy PEG5K was from Sunbio (Anyang, South Korea).

2) Synthesis of R-PEG-PMT

PMT was synthesized with mannitol diacrylate and BPEI (1200 kDa) by

Michael addition reaction as previously reported (Park, T.E. *et al.*, 2012). R-PEG-PMT and methoxy PEG-conjugated PMT (PEG-PMT) were synthesized according to the previous method (Hwang do, W. *et al.*, 2011) with slight modification. Briefly, PMT and MAL-PEG5K-NHS with reactant molar ratio of 20:1 were dissolved in anhydrous methanol and DMSO in the proportion of 1:5 (v/v). After 4 h of stirring at room temperature (RT), RVG peptide was added to the solution with a molar ratio of 1.2 equivalent to MAL-PEG-NHS. The reaction mixture was stirred for another 48 h at RT. PEG-PMT as a control was synthesized by reaction of PMT and methoxy PEG in anhydrous methanol and DMSO in the proportion of 1:3 (v/v) for 24 h at RT. The reaction mixtures were dialyzed using dialysis membrane (MW cut off 10,000 for R-PEG-PMT and 8,000 for PEG-PMT) at 4°C for 48 h. The dialyzed polymer solution was lyophilized for 3 days. R-PEG-PMT was characterized by ^{1}H high resolution NMR spectrometer (AVANCE 600, Germany, Bruker - 600 mHz) to estimate the composition of PEG and RVG in PMT.

3) Measurement of particle size and zeta-potential

Particle size and zeta-potential of nanoparticles were measured using a dynamic light scattering spectrophotometer (DLS-7000; Otsuka Electronics, Japan). To measure nanoparticle size, R-PEG-PMT/siRNA and PEG-PMT/siRNA complexes were made at N/P 10. The zeta potential of the complexes at N/P 10 were measured with a 20° scattering angle at 25°C.

4) Gel retardation assay and RNase protection assay

Gel retardation assay was carried out using gel electrophoretic technique. Agarose gels were casted with 2% agarose dissolved in Tris-borate-EDTA (TBE) buffer. Polymers and control siRNA duplexes (0.25 μg) were complexed at various N/P ratios at RT for 45 min. After adding 6× dye, complexes were loaded in gels and electric current (60 V) applied for 45 min. Gels were illuminated by the ultraviolet lamp and analyzed. For RNase protection and relase assay, complexes and naked siRNAs were treated with RNaseA (0.1 μg/μl) for 30 min at 37°C and then RNase inhibitor was added and incubated for 5 min at 70°C. To release siRNAs from complexes, SDS solution (1%) was added to complexes and incubated for 2 h 30 min at 37°C.

5) Observation of morphology of R-PEG-PMT/siRNA complexes

The morphology of R-PEG-PMT/siRNA complexes prepared at an N/P ratio of 10 was observed by energy-filtering transmission electron microscopy (LIBRA 120; Carl Zeiss, Germany).

6) *In vitro* cell viability assay

Cell viability of Neuro2a (mouse neuroblastoma cells; ATCC number CCL-131) was measured by MTT assay. Cells were seeded at density of 10×10^4 cells/ml and grown to 80–90% confluence in 24-well plates. R-PEG-PMT, PEG-PMT and PEI were complexed with siRNA with different N/P ratios in the 500 μl serum free media. Complexes containing 50 pmoles of siRNA were added to the each well and incubated for 24 h. After incubation, MTT reagent was added to the each well and incubated for an additional 4 h. Medium was

aspirated and DMSO was added to each well to dissolve purple formazan. The optical density of colored solution was measured at 540 nm using a microplate reader (Tecan Infinite® 200 PRO; Männedorf, Switzerland).

7) *In vitro* knockdown efficiency

In vitro knockdown efficiency in six different cell lines (HepG2, A549, C2C12, HeLa, Neuro2a, SH-sy5y) was measured by luciferase assay. Cells were seeded at density of 2×10^4 cells/ml and grown to 50–60% confluence in 24-well plates as above. Purified pGL3 plasmids (0.5 μg) were delivered using Lipofectamine2000 according to the manufacture's protocol. At 24 h post-transfection, luciferase siRNA complexed with R-PEG-PMT, PEG-PMT or PEI (25 kDa) was treated to the cells and incubated for 4 h followed by replacement of media into serum-containing media. After 48 h of additional incubation, cells were lysed using passive lysis buffer and luciferase assay was carried out according to the manufacture's protocol (luciferase assay system protocol-Promega). Chemiluminometer (Tecan Infinite® 200 PRO; Männedorf, Switzerland) was used to measure relative light units. Relative light units (RLU) were normalized by total proteins measured by a BCA assay.

8) *In vitro* BACE1 knockdown efficiency

In vitro BACE1 knockdown efficiency was conducted by quantitative qRT-PCR and enzyme linked immunosorbent assay (ELISA). Neuro2a cells were seeded and grown in 6-well plates as described above and BACE1 siRNAs [sense:CUAGUAACUGGUGUUCUAU(dTdT)] complexed with R-PEG-

PMT, PEG-PMT, PEI or Lipofectamine 2000 were treated to the cells. At 48 h post-transfection, total RNA was extracted using TriZol solution following manufacture's protocol and cDNA was synthesized using AccuPower® CycleScript RT PreMix (oligo dT) from Bioneer. Quantitative real-time PCR was performed by using TOPrea qPCR 2X PreMIX (SYBR Green) on iCycler Real-Time Detection System (BioRad) using following primers :

BACE1-sense:TACTACTGCCCGTGTCCACC,

BACE1-antisense:ACAACCTGAGGGGAAAGTCC,

GAPDH-sense: TTGATGG CAACAATCTCCAC

GAPDH-antisense:CGTCCCGTAGACAAAATGGT.

The BACE1 mRNA level was normalized by GAPDH mRNA level. Total protein was extracted by a cycle of freeze and thawing in PBS with protease inhibitor cocktail. The relative concentration of BACE1 protein was calculated by BACE1 ELISA kit from Mybiosource (CA, USA).

9) Construction of *in vitro* BBB model

For optimization of the *in vitro* BBB culture, poly(ethylene terephthalate) membrane of cell culture inserts (24 well, 1.0 μm pore size) were coated with collagen I and IV mixture with concentration of 5 $\mu g/cm^2$ (40:60, collagen I: collagen IV, w/w) and dried overnight. Three different modes of transwell culture system was used. bEnd.3 cells (mouse brain endothelialpolyoma cells; ATCC number CRL-2299) was monolayer cultured or co-cultured with B-23 cells (rat astrocytoma cells; KCLB number 60049) with contact or non-contact method (Figure 42).

For monolayer culture, bEnd 3 cells were seeded on the luminal side of the insert at a density of 10×10^3 cells per filter. For non-contact co-culture, B-23 cells were seeded at density of 5×10^3 cells/ml and cultured in 24 well plates. At 18 h after culture of B-23, cell culture inserts were put into the plates and bEnd.3 cells were seeded on the luminal side of the insert at a density of 10×10^3 cells per filter. The contact co-cultured cells were prepared as follow: B-23 cells were plated on the bottom of the inserts and bEnd3 cells were cultured onto the membrane of insert.

The media was changed every other day and trans-epithelial electric resistance (TEER) was recorded using EVOM resistance meter (World Precision, FL, USA). Paracellular permeability of *in vitro* BBB cultures was tested using FITC-dextran (4 kDa). FITC-dextran was added to apical chamber of cultures at a density of 0.5 mg/ml and inserts were 100 ul of PBS in basal chamber was removed every 15 min to be analyzed and fresh PBS was added to the basal chamber. The amount of diffused dextran was determined using calibration curves established with stock solution. After TEER reaches 250 ohm•cm^2 by subtraction of the resistance of a collagen-coated filter without cells, *in vitro* BBB culture was used for permeability assay.

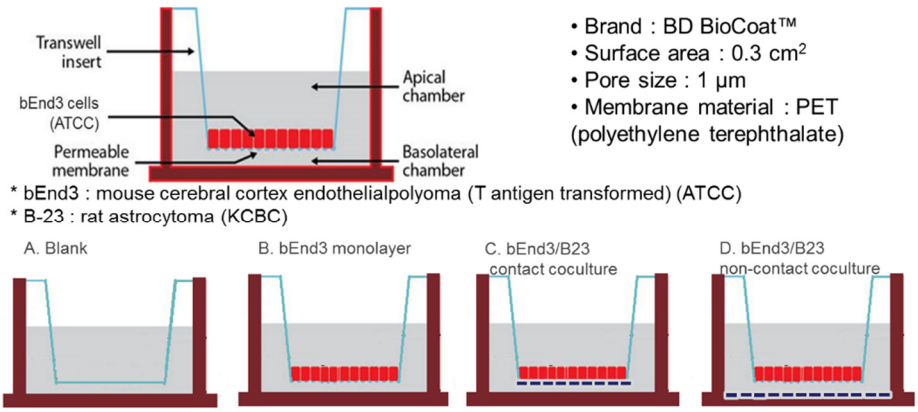

Figure 42. Schematic illustration of BBB culture systems *in vitro*

9) *In vitro* BBB permeability assay

Non-contact cultures of bEnd3 and B-23 cells on collagen coated inserts were prepared. After TEER reaches 250 ohm•cm^2 by subtraction of the resistance of a collagen-coated filter without cells, *in vitro* BBB culture was used for permeability assay. R-PEG-PMT, PEG-PMT and R-PEG-PEI were FITC labeled and complexed with 2.5 μg of control siRNA per well in PBS at N/P ratio of 10. At 15, 30, 45 and 60 min post-treatment, inserts were moved to new well where fresh PBS is contained. The concentrations of transported complexes were measured by multiple plate reader (Victor3; Perkin Elmer, USA) and analyzed using standard curve method. The apparent permeability coefficient (Papp, cm/s) for the complexes were calculated according to the equation : $\text{Papp} = \frac{\Delta Q/\Delta t}{A \times C0}$ where ΔQ/Δt is the rate of appearance of the complexes in the receiver chamber, C0 is the initial concentration of the solute in the donor chamber and A is the surface area (cm^2) of the filter.

10) *In vitro* BBB penetration mechanism

To determine the effect of cellular uptake inhibitors on permeability of R-PEG-PMT/siRNA complexes, *in vitro* BBB cultures were pre-treated with 12 μg/ml CH, 2 μg/ml of FI, 200 μM of GE or 400 nM of WO for 30 min and 150 nM of OD was treated at 10 min post-treatment of complexes. For competition assay, 10 mg/ml of GABA, 10 mg/ml of nACh or 1 mg/ml of RVG peptide was pre-treated for 30 min. To examine the energy-dependent transcytosis of R-PEG-PMT/siRNA complexes, permeability assay was conducted in 4°C and 37°C. The transported complexes were quantified and Papp was determined as described above.

11) Caveolin1 localization assay

At 30 min post-treatment of complexes, *in vitro* BBB culture was fixed by 4% of paraformaldehyde and immune-stained using caveolin1 antibody. Briefly, rabbit anti-caveolin 1 (1:100) was treated to fixed cell culture in blocking solution (3% BSA and 0.2% Triton X-100 in PBS) and incubated overnight at 4°C in humid chamber. The Alexa 594 anti-rabbit IgG (1:500) in blocking solution was incubated for 1 h at RT in humid chamber and nucleus was stained by DAPI solution for 2 min. The membranes of cell culture inserts were carefully scalped and put on the slide glasses. The location of caveolin1 was observed under confocal microscopy (SP8 X STED; Leica, Germany).

12) Optical imaging of distribution of R-PEG-PMT/siRNA complexes

For *in vivo* fluorescence study, cy5.5-labled BACE1 siRNAs (2 nmoles)

complexed with PEI, R-PEG-PEI, PEI, PEG-PMT or R-PEG-PMT were intravenously injected into 7-week-old BALB/c mice. At 4 h post administration, mice were sacrificed and organs were isolated and rinsed with ice-cold PBS immediately. The fluorescence images were acquired under excitation of 695 nm using the Optix-MX3 (Advanced Research Technologies, Canada). The fluorescence intensities in the regions of interest (ROI) were analyzed from the fluorescence images.

3. Results and Discussion

1) Synthesis and physiochemical characteristics of R-PEG-PMT

The proposed reaction scheme of the synthesis of R-PEG-PMT and PEG-PMT is shown in Figure 43. The compositions of the prepared R-PEG-PMT and PEG-PMT were confirmed by ^{1}H NMR spectroscopy (Figure 44). The morphology, particle size and zeta-potential of complexes account for *in vitro* and *in vivo* brain toxicity, endocytic pathways and tissue distribution (Rejman, J. *et al.*, 2004;Polo, S. and Di Fiore, P.P., 2006;Georgieva, J.V. *et al.*, 2011). Representative morphologies of the R-PEG-PMT/siRNA and PEG-PMT/siRNA complexes observed by TEM analysis is shown in Figure 45. As shown in Table 8, the conjugation of PEG on the surface of nanoparticles produced smaller sizes of R-PEG-PMT/siRNA (182.3 nm) and PEG-PMT/siRNA complexes (200 nm) compared to PMT/pDNA complexes (228.7 nm) (Park, T.E. *et al.*, 2012) at N/P ratio of 10. The nano-scaled R-PEG-PMT/siRNA and mPET-PMT/siRNA complexes (< 200 nm) could be suitable to be internalized via clathrin-mediated endocytosis and caveolae-mediated endocytosis (Canton, I. and Battaglia, G., 2012). The relatively neutral surface charges of R-PEG-PMT complexes and PEG-PMT ones at N/P ratio of 10 show suggested display of PEG on the particle surfaces (Table 8).

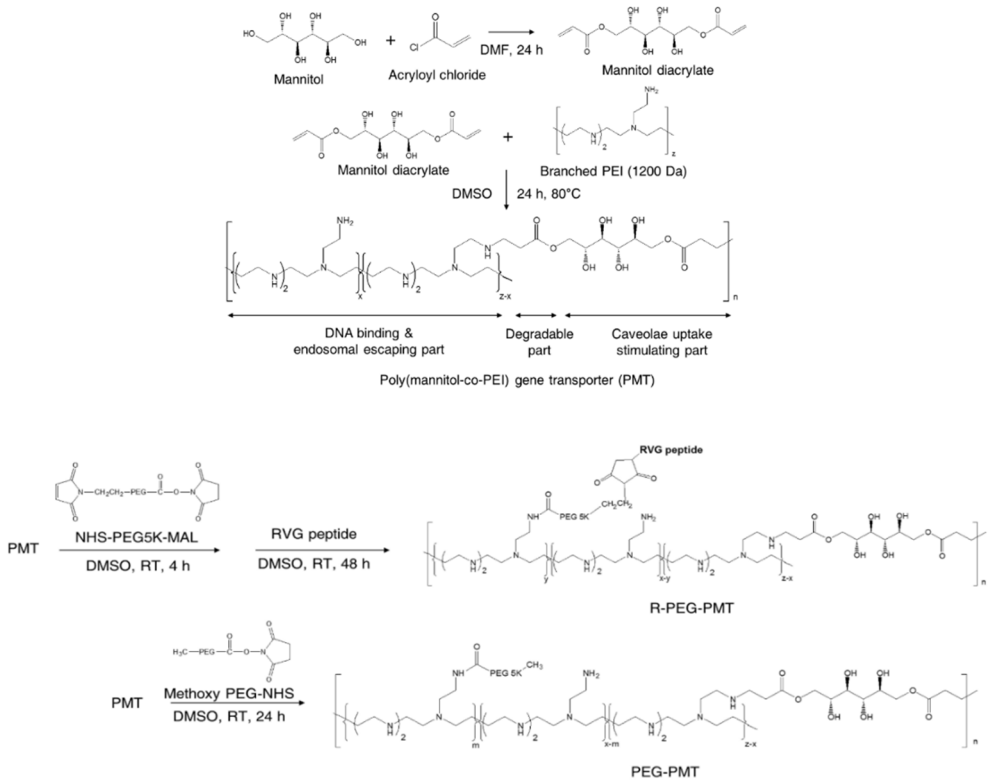

Figure 43. Schematic illustration of synthesis of R-PEG-PMT and PEG-PMT.

Table 7. The reactant concentration and synthetic yield of R-PEG-PMT

	Mass of reactants		Volume of solvent	Synthetic yield
R-PEG-PMT	RVG	20 mg	13 ml of methanol/DMSO (1:5 v/v)	54%
	NHS-PEG-MAL	27 mg		
	PMT	123 mg		
PEG-PMT	Methoxy PEG	26 mg	13 ml of methanol/DMSO (1:3 v/v)	68%
	PMT	123 mg		
R-PEG-PEI	RVG	20 mg	13 ml of methanol/DMSO (1:5 v/v)	57%
	NHS-PEG-MAL	27 mg		
	PMT	113 mg		

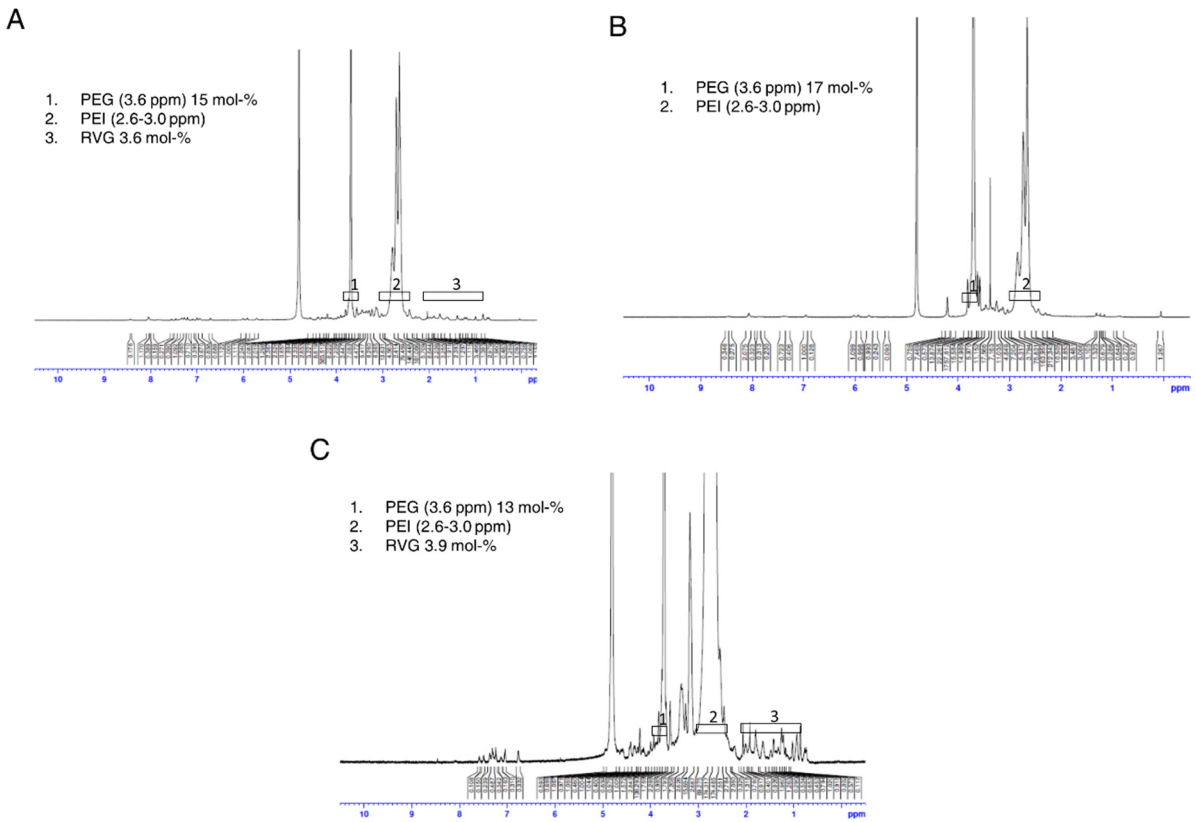

Figure 44. ^{1}H NMR analysis of (A) R-PEG-PMT, (B) PEG-PMT and (C) R-PEG-PEI.

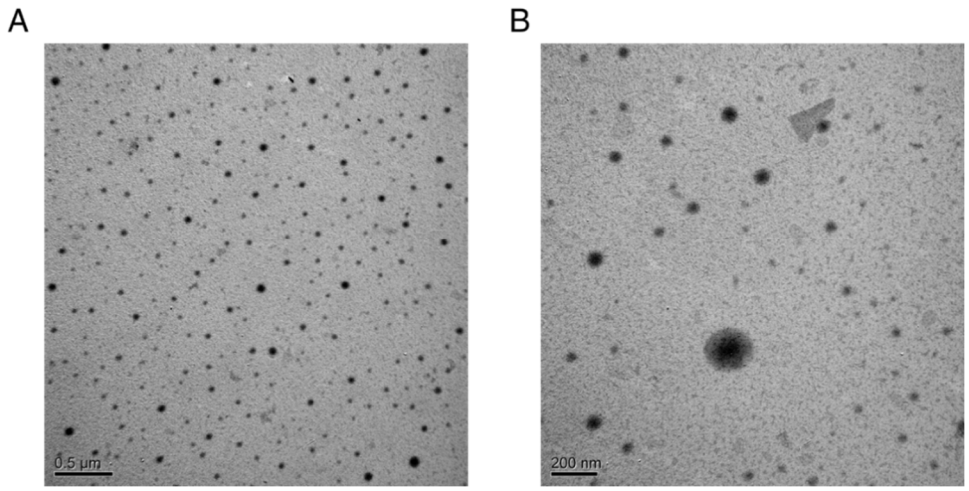

Figure 45. TEM images of (A) R-PEG-PMT/siRNA complexes (bar scale = 0.5 mm) and (B) PEG-PMT/siRNA complexes (bar scale = 200 nm) at N/P ratio of 10.

Table 8. Size and zeta potential of R-PEG-PMT/siRNA complexes

	Size (nm)	Zeta potential (mV)
R-PEG-PMT/siRNA complexes (N/P 10)	182.3 ± 3.4	10.4 ± 2.5
PEG-PMT/siRNA complexes (N/P 10)	200 ± 2.1	12.7 ± 1.3
R-PEG-PEI/siRNA complexes (N/P 10)	190.8 ± 5.7	11.5 ± 0.7

The most critical factors limiting the utility of siRNAs as therapeutics are their inherently unfavorable physiochemical properties to penetrate the negatively charged plasma membrane, their unstability and bioavailability in plasma (Castanotto, D. and Rossi, J.J., 2009). Naked siRNAs are vulnerable to RNase attack resulting in short half-life of only several minutes in plasma (Hickerson, R.P. *et al.*, 2008). Thus, efficient protection of siRNAs from harsh environment by cell uptake-favorable gene carrier is a vital prerequisite for RNAi therapeutics. Gel retardation assays confirmed the siRNA complexation by R-PEG-PMT. The cationic charged carriers form complexes with anionic charged siRNA through ionic interaction between amine groups of PEI and phosphate groups of siRNAs. From an N/P ratio 1, free siRNA moving toward the positive electrode was almost not detected, suggesting the neutralization and condensation of siRNAs by both gene carriers (Figure 46A). A small amount of free siRNAs observed at ratio of N/P 1 is associated with their inherent poor binding ability to cationic polymer because of stiff backbone structure (Liu, H. *et al.*, 2014). Next, siRNA protection and release assay was carried out under RNase environment to determine if complexation with R-PEG-PMT protects the siRNA from enzymatic degradation. The compact complexation of siRNA molecules with R-PEG-PMT and PEG-PMT efficiently prevented RNase-mediated siRNA degradation while naked siRNAs were degraded with 0.1 μg/μl of RNase (Figure 46B). This result indicated that both of R-PEG-PMT and PEG-PMT formed stable complexes with siRNAs protecting from the nuclease rich environment.

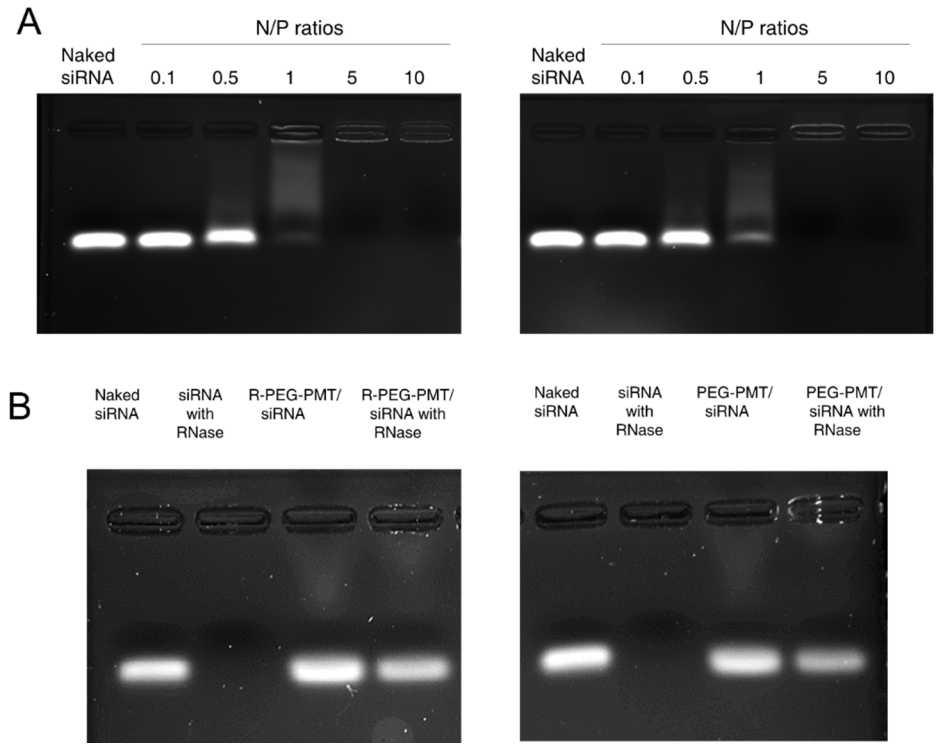

Figure 46. Gel retardation and RNase protection assay. (A) Gel electrophoresis of R-PEG-PMT/siRNA (left) and PEG-PMT complexes (right) at various N/P ratios. (B) siRNAs (0.2 nmoles) were released from R-PEG-PMT (left) and PEG-PMT (right) by addition of 1% SDS (lane 1: siRNA without RNaseA, lane 2: siRNA treated with RNaseA, lane 3: R-PEG-PMT/siRNA complexes without RNaseA, lane 4: PEG-PMT/siRNA complex with RNase).

2) *In vitro* cytotoxicity of R-PEG-PMT/siRNA complexes

Clinical application of cationic polymers for delivery of nucleic acids has been limited by its cellular toxicity. PEI which formed complexes with nucleic acids generally have lower toxicity although free PEIs damage body by interacting with anionic serum protein and red blood cells during circulation (Godbey, W.T. *et al.*, 1999). And the restored free PEIs in cytoplasm after release of nucleic acids also caused adverse effects by inhibiting normal cellular processing (Godbey, W.T. *et al.*, 2001). As main approaches to solve this problem while increasing the transfection efficiency, PEI has been modified to be degraded hydrolytically or enzymatically and modified with targeting ligands (Liu, K. *et al.*, 2012) with PEG spacer (Kircheis, R. *et al.*, 1999;Park, M.R. *et al.*, 2005;Park, M.R. *et al.*, 2008). Therefore, PMT (~14 kDa) was previously designed to have ester groups to be easily hydrolyzed in physiological condition producing low MW PEIs and mannitols and to quench the remained positive charges with partially negative charges of mannitols not too hard on the cells (Park, T.E. *et al.*, 2012). The employment of RVG peptide with PEG spacer to PMT is also expected to decrease the non-specific interaction with negatively charged cellular components. An *in vitro* cytotoxicity test was carried out using Neuro2a (neuroblastoma cells) by MTT method. The results showed that the R-PEG-PMT/siRNA and PEG-PMT/siRNA complexes were less cytotoxic compared to high molecular weight PEI (25 kDa) in broad N/P ratios implying that the above mentioned strategy markedly decrease the inherent cytotoxicity of cationic gene carriers (Figure

47A).

3) *In vitro* targeting specificity of R-PEG-PMT/siRNA complexes

Neuronal cell targeting specificity of gene carrier is an important factor for spatially controlled gene delivery while reducing undesired side effects elsewhere. It is well known that RVG peptide from rabies virus which preferentially infects the nervous system is able to direct the delivery of drugs to the brain neuronal cells via binding to the nAChRs. To verify the neuronal cell targeting specificity of R-PEG-PMT/siRNA complexes *in vitro* , R-PEG-PMT/siLUC (luciferase siRNA) and PEG-PMT/siLUC complexes were treated to various cell types and ratios of silencing efficiencies were examined. As shown in Figure 47B, employment of RVG peptide on the surfaces of complexes largely increased the silencing efficiency more than two folds using Neuro2a and SH-sy5y cell lines which are originated from neuronal cells while there was no evident increase of silencing effect using HepG2, A549, C2C12 and HeLa cells. This result suggests that R-PEG-PMT/siRNA complexes can be utilized for CNS targeted RNAi therapeutics.

4) *In vitro* BACE1 silencing effects of R-PEG-PMT/siRNA complexes

BACE1 was targeted gene known as beta-site APP cleaving enzyme 1 which generates the 40 or 42 amino acid-long amyloid-β peptides in the brain of Alzheimer's patients by cleavage of the APP. Several studies indicated that protein levels of BACE1 are elevated in brain region affected by AD, implying that abnormal BACE1 activity contributes to AD pathogenesis (Jiang, S. *et al.*,

2014). A great effort has been made to down-regulate BACE1 using specific inhibitors although open structure of the active sites of BACE1 interfere with their usefulness (Vassar, R., 2002). Thus, controlling BACE1 expression in genetic level has been regarded as a promising way for efficient treatment of AD (Singer, O. *et al.*, 2005;Alvarez-Erviti, L. *et al.*, 2011). Neuro2a cells were transfected with R-PEG-PMT/siBACE1 complexes for 48 h and silencing effect was analyzed in levels of mRNA and protein via qRT-PCR and ELISA method, respectively. As shown in Figure 48A, the increase of BACE1 silencing efficiencies was observed by increasing the concentrations of treated siRNAs. R-PEG-PMT/siBACE1 complexes down-regulated BACE1 expression with similar efficacies of PEI 25K and Lipofectamine2000 used as positive controls. However, PEG-PMT/siBACE1 complexes significantly provided the lower silencing effect in a broad range of N/P ratios compared to R-PEG-PMT/siBACE1 complexes. Similar patterns of silencing efficiencies of complexes and lipoplexes were observed in BACE1 protein level measured using ELISA method (Figure 48B). It is reasonable to assume that employment of PEG to PMT decreased the transfection efficiency *in vitro* because of reduced attachment to cellular membrane by shielding cationic charges on surfaces of the complexes (Park, M.R. *et al.*, 2005) while RVG ligands facilitated the cellular uptake of complexes with offsetting against the PEG effect.

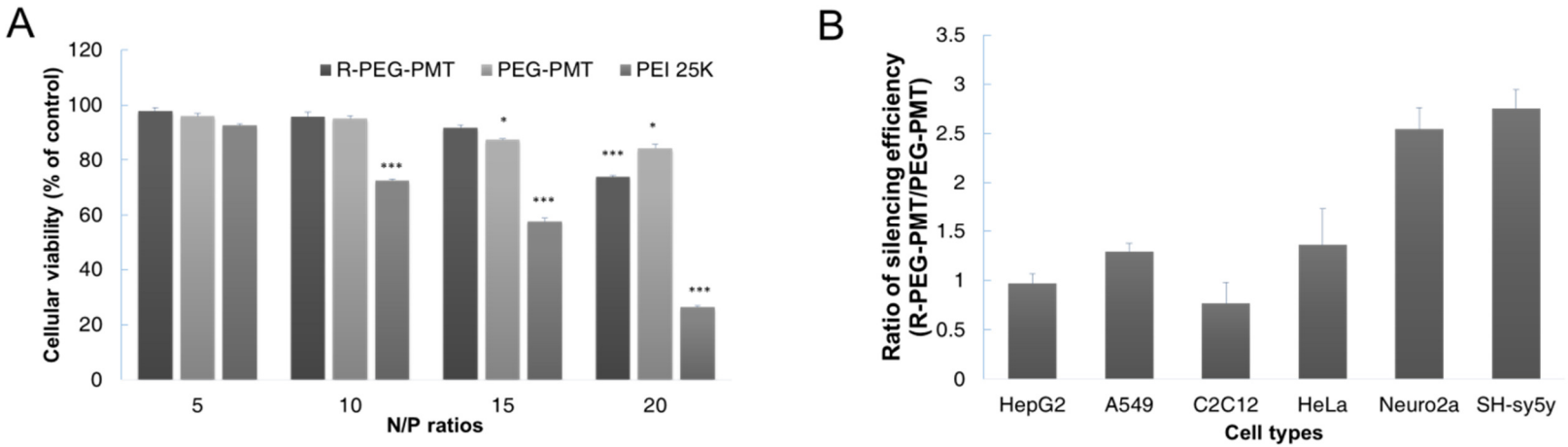

Figure 47. Cytotoxicity and specificity of R-PEG-PMT /siRNA complexes *in vitro* . (A) *In vitro* cytotoxicity of complexes at various N/P ratios was measured using MTT assay method and given as percentage of control in Neuro2A cells. (B) *In vitro* targeting specificity of R-PEG-PMT/siRNA complexes was examined using variety of cell lines. HepG2, A549, C2C12, HeLa, Neuro2A and SH-sy5y cells pre-transfected with same amount of pGL3 plasmids were treated with R-PEG-PMT/siLuciferase and PEG-PMT/siLuciferase complexes. The ratio of silencing efficiency of complexes in each cell line was analyzed by measuring luminescence at 48 h post-transfection (n = 3, error bar represents standard deviation; *$p < 0.1$, **$p < 0.05$, ***$p < 0.01$, one-way ANOVA)

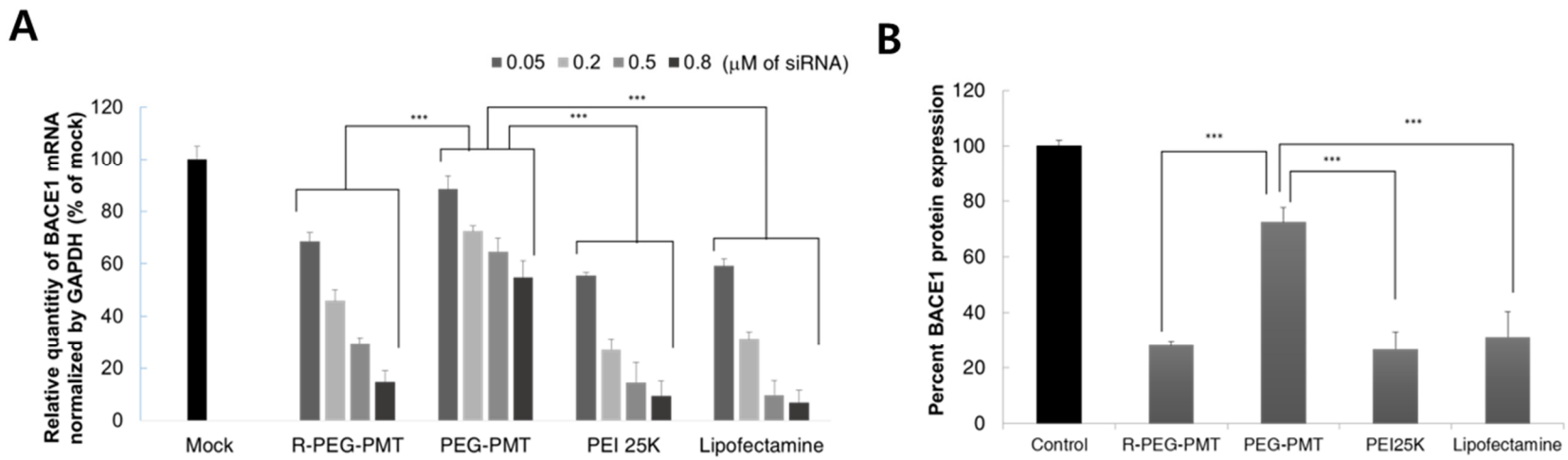

Figure 48. Silencing efficiency of R-PEG-PMT/siRNA complexes *in vitro* . BACE1 siRNAs complexed with R-PEG-PMT, PEG-PMT or PEI 25 kDa or encapsulated with Lipofectamine2000 were delivered in Neuro2a cells. At 48 h post-transfection, silencing efficiencies of complexes and lipoplexes were determined in levels of (A) BACE1 mRNA expression by qRT-PCR and (B) protein expression by ELISA method. (n = 3, error bar represents standard deviation; *p < 0.1, **p < 0.05, ***p < 0.01, one-way ANOVA)

5) *In vitro* BBB permeability of R-PEG-PMT/siRNA complexes

As a quick assay method of permeability of nanoparticles through BBB, cell culture model has been widely utilized (Ragnaill, M.N. *et al.*, 2011;Hanada, S. *et al.*, 2014). For BBB permeability studies, *in vitro* BBB model was built by non-contact co-culture of bEnd.3 (mouse brain capillary endothelial cell line) and B-23 (rat astrocytoma cell line) on trans-wells coated with mixture of collagen I and collagen IV. To determine the establishment of *in vitro* BBB model, TEER of *in vitro* model and diffusive permeability of FITC-dextran (4 kDa) were measured (Figure 49). The *in vitro* BBB permeability of FITC-labeled complexes were analyzed by measuring fluorescence intensity of transported complexes. To determine the function of mannitol backbone in PMT on BBB permeability, PEI (25 kDa) modified with RVG ligand with bridge of PEG (5 kDa) (R-PEG-PEI) was employed as a control group. Some pharmaceutical nanoparticles use the paracellular route to cross over BBB by accelerating the breakdown of the tight junction (Brun, E. *et al.*, 2012), while other use the transcellular transport via specific interaction with surface of endothelial cells (Karkan, D. *et al.*, 2008;Liu, Y. *et al.*, 2009). The integrity of *in vitro* BBB tight junction at pre- and pro-treatment of complexes was examined to assess the possible risk by breakdown of BBB. The TEER values of the monolayers did not change significantly during the experimental period (date is not shown) ensuring little effects of complexes on integrity of monolayer.

The Papp of FITC-labled R-PEG-PMT, PEG-PMT and R-PEG-PEI/siRNA complexes at 4°C and 37°C are shown in Table 9. At the same concentrations,

the flux of R-PEG-PMT/siRNA complexes was 2.2-fold higher than PEG-PMT/siRNA complexes indicating the efficacy of RVG-mediated surface modification on BBB permeability. The energy dependence on transport of complexes was examined by comparing the Papp values between at 37°C and 4°C which inhibits energy-dependent pathways. At normal internal body temperature, the R-PEG-PMT/siRNA and R-PEG-PEI/siRNA complexes showed 3.73-fold and 3.06-fold higher Papp values respectively than those at energy-blocked temperature implying the energy dependent mechanism of RVG ligand-mediated internalization at BBB rather than passive diffusion. On the other hand, PEG-PMT/siRNA complexes showed only 1.37-fold higher Papp values at 37°C than at 4°C. Furthermore, a possible role of PMT in BBB penetration was demonstrated by 1.26-fold higher Papp value of R-PEG-PMT/siRNA complexes than that of R-PEG-PEI/siRNA complexes.

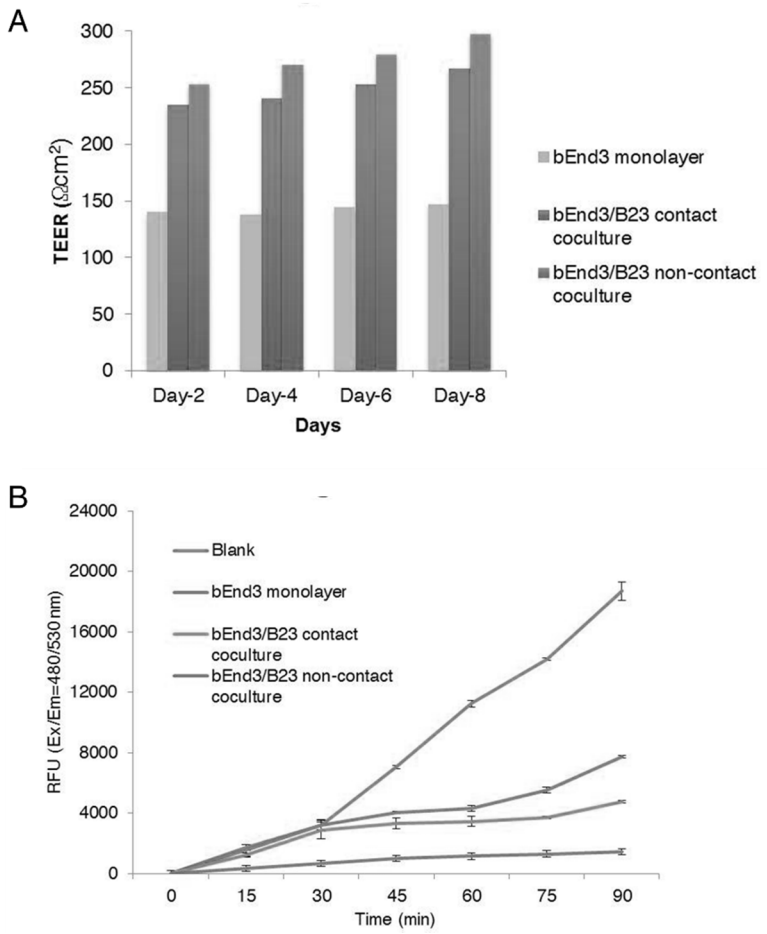

Figure 49. TEER and permeability of FITC-dextran (4 kDa) in different *in vitro* BBB cell layers. (A) TEER was measured using EVOM on day 2, 4, 6 and 8 and (B) penetration of FITC-dextran (4 kDa) across *in vitro* BBB culture was analyzed using multiple plate reader (Victor 3, Perkin Elmerin, USA) in monocultured cell layer (bEnd.3 cell line), contact co-culture of bEnd.3 cell line and B-23 cell line, and non-contact co-culture of bEnd.3 cell line and B-23 cell line on collagen-coated 24-well insert systems (n = 3, error bar represents standard deviation; *$p < 0.1$, **$p < 0.05$, ***$p < 0.01$, one-way ANOVA compared to that of control).

Table 9. BBB permeability of complexes *in vitro*

Complexes	**Temperature (°C)**	**Papp (10^{-5}cm/sec)**
R-PEG-PMT/siRNA	37	15.1±2.66
	4	4.01±0.84
PEG-PMT/siRNA	37	6.76±0.42
	4	4.95±1.27
R-PEG-PEI/siRNA	37	11.9±0.48
	4	3.88±1.01

To confirm the uptake mechanism of R-PEG-PMT/siRNA complexes, a competition assay was conducted by pre-treatment of RVG peptide, nACh and GABA which are possibly associated with uptake of the complexes. There are considerable evidences that nAChR is a specific binding site of RVG which is a component of rabies virus (Gastka, M. *et al.*, 1996). Liu et al. suggested that $GABA_B$ receptor was possibly involved in the mechanism of RVG-mediated endocytosis pathway of RVG modified poly(amido amine) dendrimer. Hence, RVG ligand-mediated internalization of R-PEG-PMT/siRNA complexes can be assumed to be via nAChRs and/or $GABA_B$ receptors expressed on brain endothelial cells. As shown in Table 10, pre-treatment of RVG peptide and nACh significantly reduced the permeability of R-PEG-PMT/siRNA complexes by 65 and 71 percent respectively, while there was little change in permeability by treatment of $GABA_B$ (2.6 percent reduction). This result suggests that BBB penetration of R-PEG-PMT/siRNA complexes is mediated by receptor-mediated transcytosis following binding of RVG ligands to nAChRs.

Table 10. Competition assay of R-PEG-PMT/siRNA complexes

Pre-treated compounds	**Papp (10^{-5}cm/sec)**
No compound	15.1±2.66
GABA	14.7±1.35
RVG	5.24 ±1.21
nACh	4.31±0.54

6) Mechanistic study of *in vitro* BBB penetration of R-PEG-PMT/siRNA complexes

The entry pathway into BBB is a decisive factor in subcellular trafficking and thereby the nanoparticles' fates. The mode of endocytosis of R-PEG-PMT/siRNA complexes was determined using *in vitro* BBB culture by analyzing the effects of metabolic inhibitors on the permeability. *In vitro* BBB cultures were treated with inhibitor drugs and FITC-labeled polyplexes were added to apical sides of inserts at 30 min post-treatments. CH and WO were utilized to disrupt clathrin-mediated endocytosis and macropinocytosis respectively. FI and GE were treated as inhibitors of caveolae-mediated endocytosis. OD, otherwise, a drug which increases the mobility of caveolae was treated at 10 min post-treatment of complexes to stimulate the caveolae-mediated endocytosis. Decrease of permeability of complexes by specific metabolic inhibitor reflects the dependence of specific uptake pathway. As shown in Figure 50, it was confirmed that clathrin-mediated endocytosis, caveolae-mediated endocytosis and macropinocytosis are all involved in uptakes of those complexes to greater or lesser degree. When it comes to R-PEG-PMT/siRNA and PEG-PMT/siRNA complexes, caveolae-mediated endocytosis most largely contributed to entry into BBB, on the other hand, penetration of R-PEG-PEI/siRNA complexes into BBB was less dependent on caveolae-mediated endocytosis. Treatment of OD significantly increased the permeability of R-PEG-PEI/siRNA complexes by 1.4-fold implying the importance of stimulation of caveolae-mediated endocytosis on enhancing transcytosis of complexes across BBB. No effect of OD on permeability of

PMT-based complexes indicates that caveolae has already been stimulated and thereby mobilized from plasma-membrane to near the nucleus.In caption 1, it was demonstrated that osmotic active PMT specifically stimulated the caveolar endocytosis whose trafficking pathway efficiently avoids the lysosomal degradation. The selective stimulation of caveolar endocytosis is associated with induction of caveolin-1 phosphorylation through activation of Src-kinase in response to hyperosmotic properties of the PMT. To confirm the stimulation of caveolar endocytosis by PMT, caveolin-1 was stained at 30 min post-treatment of R-PEG-PMT/siRNA or PVG-PEI/siRNA complexes. The caveolar endocytosis has been known to occur via stimulation by certain ligands or cellular stress, which differs from a type of constitutive endocytosis including clathrin-mediated endocytosis. When stimulated, caveolae which are normally immobile at plasma membrane are budded and pinched off following phosphorylatation of caveolin-1. As shown in Figure 51, plasma membrane-bound caveolae vesicles were localized nearby nucleus by treatment of R-PEG-PMT/siRNA complexes while R-PEG-PEI/siRNA complexes a little affected the mobility of caveolae vesicles. The importance of caveolin-1 mediated signaling on entry of pathogen into brain endothelial cells via nAChRs has been reported (Chi, F. *et al.*, 2011). It is reasonable to assume that osmotically-active PMT provided stimuli on *in vitro* BBB culture enhancing the caveolae-mediated endocytosis and thereby enhanced the permeability across the BBB (Park, T.E. *et al.*, 2012).

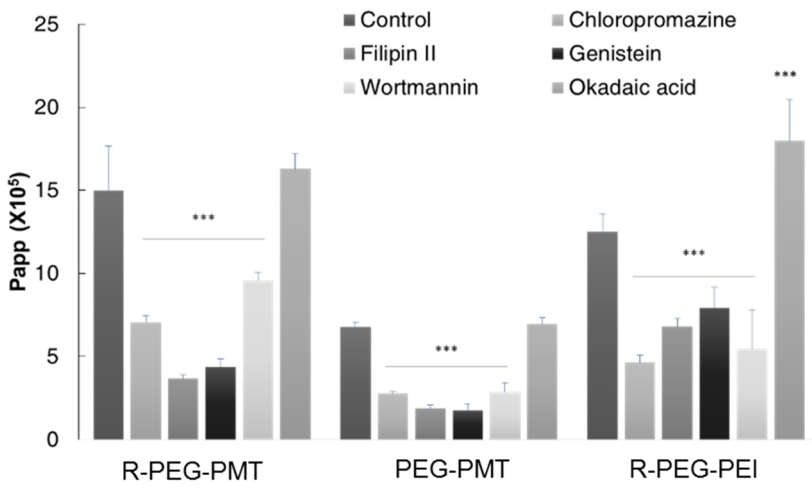

Figure 50. Endocytosis mechanism for the penetration of complexes through BBB *in vitro* . (A) *In vitro* BBB cultures were pre-treated with endocytosis inhibitors-12 ug/ml of CH, 2 ug/ml of FI, 200 uM of GE or 400 nM of WO and FITC-labeled complexes were added to the apical side of inserts. 150 nM of OD, a drug that stimulate the caveolar endocytosis, was treated at 10 min post-treatment of complexes. Effect of endocytosis inhibitors or stimulator on the penetration of complexes was determined by measuring fluorescence intensities of transported complexes. (n = 4, error bar represents standard deviation; *p < 0.1, **p < 0.05, ***p < 0.01, one-way ANOVA compared to that of control without metabolic drug)

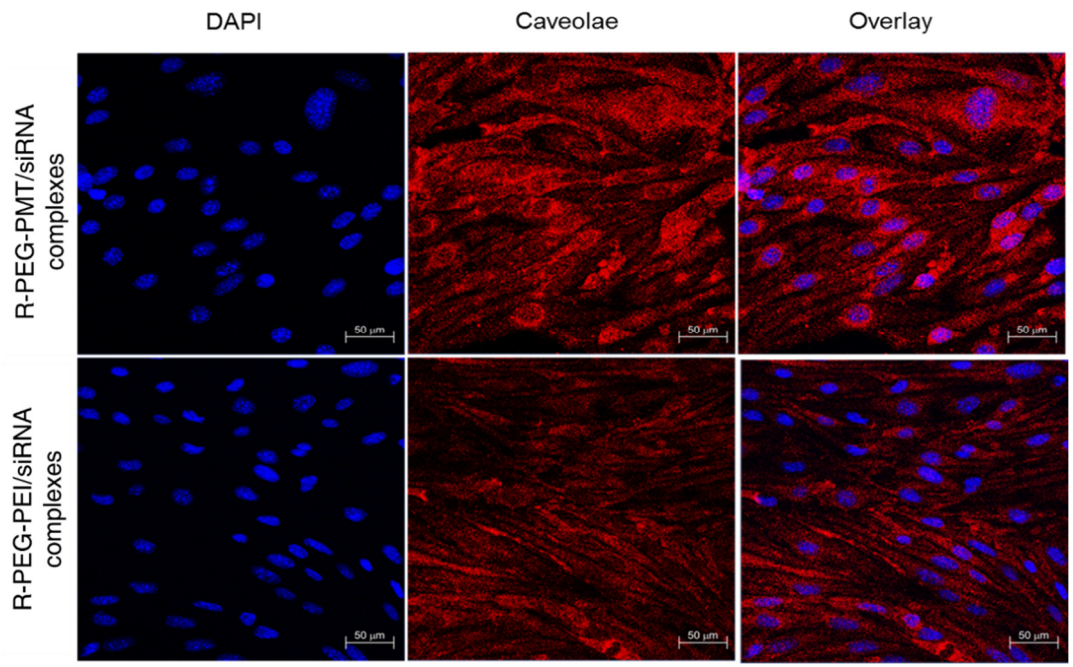

Figure 51. The localization of caveolae vesicles was observed under confocal microscopy. The caveolin-1 was immunostained (red signal) at 30 min post-treatment of R-PEG-PMT/siRNA or R-PEG-PEI/siRNA complexes to determine the stimulation of caveolar endocytosis by PMT.

7) Optical imaging of distribution of R-PEG-PMT/siRNA complexes

Increased brain uptake of R-PEG-PMT/siRNA complexes was examined using Optix MX3 imaging system. The cy5.5-labeled siRNAs complexed with variety of polymeric carriers were intravenously injected. At 4 h post-administration, intensity of fluorescence signal from isolated tissues were immediately measured by Optix MX3 system and analyzed by OptiView analysis software. As shown in Figure 52, much higher accumulation of cy5.5-siRNAs in brain region was observed in the R-PEG-PMT mediated delivery group implying the improved brain uptake efficiency. The fluorescence intensity in brain of mouse given R-PEG-PMT/cy5.5-siRNA complexes was approximately 1.8-fold higher than those of PEI and R-PEG-PEI/cy5.5-siRNA complexes groups and 5.8-fold higher than PEG-PMT/cy5.5-siRNA complexes group. Many cationic nanoparticle are rapidly removed from the circulation by macrophages in few hours. Therefore, organs such as liver and lungs which have a large population of resident macrophage retain majority of circulating nanoparticles inducing off-target effect (Kirtane and Panyam, 2013). The R-PEG-PEI, PEG-PMT, and R-PEG-PMT/siRNA complexes appear to be less captured in lungs and liver compared to PEI/siRNA complexes due to avoidance of macrophage uptake by modification with PEG. Furthermore, RVG-mediated delivery groups showed lower fluorescence intensity in lungs than PEG-PMT mediated delivery group indicating that RVG ligand provided the evasion of accumulation in lungs.

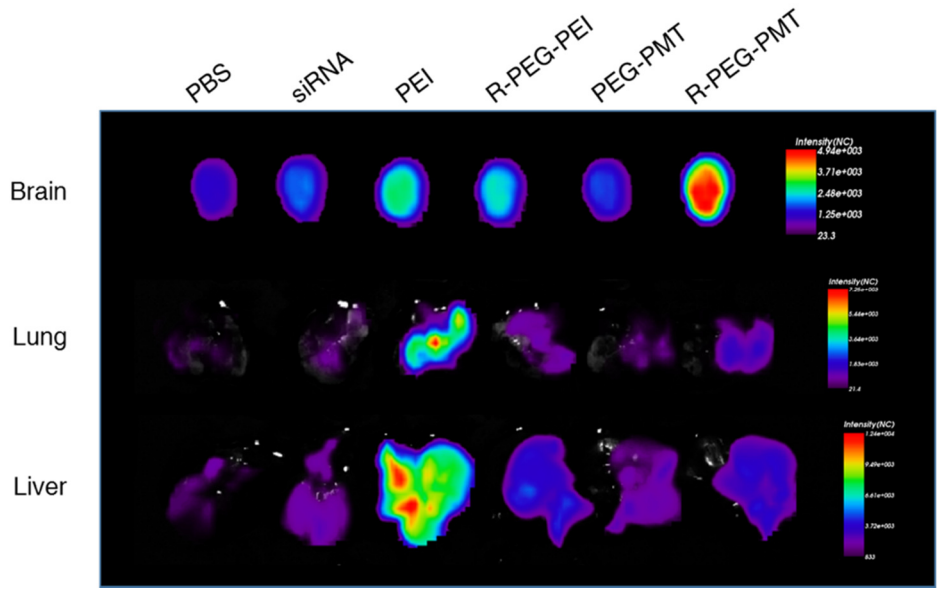

Figure 52. Accumulation of cy5.5 labeled siRNAs complexed with variety of gene carriers in brain. At 4 h post-treatment of complexes, isolated organs were imaged in an Optix MX3 system by organ type. Higher accumulation of cy5.5-siRNAs complexed with R-PEG-PMT in the brain was determined by strong fluorescence intensity.

4. Conclusion

The development of effective gene delivery system remains a key requirement for clinical application of RNAi therapeutics in brain diseases. In order to deliver siRNAs to brain neuronal cells, non-viral gene carriers are required to cross over BBB and overcome intracellular barrier by avoiding lysosomal degradation. For, a novel gene carrier, PMT modified with RVG (R-PEG-PMT) was synthesized which provides enhanced brain-targeted RNAi effect *in vitro*. It was previously suggested that osmotically active PMT specifically stimulates the caveolae-mediated endocytosis and thus avoids the lysosomal degradation as an obvious way of increasing transfection efficiency. In this study, it was determined that employment of RVG ligand to PMT provided synergistic effect on improved BBB penetration via receptor-mediated transcytosis with well-regulated mode of uptake pathway and enhanced siRNA delivery.

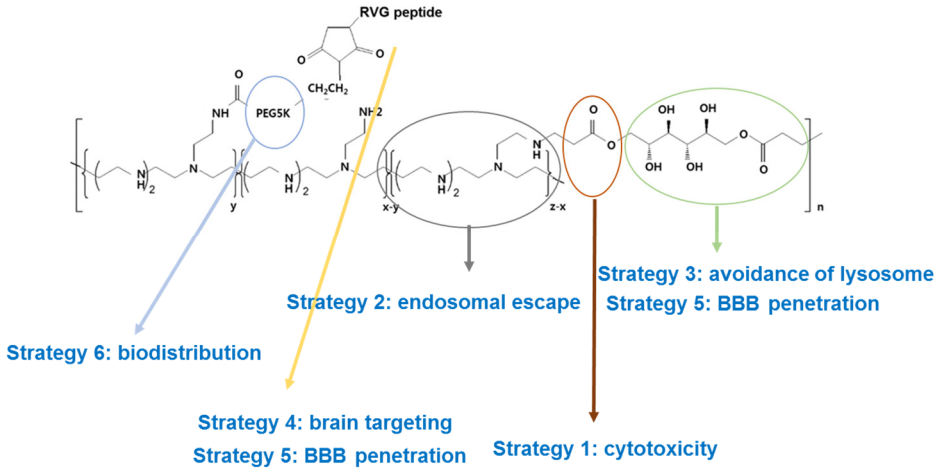

Figure 53. Functional parts of R-PEG-PMT

Chapter 3. RNA interference therapeutic potential of poly(manntiol-co-PEI) modified with rabies virus glycoprotein in AD

1. Introduction

Age related-neurodegenerative disease such as Alzheimer's disease (AD) is a major medical problem worldwide. While the prevalence of neurodegenerative diseases is escalating, treatment to prevent the progression of AD has not been identified. In situation in which conventional therapies are unavailable, RNAi therapeutic is a promising strategy for ultimate treatment of AD. For successful clinical application of brain RNAi therapeutics, R-PEG-PMT was designed to overcome intracellular and extracellular barriers (Table 1) and whether it could conquer the challenges was examined *in vitro* through first and second approaches. Although the R-PEG-PMT/siRNA complexes have shown great potential for use in brain gene delivery *in vitro* , a real biological environment may actually hinder benefits of R-PEG-PMT.

In this study, *in vivo* therapeutic potential of R-PEG-PMT was examined. β–secretase 1 (BACE1) which plays an early role in amyloid plaque generation was targeted to evaluate the therapeutic potential of R-PEG-PMT system for AD. Although BACE1 is rate-limiting factor for production of pathogenic Aβ42, pharmaceutical BACE1 inhibition has presented many challenges because active site of BACE1 is more open and less hydrophobic than other protease (Singer, O. *et al.*,

2005). Therefore, post-transcriptional regulation of BACE1 is considered as alternative approach. R-PEG-PMT was validated as a brain targeted non-viral vector by its capability of central nerve system (CNS) targeting specificity and siRNA delivery efficiency *in vivo*.

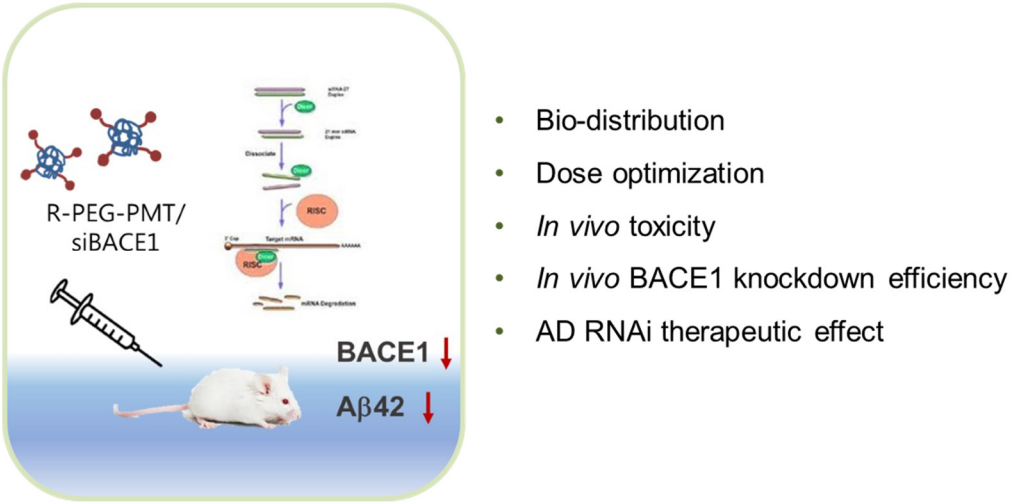

Figure 54. Experimental flow of the study

2. Materials and method

1) *In vivo* transfection

Intravenous administration of GAPDH siRNA [sense: CUAGUAACUGGUGU UCUAU(dTdT)] or BACE1 siRNA complexed with polymers was performed in six-week-old BALB/C (5 mice/group) following the policy and regulations for the care and use of laboratory animal (Laboratory Animal Center, Seoul National University, Korea). Mice were kept in the laboratory animal facility with temperature and relative humidity maintained at 23 ± 2 °C and 50 ± 20%, and a 12 h light/dark cycle. All experimental protocols were reviewed and approved by the Animal Care and Use Committee at Seoul National University (SNU-130705-3-2). The complexes were intravenously injected three times at 3, 8 and 13 days before euthanization. Mice were sacrificed and whole organs were isolated immediately for extraction of total RNA and proteins using TRizol solution and RIPA buffer respectively. The blood samples were collected and serum alanine transaminase (ALT), aspartate transaminase (AST), and blood urea nitrogen (BUN) concentrations were assayed by a commercial laboratory (Neodin Vetlab, Seoul, South Korea).

2) *In vivo* transfection efficiency (qRT-PCR)

cDNA was synthesized using AccuPower® CycleScript RT PreMix (oligo dT) from Bioneer. Quantitative real-time PCR was performed by using TOPrea qPCR 2X PreMIX (SYBR Green) on iCycler Real-Time Detection System (BioRad) using following primers : BACE1-sense:TACTACTGCCCGTGTCCACC, BACE1-

antisense: ACAACCTGAG GGGAAAGTCC, GAPDH-sense: TTGATGGCAACAATCTCCAC and GAPDH-antisense: CGTCCCGTAGACAAAATGGT. The BACE1 mRNA level was normalized by GAPDH mRNA level.

3) *In vivo* transfection efficiency (western blotting)

For western blotting, one of the five samples from each group whose knock down efficiency approaches mean value based on qRT-PCR data was loaded on the SDS-PAGE (4~15%) and run at 150 V for 80 min. Protein was transferred to the nitrocellulose membranes using a wet transfer method on 12 V for 60 min and pre-blocked with 5% skim milk in Tris-buffered saline Tween 20 solution overnight at 4°C with agitation, and incubated with bace-1 IgG (rabbit polyclonal antibody) or gapdh IgG (rabbit polyclonal antibody) overnight at 4 °C. After washing three times for each 15 min, goat anti-rabbit IgG-HRP was treated and incubated for 1 h with agitation. Bands of interest were imaged with a CCD camera gel documentation system (Chemidoc; Bio-rad, USA).

3. Results and discussion

1) Targeting specificity of R-PEG-PMT/siRNA complexes

The potential for brain-targeted R-PEG-PMT-mediated siRNA delivery was examined *in vivo*. For validation of tissue distribution of R-PEG-PMT/siRNA complexes, siRNAs against GAPDH as a housekeeping gene, were complexed and intravenously injected in mice three times at intervals of five days. As shown in Figure 55A-D, difference of decrease in GAPDH mRNA expression was observed among tissue types and delivery vehicles. The treatment of R-PEG-PMT/siGAPDH complexes showed significant decrease in expression level of GAPDH mRNA in brain region without effect on other types of tissues whereas PEG-PMT and PEI/siGAPDH complexes provided no effect on brain. Injection of R-PEG-PEI/siGAPDH resulted in significant decrease of GAPDH expression in brain region although it also had effect on kidney region. The result of tissue specificity study confirmed that RVG-assisted delivery of complexes is useful for the brain-directed siRNA delivery.

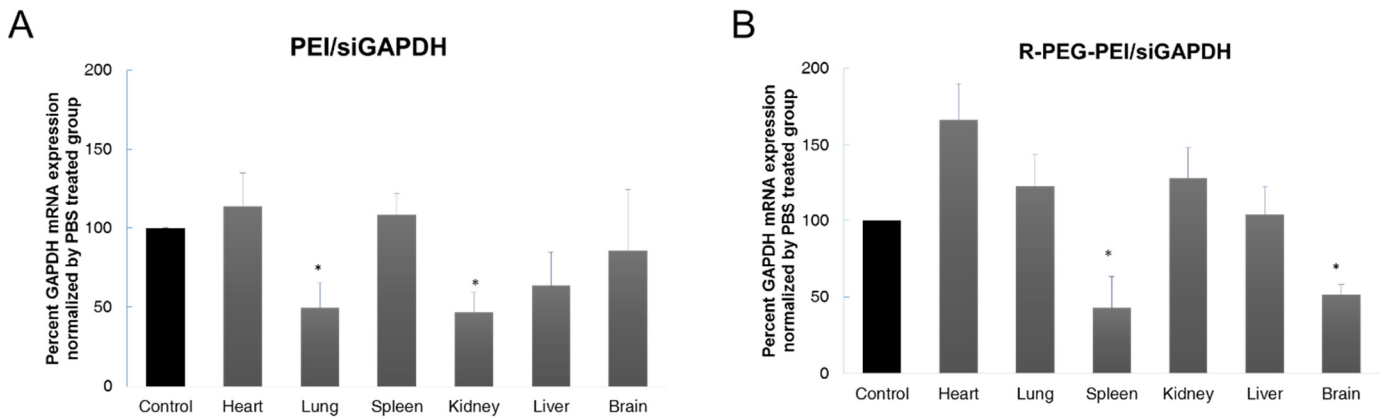

Figure 55. Tissue specificity of R-PEG-PMT/siRNA complexes *in vivo.* 2 nmoles of GAPDH siRNAs complexed with (A) PEI, (B), R-PEG-PEI were intravenously injected to mice three times at intervals of five days. Mice were sacrificed and whole organs were isolated immediately for extraction of total RNA. The level of GAPDH mRNA expression compared to β-Actin mRNA expression was analyzed using qRT-PCR and normalized by PBS group. (n = 5, error bar represents standard deviation; *p < 0.1, **p < 0.05, ***p < 0.01, one-way ANOVA) (continue)

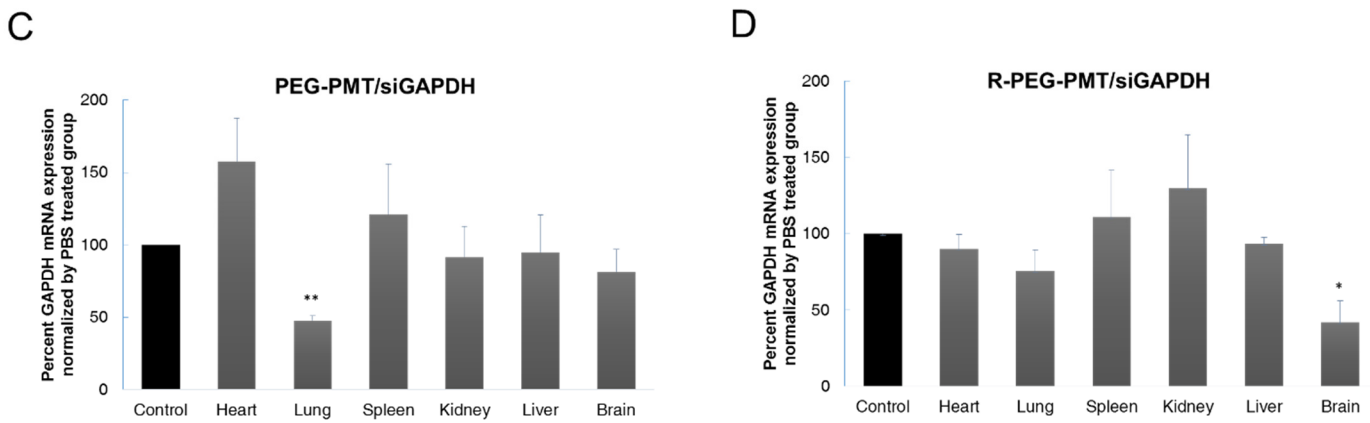

Figure 55. *In vivo* tissue specificity of R-PEG-PMT/siRNA complexes. 2 nmoles of GAPDH siRNAs complexed with ((C) PEG-PMT, or (D) R-PEG-PMT were intravenously injected to mice three times at intervals of five days. Mice were sacrificed and whole organs were isolated immediately for extraction of total RNA. The level of GAPDH mRNA expression compared to β-Actin mRNA expression was analyzed using qRT-PCR and normalized by PBS group. (n = 5, error bar represents standard deviation; *p < 0.1, **p < 0.05, ***p < 0.01, one-way ANOVA)

2) Dose optimization of R-PEG-PMT/siRNA complexes

Dose optimization for treatment of complexes was preceded by systemically delivering different amounts of BACE1 siRNAs (0.04, 0.4, 2, 4 nmoles) complexed with carriers three times at intervals of five days. Mice administrated below 2 nmoles of siRNAs complexed with R-PEG-PMT and PEG-PMT were maintained under normal condition, however, 4 nmoles of complexed siRNAs instantly killed 75 percentage of mice. The relative quantities of BACE1 mRNA normalized by GAPDH mRNA were analyzed in cortex and hippocampus parts of mice given 0.04, 0.4 or 2 nmoles of complexed BACE1 siRNAs. The result of dose optimization study showed that the amount of complexed siRNAs which have effect on both cortex and hippocampus parts is level of 2 nmoles (Figure 56).

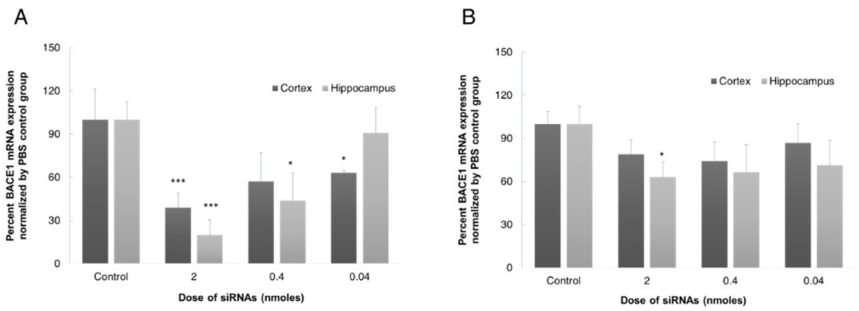

Figure 56. Dose optimization of R-PEG-PMT and PEG-PMT/siRNA complexes. Different amounts of BACE1 siRNAs (0.04, 0.4, 2 and 4 nmoles) complexed with (A) R-PEG-PMT or (B) PEG-PMT three times at intervals of five days. Four nanomoles of siRNAs complexed with R-PEG-PMT and PEG-PMT killed 75 percentage of mice instantly and killed 25 percentage of mice within two days. The relative quantities of BACE1 mRNA normalized by GAPDH mRNA were analyzed in cortex and hippocampus parts using qRT-PCR (n = 5, error bar represents standard deviation; *p < 0.1, **p < 0.05, ***p < 0.01, one-way ANOVA compared to that of control).

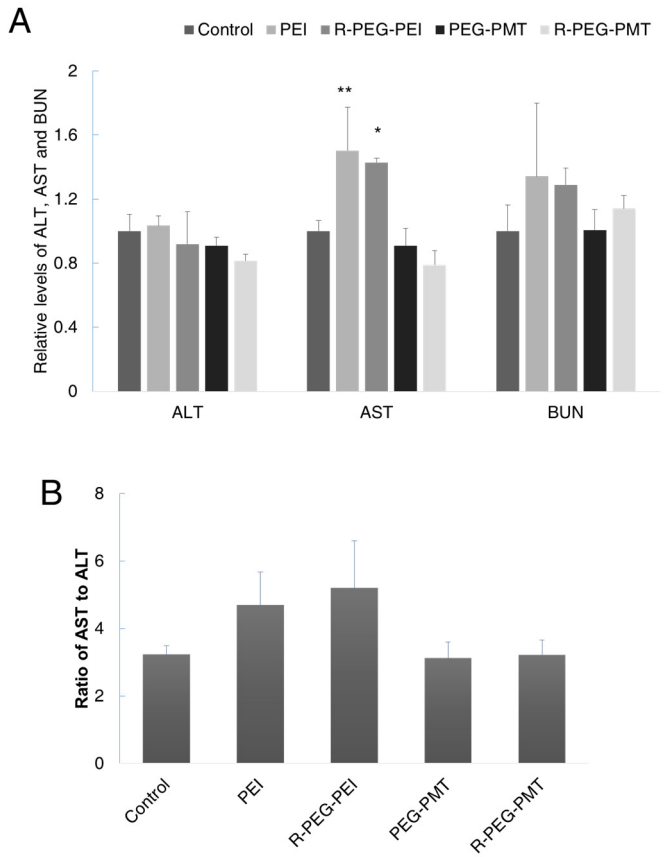

Figure 57. ALT, AST and BUN levels in serum. After finishing the course of administration, blood sampling was conducted and serum ALT, AST and BUN levels were measured. (A) Relative levels of ALT, AST, and BUN and (B) the ratio of AST to ALT was analyzed to examine the possible damage in liver and kidney by administration of complexes (n = 5, error bar represents standard deviation; *$p < 0.1$, **$p < 0.05$, ***$p < 0.01$, one-way ANOVA compared to that of control).

A drug-induced injury in liver and kidney at optimized dosing was also determined by measuring serum AST, ALT and BUN levels after finishing course of drug administration (Figure 57). No significant change in serum levels of AST, ALT and BUN occurred in mice given R-PEG-PMT and PEG-PMT/siBACE1 complexes. Although increase in serum level of ALT was observed in mice given PEI and R-PEG-PEI/siBACE1 complexes, the ratio of AST to ALT was not significantly changed implying no possible damage in liver. The result of *in vivo* toxicity indicates that liver and renal functions are maintained in all groups in the course of administration.

3) BACE1 knock down efficiency of R-PEG-PMT/siRNA complexes

The BACE1 silencing efficiency of R-PEG-PMT/siBACE1 complexes was determined in the levels of mRNA and protein expression in hippocampus and cortex parts mostly affected in AD (Figure 58). R-PEG-PMT/siBACE1 complexes efficiently showed *in vivo* gene silencing in both cortex and hippocampus parts showing 2.32-fold and 3.03-fold reduction of BACE1 expression, respectively. Although PEI, R-PEG-PEI and PEG-PMT/siBACE1 complexes also showed significant down-regulation of BACE1 mRNA expression in cortex part, they did not induce significant reduction of BACE1 mRNA in hippocampus part.

The suppression of BACE1 through R-PEG-PMT was further confirmed by analyzing BACE1 protein level by western blotting (Figure 59). The results of western blot and qRT-PCR showed obviously higher BACE1 silencing effect

of R-PEG-PMT/siBACE1 complexes than those of other complexes. Down-regulation of BACE1 is strongly related to reduction of $A\beta_{42}$ level because the generation of $A\beta_{42}$ is performed by sequential actions of BACE1 and γ-secretase on APP. Therefore, we measured $A\beta_{42}$ level using ELISA method to confirm the reduced BACE1 activity *in vivo*. As shown in Figure 60, the generation of $A\beta_{42}$ was obviously reduced by both R-PEG-PMT and R-PEG-PEI/BACE1siRNA treatments, which could possibly2 reduce the risk for development of dementia. In accordance with above results, the efficacy of R-PEG-PMT on decrease of $A\beta_{42}$ was higher than R-PEG-PEI. Based on the result of *in vitro* permeability study, enhanced gene silencing efficiency of R-PEG-PMT compared to R-PEG-PEI/siRNA complexes reflects the preferential entry of R-PEG-PMT/siRNA complexes into BBB by controlled endocytosis pathway.

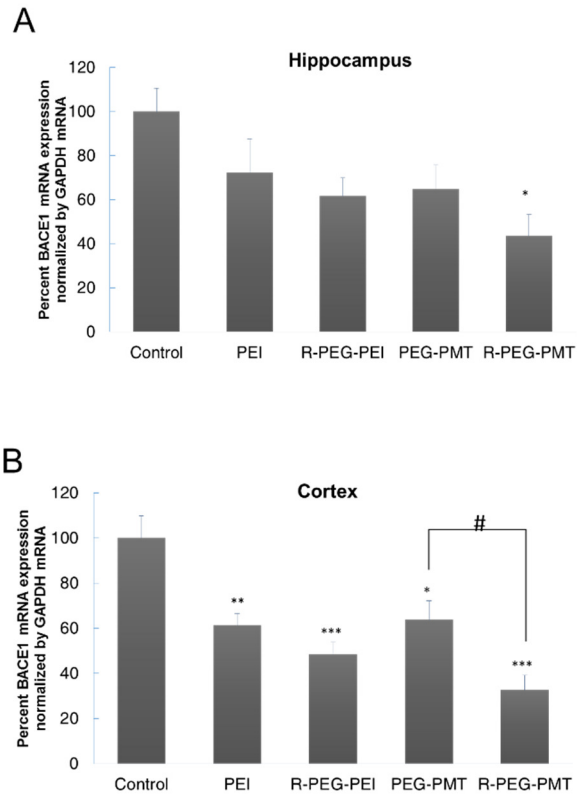

Figure 58. RNAi effect of R-PEG-PMT/siBACE1 complexes in mRNA levels. The BACE1 siRNAs complexed with variety of gene carriers were intravenously injected to mice three times at intervals of five days. Expression of BACE1 mRNA compared to GAPDH mRNA was measured by qRT-PCR in (A) hippocampus and (B) cortex parts of brain region (n = 5, error bar represents standard deviation; *$p < 0.1$, **$p < 0.05$, ***$p < 0.01$, one-way ANOVA compared to that of control; #$p < 0.1$, one-way ANOVA compared to that of PEG-PMT).

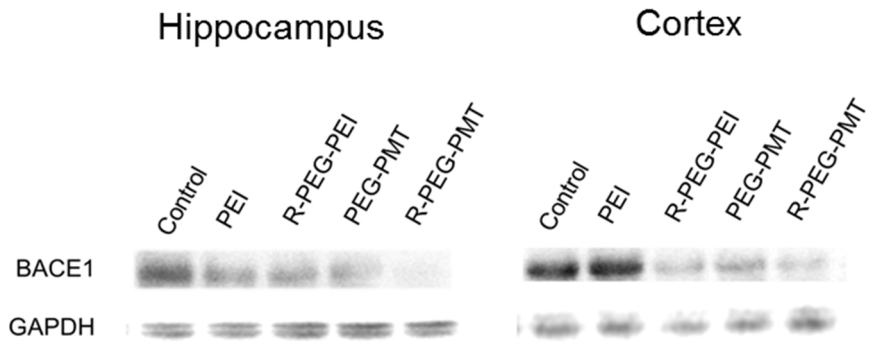

Figure 59. RNAi effect of R-PEG-PMT/siBACE1 complexes in protein level. The BACE1 siRNAs complexed with variety of gene carriers were intravenously injected to mice three times at intervals of five days. The BACE1 protein levels were analyzed by western blotting showing that R-PEG-PMT/siBACE1 complexes efficiently down-regulated the BACE1 expression both in hippocampus and cortex parts.

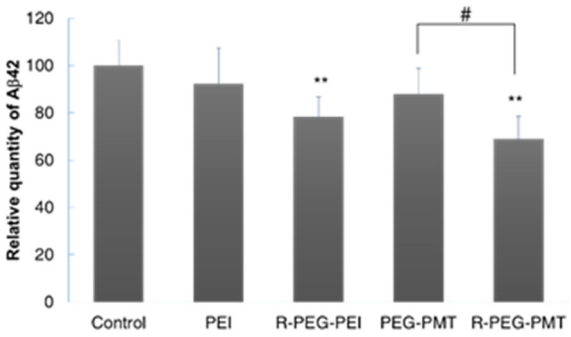

Figure 60. Functional effect of RNAi effect of R-PEG-PMT/siBACE1 complexes. The decrease of production of Aβ42 was measured using ELISA method to determine the down-regulated BACE1 activity by R-PEG-PMT/siBACE1 complexes (n = 5, error bar represents standard deviation; *p < 0.1, **p < 0.05, ***p < 0.01, one-way ANOVA compared to that of control; #p < 0.1, one-way ANOVA compared to that of PEG-PMT).

4. Conclusion

PMT modified with RVG (R-PEG-PMT) which was designed to overcome intracellular and extracellular barriers provided enhanced brain-targeted RNAi effect *in vivo*. R-PEG-PMT/siRNA complexes have shown brain specific accumulation and silencing effect without *in vivo* toxicity. Hippocampus and cortex where pathology is seen in the earliest stage of AD could be targeted by R-PEG-PMT although other complexes could not provide silencing effect on both regions. Successful brain-targeted BACE1 suppression indicates that R-PEG-PMT is a promising tool in RNAi therapeutics for brain diseases.

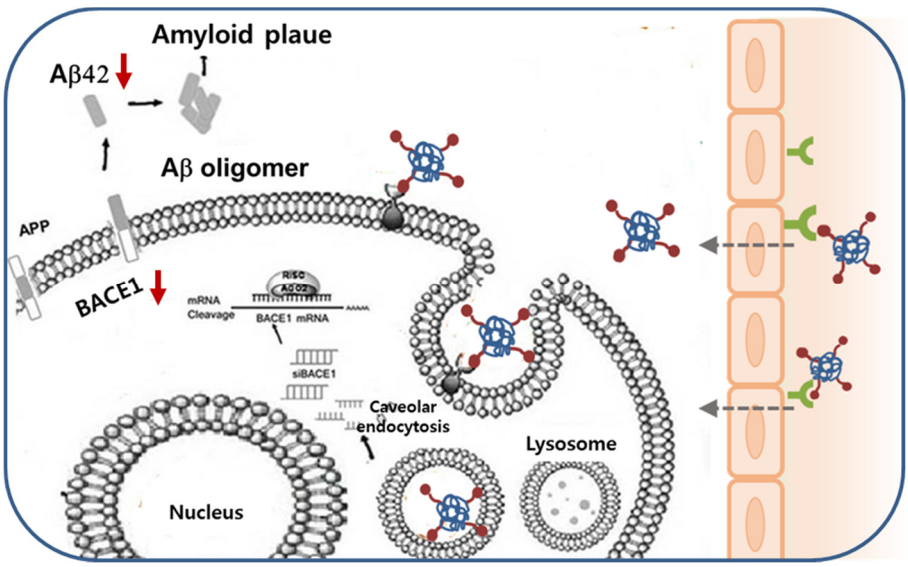

Figure 61. Schematic illustration of result of the study

Overall Conclusion and Future Prospects

AD is the world's most common dementing illness, but no defensive treatments are available currently. As an alternative to the traditional pharmacological approaches, RNAi therapeutics holds one of promising tools by directly down-regulating AD causative gene such as BACE1. Delivery of therapeutic siRNA to the brain is one of the biggest challenges for successful gene therapy because BBB permits selective entry of only few substances into the brain. In addition, immune clearance and non-specific cellulr binding also disturb siRNAs to reach their target cells. After therapeutic genes are arrived in target cells, intracellular barriers including poor endosomal escape and lysosomal degradation inhibit their RNAi activity. The aim of the study was the development of safe and efficient non-viral gene carrier for brain targeted RNAi therapeutics for AD. To obtain the maximal therapeutic effect, polymeric gene carrier was designed according to the coping strategies against intracellular and extracellular barriers (Table 1 and Figure 62).

In study 1, PMT was generated by reflecting coping strategy for intracellular barriers. Overall results of study 1 indicate that PMT itself overcomes intracellular barriers including cytotoxicity, endosomal escape, and lysosomal degradation. First, PMT/DNA complexes has shown enhanced cytotoxicity compared to PEI/DNA complexes due to degradable ester groups in PMT which undergo hydrolysis in physiological condition. Second, PEI backbone of PMT played a role in endosomal escape. Third, mannitol backbone of PMT enhanced

the transfection efficiency by regulating the mode of endocytosis and consequently allowing avoidance of lysosomal degradation. In mechanistic study, stimulation of caveolar endocytosis was determined to be associated with activation of Src kinase by mannitol part (Table 11).

In study 2, extracellular barriers were conquered by modification of PMT generating R-PEG-PMT. First, RVG ligand provided the targeting specificity to brain neuronal cell *in vitro* . Second, RVG directed the complexes across the BBB via receptor-mediated transcytosis. The improved BBB penetration of RVG-modified PMT was deteremined using *in vitro* BBB culture implying that R-PEG-PMT is well suited for 'Trojan horse strategy'. Mechanistic study on transcytosis pathway of R-PEG-PMT showed that PMT stimulated the caveolae-mediated transcytosis on *in vitro* BBB culture facilitating the budding and trafficking of caveolae vesicles. The synergistic effect of stimulation of caveolar endocytosis via PMT and 'Trojan horse strategy' via RVG ligand provided the enhanced BBB penetration. Third, PEG linker used for conjugation of RVG to amine group of PEI provided the stealth effect *in vivo*, which enhanced the accumulation of siRNAs in brain region with less off-target effect. (Table 11).

As shown in Table 11, coping strategies reflected on design of R-PEG-PMT provided solutions against extracellular and intracellular barriers, which brought the AD RNAi therapeutic potential. In study 3, R-PEG-PMT-mediated BACE1 siRNA delivery has shown brain-targeted BACE1 silencing effect on levels of mRNA and protein without significant systemic toxicity. Furthermore,

suppression of BACE1 led to decrease in Aβ42 production.

The virtue of non-viral vector is easy of modification depending on the purposes. R-PEG-PMT is transformable into various types of brain targeted non-viral vector. For example, i) RVG can be replaced to more efficient and safe 'Trojan horse' for enhanced brain specificity, ii) other funtional linkers which can act as physical, chemical, biological, geometrical cues can be used to regulate the endocytosis pathway, iii) prolonged gene expression or silencing can be available via targeted genome editing, and iv) chemical drugs can be conjugated to gene carrier as co-delivery system (Figure 63).

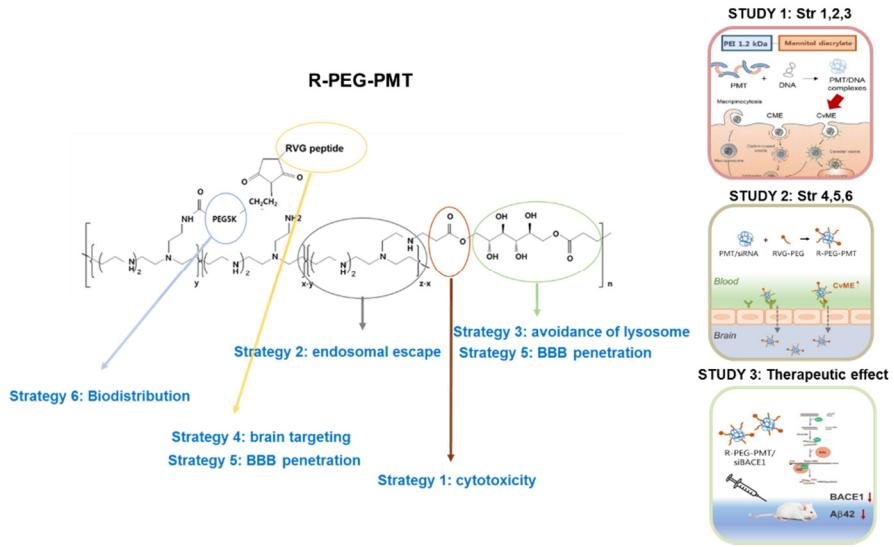

Figure 62. A schematic illustration of overall research approach

Table 11. Challenges of brain-targeted non-viral gene delivery and solutions achieved by R-PEG-PMT-mediated gene delivery

	Challenges	Solutions
	Intracellular barriers (Chapter 1)	
1	Cytotoxicity	PMT/DNA and R-PEG-PMT/siRNA showed significantly lower cytotoxicity compared to PEI
2	Endosomal escape	Endosomal escape of PMT/DNA complexes was based on the proton sponge effect of PEI
3	Avoidance of lysosomal degradation	PMT provided successful avoidance of lysosomal degradation via stimulation of caveolar endocytosis
	Extracellular barriers (Chapter 2)	
4	Brain targeting	R-PEG-PMT/siRNA provided CNS-targeted RNAi effect
5	BBB penetration	1. R-PEG-PMT penetrated BBB via RMT (RVG and nAchr) 2. Selective stimulation of caveolar endocytosis to avoid lysosomal fusion during transcytosis
6	Bio-distribution	Stealth effect of PEG provided less off-target effect in vivo and enhanced accumulation of siRNA in brain

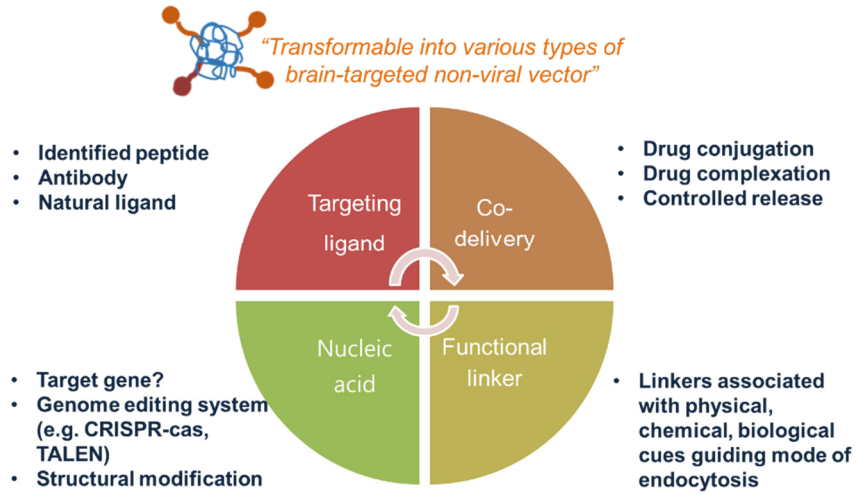

Figure 63. Possible strategies for enhanced brain delivery by modification of R-PEG-PMT

Literature Cited

Abbott, N. J., Patabendige, A. A., Dolman, D. E., Yusof, S. R. and Begley, D. J. 2010. Structure and function of the blood-brain barrier. *Neurobiol Dis*. 37(1), 13-25.

Abbott, N. J., Ronnback, L. and Hansson, E. Carver, L. A. 2006. *Nat Rev Neurosci*. 7(1), 41-53.

Akinc, A., Thomas, M., Klibanov, A. M. and Langer, R. 2005. Exploring polyethylenimine-mediated DNA transfection and the proton sponge hypothesis. *J Gene Med*. 7(5), 657-663.

Akiyama, T. and Ogawara, H. 1991. Use and specificity of genistein as inhibitor of protein-tyrosine kinases. *Methods Enzymol*. 201(362-370.

Alvarez-Erviti, L., Seow, Y., Yin, H., Betts, C., Lakhal, S. and Wood, M. J. 2011. Delivery of siRNA to the mouse brain by systemic injection of targeted exosomes. *Nat Biotechnol*. 29(4), 341-345.

Apodaca, G. 2002. Modulation of membrane traffic by mechanical stimuli. *Am J Physiol Renal Physiol*. 282(2), F179-190.

Arima, H., Kihara, F., Hirayama, F. and Uekama, K. 2001. Enhancement of gene expression by polyamidoamine dendrimer conjugates with [alpha]-, [beta]-, and [gamma]-cyclodextrins. *Bioconjug. Chem.* 12(476-484.

Arote, R., Kim, T. H., Kim, Y. K., Hwang, S. K., Jiang, H. L., Song, H. H., Nah,

J. W., Cho, M. H. and Cho, C. S. 2007. A biodegradable poly(ester amine) based on polycaprolactone and polyethylenimine as a gene carrier. *Biomaterials*. 28(4), 735-744.

Arote, R. B., Hwang, S. K., Yoo, M. K., Jere, D., Jiang, H. L., Kim, Y. K., Choi, Y. J., Nah, J. W., Cho, M. H. and Cho, C. S. 2008. Biodegradable poly(ester amine) based on glycerol dimethacrylate and polyethylenimine as a gene carrier. *J Gene Med*. 10(11), 1223-1235.

Arvanitakis, Z., Tuszynski, M. H., Bakay, R., Arends, D., Potkin, S., Bartus, R. and Bennett, D. 2007. Interim data from a phase 1 clinical trial of AAV-NGF (CERE-110) gene delivery in Alzheimer's disease. *Neurology*. 68(12), A233-A234.

Balazs, D. A. and Godbey, W. 2011. Liposomes for use in gene delivery. *J Drug Deliv*. 2011(326497.

Barreto, J. A., O'Malley, W., Kubeil, M., Graham, B., Stephan, H. and Spiccia, L. 2011. Nanomaterials: applications in cancer imaging and therapy. *Adv Mater*. 23(12), H18-40.

Benjaminsen, R. V., Mattebjerg, M. A., Henriksen, J. R., Moghimi, S. M. and Andresen, T. L. 2013. The possible "proton sponge " effect of polyethylenimine (PEI) does not include change in lysosomal pH. *Mol Ther*. 21(1), 149-157.

Blaese, R. M., Culver, K. W., Miller, A. D., Carter, C. S., Fleisher, T., Clerici, M., Shearer, G., Chang, L., Chiang, Y., Tolstoshev, P., Greenblatt, J. J., Rosenberg, S. A., Klein, H., Berger, M., Mullen, C. A., Ramsey, W. J., Muul,

L., Morgan, R. A. and Anderson, W. F. 1995. T lymphocyte-directed gene therapy for ADA- SCID: initial trial results after 4 years. *Science*. 270(5235), 475-480.

Boussif, O., Lezoualc'h, F., Zanta, M. A., Mergny, M. D., Scherman, D., Demeneix, B. and Behr, J. P. 1995. A versatile vector for gene and oligonucleotide transfer into cells in culture and *in vivo*: polyethylenimine. *Proc Natl Acad Sci U S A*. 92(16), 7297-7301.

Broadwell, R. D. 1989. Transcytosis of macromolecules through the blood-brain barrier: a cell biological perspective and critical appraisal. *Acta Neuropathol*. 79(2), 117-128.

Brookmeyer, R., Johnson, E., Ziegler-Graham, K. and Arrighi, H. M. 2007. Forecasting the global burden of Alzheimer's disease. *Alzheimers Dement*. 3(3), 186-191.

Brun, E., Carriere, M. and Mabondzo, A. 2012. *In vitro* evidence of dysregulation of blood-brain barrier function after acute and repeated/long-term exposure to TiO(2) nanoparticles. *Biomaterials*. 33(3), 886-896.

Campbell, R. N. 2008. Gene therapy and cancer research focus. New York, Nova Biomedical Books.

Cantin, E. M. and Rossi, J. J. 2007. Molecular medicine: entry granted. *Nature*. 448(7149), 33-34.

Canton, I. and Battaglia, G. 2012. Endocytosis at the nanoscale. *Chem Soc Rev*.

41(7), 2718-2739.

Carver, L. A. and Schnitzer, J. E. 2003. Caveolae: mining little caves for new cancer targets. *Nat Rev Cancer*. 3(8), 571-581.

Castanotto, D. and Rossi, J. J. 2009. The promises and pitfalls of RNA-interference-based therapeutics. *Nature*. 457(7228), 426-433.

Chen, S., Ge, X., Chen, Y., Lv, N., Liu, Z. and Yuan, W. 2013. Advances with RNA interference in Alzheimer's disease research. *Drug Des Devel Ther*. 7(117-125.

Chi, F., Wang, L., Zheng, X., Jong, A. and Huang, S. H. 2011. Recruitment of alpha7 nicotinic acetylcholine receptor to caveolin-1-enriched lipid rafts is required for nicotine-enhanced Escherichia coli K1 entry into brain endothelial cells. *Future Microbiol*. 6(8), 953-966.

Chidlow, J. H., Jr. and Sessa, W. C. 2010. Caveolae, caveolins, and cavins: complex control of cellular signalling and inflammation. *Cardiovasc Res*. 86(2), 219-225.

Christine, C. W., Starr, P. A., Larson, P. S., Eberling, J. L., Jagust, W. J., Hawkins, R. A., VanBrocklin, H. F., Wright, J. F., Bankiewicz, K. S. and Aminoff, M. J. 2009. Safety and tolerability of putaminal AADC gene therapy for Parkinson disease. *Neurology*. 73(20), 1662-1669.

Chung, Y. C., Cheng, T. Y. and Young, T. H. 2011. The role of adenosine receptor and caveolae-mediated endocytosis in oligonucleotide-mediated

gene transfer. *Biomaterials*. 32(19), 4471-4480.

de Boer, A. G. and Gaillard, P. J. 2007. Drug targeting to the brain. *Annu Rev Pharmacol Toxicol*. 47(323-355.

Demeneix, B. and Behr, J. P. 2005. Polyethylenimine (PEI). *Non-Viral Vectors for Gene Therapy, 2nd Edition: Part 1*. 53(217-230.

Dhaliwal, A., Maldonado, M., Han, Z. and Segura, T. 2010. Differential uptake of DNA-poly(ethylenimine) polyplexes in cells cultured on collagen and fibronectin surfaces. *Acta Biomater*. 6(9), 3436-3447.

Di Stefano, A., Iannitelli, A., Laserra, S. and Sozio, P. 2011. Drug delivery strategies for Alzheimer's disease treatment. *Exp Opin Drug Deliv.* 8(5), 581-603.

Dokka, S. and Rojanasakul, Y. 2000. Novel non-endocytic delivery of antisense oligonucleotides. *Adv Drug Deliv Rev*. 44(1), 35-49.

Doran, S. E., Ren, X. D., Betz, A. L., Pagel, M. A., Neuwelt, E. A., Roessler, B. J. and Davidson, B. L. 1995. Gene expression from recombinant viral vectors in the central nervous system after blood-brain barrier disruption. *Neurosurgery*. 36(5), 965-970.

Du, L., Kayali, R., Bertoni, C., Fike, F., Hu, H., Iversen, P. L. and Gatti, R. A. 2011. Arginine-rich cell-penetrating peptide dramatically enhances AMO-mediated ATM aberrant splicing correction and enables delivery to brain and cerebellum. *Hum Mol Genet*. 20(16), 3151-3160.

Edelstein, M. L., Abedi, M. R. and Wixon, J. 2007. Gene therapy clinical trials worldwide to 2007--an update. *J Gene Med*. 9(10), 833-842.

Ewert, K. K., Zidovska, A., Ahmad, A., Bouxsein, N. F., Evans, H. M., McAllister, C. S., Samuel, C. E. and Safinya, C. R. 2010. Cationic liposome-nucleic acid complexes for gene delivery and silencing: pathways and mechanisms for plasmid DNA and siRNA. *Top Curr Chem*. 296(191-226.

Felgner, P. L., Gadek, T. R., Holm, M., Roman, R., Chan, H. W., Wenz, M., Northrop, J. P., Ringold, G. M. and Danielsen, M. 1987. Lipofection: a highly efficient, lipid-mediated DNA-transfection procedure. *Proc Natl Acad Sci U S A*. 84(21), 7413-7417.

Fernandez-Carneado, J., Kogan, M. J., Pujals, S. and Giralt, E. 2004. Amphipathic peptides and drug delivery. *Biopolymers*. 76(2), 196-203.

Ferrari, A., Pellegrini, V., Arcangeli, C., Fittipaldi, A., Giacca, M. and Beltram, F. 2003. Caveolae-mediated internalization of extracellular HIV-1 tat fusion proteins visualized in real time. *Mol Ther*. 8(2), 284-294.

Forrest, M. L., Gabrielson, N. and Pack, D. W. 2004. Cyclodextrin-polyethylenimine conjugates for targeted *in vitro* gene delivery. *Biotechnol. Bioeng*. 89(416-423.

Franz, C. K., Federici, T., Yang, J., Backus, C., Oh, S. S., Teng, Q., Carlton, E., Bishop, K. M., Gasmi, M., Bartus, R. T., Feldman, E. L. and Boulis, N. M. 2009. Intraspinal cord delivery of IGF-I mediated by adeno-associated virus

2 is neuroprotective in a rat model of familial ALS. *Neurobiol Dis*. 33(3), 473-481.

Gan, C. W. and Feng, S.-S. 2010. Transferrin-conjugated nanoparticles of poly (lactide)-D-α-tocopheryl polyethylene glycol succinate diblock copolymer for targeted drug delivery across the blood–brain barrier. *Biomaterials*. 31(30), 7748-7757.

Gastka, M., Horvath, J. and Lentz, T. L. 1996. Rabies virus binding to the nicotinic acetylcholine receptor alpha subunit demonstrated by virus overlay protein binding assay. *J Gen Virol*. 77 (Pt 10)(2437-2440.

Georgieva, J. V., Kalicharan, D., Couraud, P. O., Romero, I. A., Weksler, B., Hoekstra, D. and Zuhorn, I. S. 2011. Surface characteristics of nanoparticles determine their intracellular fate in and processing by human blood-brain barrier endothelial cells *in vitro* . *Mol Ther*. 19(2), 318-325.

Ginn, S. L., Alexander, I. E., Edelstein, M. L., Abedi, M. R. and Wixon, J. 2013. Gene therapy clinical trials worldwide to 2012 - an update. *J Gene Med*. 15(2), 65-77.

Gleeson, M. P. 2008. Generation of a set of simple, interpretable ADMET rules of thumb. *J Med Chem*. 51(4), 817-834.

Godbey, W. T., Wu, K. K., Hirasaki, G. J. and Mikos, A. G. 1999. Improved packing of poly(ethylenimine)/DNA complexes increases transfection efficiency. *Gene Ther*. 6(8), 1380-1388.

Godbey, W. T., Wu, K. K. and Mikos, A. G. 2001. Poly(ethylenimine)-mediated gene delivery affects endothelial cell function and viability. *Biomaterials*. 22(5), 471-480.

Guo, X. and Szoka, F. C., Jr. 2001. Steric stabilization of fusogenic liposomes by a low-pH sensitive PEG--diortho ester--lipid conjugate. *Bioconjug Chem*. 12(2), 291-300.

Haensler, J. and Szoka, F. C., Jr. 1993. Polyamidoamine cascade polymers mediate efficient transfection of cells in culture. *Bioconjug Chem*. 4(5), 372-379.

Hanada, S., Fujioka, K., Inoue, Y., Kanaya, F., Manome, Y. and Yamamoto, K. 2014. Cell- Based *in vitro* Blood-Brain Barrier Model Can Rapidly Evaluate Nanoparticles' Brain Permeability in Association with Particle Size and Surface Modification. *International Journal of Molecular Sciences*. 15(2), 1812-1825.

Hartsock, A. and Nelson, W. J. 2008. Adherens and tight junctions: structure, function and connections to the actin cytoskeleton. *Biochim Biophys Acta*. 1778(3), 660-669.

Hawkins, R. A., O'Kane, R. L., Simpson, I. A. and Vina, J. R. 2006. Structure of the blood-brain barrier and its role in the transport of amino acids. *J Nutr*. 136(1 Suppl), 218S-226S.

Hickerson, R. P., Vlassov, A. V., Wang, Q., Leake, D., Ilves, H., Gonzalez-Gonzalez, E., Contag, C. H., Johnston, B. H. and Kaspar, R. L. 2008. Stability study of unmodified siRNA and relevance to clinical use.

Oligonucleotides. 18(4), 345-354.

Hillaireau, H. and Couvreur, P. 2009. Nanocarriers' entry into the cell: relevance to drug delivery. *Cell Mol Life Sci*. 66(17), 2873-2896.

Hinson, H. E., Stein, D. and Sheth, K. N. 2011. Hypertonic Saline and Mannitol Therapy in Critical Care Neurology. *J Intensive Care Med*.

Huang, R.-Q., Qu, Y.-H., Ke, W.-L., Zhu, J.-H., Pei, Y.-Y. and Jiang, C. 2007. Efficient gene delivery targeted to the brain using a transferrin-conjugated polyethyleneglycol-modified polyamidoamine dendrimer. *The FASEB Journal*. 21(4), 1117-1125.

Hughes, A. B. 2009. Amino acids, peptides and proteins in organic chemistry. Weinheim, Wiley-VCH.

Hwang do, W., Son, S., Jang, J., Youn, H., Lee, S., Lee, D., Lee, Y. S., Jeong, J. M., Kim, W. J. and Lee, D. S. 2011. A brain-targeted rabies virus glycoprotein-disulfide linked PEI nanocarrier for delivery of neurogenic microRNA. *Biomaterials*. 32(21), 4968-4975.

Islam, M. A., Shin, J. Y., Firdous, J., Park, T. E., Choi, Y. J., Cho, M. H., Yun, C. H. and Cho, C. S. 2012. The role of osmotic polysorbitol-based transporter in RNAi silencing via caveolae-mediated endocytosis and COX-2 expression. *Biomaterials*. 33(34), 8868-8880.

Islam, M. A., Shin, J. Y., Yun, C. H., Cho, C. S., Seo, H. W., Chae, C. and Cho, M. H. 2014. The effect of RNAi silencing of p62 using an osmotic

polysorbitol transporter on autophagy and tumorigenesis in lungs of K-rasLA1 mice. *Biomaterials*. 35(5), 1584-1596.

Islam, M. A., Yun, C. H., Choi, Y. J., Shin, J. Y., Arote, R., Jiang, H. L., Kang, S. K., Nah, J. W., Park, I. K., Cho, M. H. and Cho, C. S. 2011. Accelerated gene transfer through a polysorbitol-based transporter mechanism. *Biomaterials*. 32(36), 9908-9924.

Ittner, L. M. and Gotz, J. 2011. Amyloid-beta and tau--a toxic pas de deux in Alzheimer's disease. *Nat Rev Neurosci*. 12(2), 65-72.

Ittner, L. M., Ke, Y. D., Delerue, F., Bi, M., Gladbach, A., van Eersel, J., Wolfing, H., Chieng, B. C., Christie, M. J., Napier, I. A., Eckert, A., Staufenbiel, M., Hardeman, E. and Gotz, J. 2010. Dendritic function of tau mediates amyloid-beta toxicity in Alzheimer's disease mouse models. *Cell*. 142(3), 387-397.

Jarraya, B., Boulet, S., Ralph, G. S., Jan, C., Bonvento, G., Azzouz, M., Miskin, J. E., Shin, M., Delzescaux, T., Drouot, X., Herard, A. S., Day, D. M., Brouillet, E., Kingsman, S. M., Hantraye, P., Mitrophanous, K. A., Mazarakis, N. D. and Palfi, S. 2009. Dopamine gene therapy for Parkinson's disease in a nonhuman primate without associated dyskinesia. *Sci Transl Med*. 1(2), 2ra4.

Jere, D., Jiang, H. L., Kim, Y. K., Arote, R., Choi, Y. J., Yun, C. H., Cho, M. H. and Cho, C. S. 2009. Chitosan-graft-polyethylenimine for Akt1 siRNA delivery to lung cancer cells. *Int J Pharm*. 378(1-2), 194-200.

Jere, D., Xu, C. X., Arote, R., Yun, C. H., Cho, M. H. and Cho, C. S. 2008.

Poly(beta-amino ester) as a carrier for si/shRNA delivery in lung cancer cells. *Biomaterials*. 29(16), 2535-2547.

Jiang, S., Li, Y., Zhang, X., Bu, G., Xu, H. and Zhang, Y. W. 2014. Trafficking regulation of proteins in Alzheimer's disease. *Mol Neurodegener*. 9(6).

Kanasty, R., Dorkin, J. R., Vegas, A. and Anderson, D. 2013. Delivery materials for siRNA therapeutics. *Nat Mater*. 12(11), 967-977.

Kang, Y. S., Ko, Y. G. and Seo, J. S. 2000. Caveolin internalization by heat shock or hyperosmotic shock. *Exp Cell Res*. 255(2), 221-228.

Kanwar, J. R., Sriramoju, B. and Kanwar, R. K. 2012. Neurological disorders and therapeutics targeted to surmount the blood-brain barrier. *Int J Nanomedicine*. 7(3259-3278.

Kapus, A., Szaszi, K., Sun, J., Rizoli, S. and Rotstein, O. D. 1999. Cell shrinkage regulates Src kinases and induces tyrosine phosphorylation of cortactin, independent of the osmotic regulation of Na+/H+ exchangers. *J Biol Chem*. 274(12), 8093-8102.

Karaman, D. S., Desai, D., Senthilkumar, R., Johansson, E. M., Ratts, N., Oden, M., Eriksson, J. E., Sahlgren, C., Toivola, D. M. and Rosenholm, J. M. 2012. Shape engineering vs organic modification of inorganic nanoparticles as a tool for enhancing cellular internalization. *Nanoscale Res Lett*. 7(1), 358.

Karkan, D., Pfeifer, C., Vitalis, T. Z., Arthur, G., Ujiie, M., Chen, Q., Tsai, S., Koliatis, G., Gabathuler, R. and Jefferies, W. A. 2008. A unique carrier for

delivery of therapeutic compounds beyond the blood-brain barrier. *PLoS One*. 3(6), e2469.

Kaspar, B. K., Llado, J., Sherkat, N., Rothstein, J. D. and Gage, F. H. 2003. Retrograde viral delivery of IGF-1 prolongs survival in a mouse ALS model. *Science*. 301(5634), 839-842.

Kaur, T. and Slavces, R. (2013). Solid Lipid Nanoparticles: Tuneable Anti-Cancer Gene/Drug Delivery Systems. Novel Gene Therapy Approaches. M. Wei. InTech, InTech.

Ke, W., Shao, K., Huang, R., Han, L., Liu, Y., Li, J., Kuang, Y., Ye, L., Lou, J. and Jiang, C. 2009. Gene delivery targeted to the brain using an Angiopep-conjugated polyethyleneglycol-modified polyamidoamine dendrimer. *Biomaterials*. 30(36), 6976-6985.

Kells, A. P., Eberling, J., Su, X., Pivirotto, P., Bringas, J., Hadaczek, P., Narrow, W. C., Bowers, W. J., Federoff, H. J., Forsayeth, J. and Bankiewicz, K. S. 2010. Regeneration of the MPTP-lesioned dopaminergic system after convection-enhanced delivery of AAV2-GDNF. *J Neurosci*. 30(28), 9567-9577.

Khalil, I. A., Kogure, K., Akita, H. and Harashima, H. 2006. Uptake pathways and subsequent intracellular trafficking in nonviral gene delivery. *Pharmacol Rev*. 58(1), 32-45.

Kim, J. Y., Choi, W. I., Kim, Y. H. and Tae, G. 2013. Brain-targeted delivery of protein using chitosan- and RVG peptide-conjugated, pluronic-based nano-carrier. *Biomaterials*. 34(4), 1170-1178.

Kircheis, R., Schuller, S., Brunner, S., Ogris, M., Heider, K. H., Zauner, W. and Wagner, E. 1999. Polycation-based DNA complexes for tumor-targeted gene delivery *in vivo*. *J Gene Med*. 1(2), 111-120.

Kiss, A. L. 2012. Caveolae and the regulation of endocytosis. *Adv Exp Med Biol*. 729(14-28.

Kiss, A. L. and Botos, E. 2009. Endocytosis via caveolae: alternative pathway with distinct cellular compartments to avoid lysosomal degradation? *J Cell Mol Med*. 13(7), 1228-1237.

Kobayashi, D., Zeller, M., Cole, T., Buttini, M., McConlogue, L., Sinha, S., Freedman, S., Morris, R. G. and Chen, K. S. 2008. BACE1 gene deletion: impact on behavioral function in a model of Alzheimer's disease. *Neurobiol Aging*. 29(6), 861-873.

Kong, H. J., Liu, J., Riddle, K., Matsumoto, T., Leach, K. and Mooney, D. J. 2005. Non-viral gene delivery regulated by stiffness of cell adhesion substrates. *Nat Mater*. 4(6), 460-464.

Koo, H., Jin, G. W., Kang, H., Lee, Y., Nam, K., Zhe Bai, C. and Park, J. S. 2010. Biodegradable branched poly(ethylenimine sulfide) for gene delivery. *Biomaterials*. 31(5), 988-997.

Kreuter, J., Shamenkov, D., Petrov, V., Ramge, P., Cychutek, K., Koch-Brandt, C. and Alyautdin, R. 2002. Apolipoprotein-mediated transport of nanoparticle-bound drugs across the blood-brain barrier. *J Drug Target*. 10(4),

317-325.

Kumar, P., Wu, H., McBride, J. L., Jung, K. E., Kim, M. H., Davidson, B. L., Lee, S. K., Shankar, P. and Manjunath, N. 2007. Transvascular delivery of small interfering RNA to the central nervous system. *Nature*. 448(7149), 39-43.

Kurosaki, T., Morishita, T., Kodama, Y., Sato, K., Nakagawa, H., Higuchi, N., Nakamura, T., Hamamoto, T., Sasaki, H. and Kitahara, T. 2011. Nanoparticles electrostatically coated with folic acid for effective gene therapy. *Mol Pharm*. 8(3), 913-919.

Le Roy, C. and Wrana, J. L. 2005. Clathrin- and non-clathrin-mediated endocytic regulation of cell signalling. *Nat Rev Mol Cell Biol*. 6(2), 112-126.

LeWitt, P. A., Rezai, A. R., Leehey, M. A., Ojemann, S. G., Flaherty, A. W., Eskandar, E. N., Kostyk, S. K., Thomas, K., Sarkar, A., Siddiqui, M. S., Tatter, S. B., Schwalb, J. M., Poston, K. L., Henderson, J. M., Kurlan, R. M., Richard, I. H., Van Meter, L., Sapan, C. V., During, M. J., Kaplitt, M. G. and Feigin, A. 2011. AAV2-GAD gene therapy for advanced Parkinson's disease: a double-blind, sham-surgery controlled, randomised trial. *Lancet Neurol*. 10(4), 309-319.

Li, J., Feng, L., Fan, L., Zha, Y., Guo, L., Zhang, Q., Chen, J., Pang, Z., Wang, Y., Jiang, X., Yang, V. C. and Wen, L. 2011. Targeting the brain with PEG-PLGA nanoparticles modified with phage-displayed peptides. *Biomaterials*. 32(21), 4943-4950.

Li, S. and Huang, L. 2000. Nonviral gene therapy: promises and challenges.

Gene Ther. 7(1), 31-34.

Li, S., Wang, Y., Zhang, J., Yang, W. H., Dai, Z. H., Zhu, W. and Yu, X. Q. 2011. Biodegradable cross-linked poly(amino alcohol esters) based on LMW PEI for gene delivery. *Mol Biosyst*. 7(4), 1254-1262.

Liu, H., Li, Y., Mozhi, A., Zhang, L., Liu, Y., Xu, X., Xing, J., Liang, X., Ma, G., Yang, J. and Zhang, X. 2014. SiRNA-phospholipid conjugates for gene and drug delivery in cancer treatment. *Biomaterials*. 35(24), 6519-6533.

Liu, K., Wang, X., Fan, W., Zhu, Q., Yang, J., Gao, J. and Gao, S. 2012. Degradable polyethylenimine derivate coupled to a bifunctional peptide R13 as a new gene-delivery vector. *Int J Nanomedicine*. 7(1149-1162.

Liu, Y., Huang, R., Han, L., Ke, W., Shao, K., Ye, L., Lou, J. and Jiang, C. 2009. Brain-targeting gene delivery and cellular internalization mechanisms for modified rabies virus glycoprotein RVG29 nanoparticles. *Biomaterials*. 30(25), 4195-4202.

Liu, Y., Li, J., Shao, K., Huang, R., Ye, L., Lou, J. and Jiang, C. 2010. A leptin derived 30-amino-acid peptide modified pegylated poly-L-lysine dendrigraft for brain targeted gene delivery. *Biomaterials*. 31(19), 5246-5257.

Luu, Q. P., Shin, J. Y., Kim, Y. K., Islam, M. A., Kang, S. K., Cho, M. H., Choi, Y. J. and Cho, C. S. 2012. High gene transfer by the osmotic polysorbitol-mediated transporter through the selective caveolae endocytic pathway. *Mol Pharm*. 9(8), 2206-2218.

Madani, F., Lindberg, S., Langel, U., Futaki, S. and Graslund, A. 2011. Mechanisms of cellular uptake of cell-penetrating peptides. *J Biophys*. 2011(414729.

Maguire, A. M., High, K. A., Auricchio, A., Wright, J. F., Pierce, E. A., Testa, F., Mingozzi, F., Bennicelli, J. L., Ying, G. S., Rossi, S., Fulton, A., Marshall, K. A., Banfi, S., Chung, D. C., Morgan, J. I., Hauck, B., Zelenaia, O., Zhu, X., Raffini, L., Coppieters, F., De Baere, E., Shindler, K. S., Volpe, N. J., Surace, E. M., Acerra, C., Lyubarsky, A., Redmond, T. M., Stone, E., Sun, J., McDonnell, J. W., Leroy, B. P., Simonelli, F. and Bennett, J. 2009. Age-dependent effects of RPE65 gene therapy for Leber's congenital amaurosis: a phase 1 dose-escalation trial. *Lancet*. 374(9701), 1597-1605.

Marks, W. J., Jr., Bartus, R. T., Siffert, J., Davis, C. S., Lozano, A., Boulis, N., Vitek, J., Stacy, M., Turner, D., Verhagen, L., Bakay, R., Watts, R., Guthrie, B., Jankovic, J., Simpson, R., Tagliati, M., Alterman, R., Stern, M., Baltuch, G., Starr, P. A., Larson, P. S., Ostrem, J. L., Nutt, J., Kieburtz, K., Kordower, J. H. and Olanow, C. W. 2010. Gene delivery of AAV2-neurturin for Parkinson's disease: a double-blind, randomised, controlled trial. *Lancet Neurol*. 9(12), 1164-1172.

Mazanetz, M. P. and Fischer, P. M. 2007. Untangling tau hyperphosphorylation in drug design for neurodegenerative diseases. *Nat Rev Drug Discov*. 6(6), 464-479.

McBride, J. L., Pitzer, M. R., Boudreau, R. L., Dufour, B., Hobbs, T., Ojeda, S. R. and Davidson, B. L. 2011. Preclinical safety of RNAi-mediated HTT suppression in the rhesus macaque as a potential therapy for Huntington's disease. *Mol Ther*. 19(12), 2152-2162.

McCarty, D. M., DiRosario, J., Gulaid, K., Muenzer, J. and Fu, H. 2009. Mannitol-facilitated CNS entry of rAAV2 vector significantly delayed the neurological disease progression in MPS IIIB mice. *Gene Ther*. 16(11), 1340-1352.

McIntosh, D. P., Tan, X. Y., Oh, P. and Schnitzer, J. E. 2002. Targeting endothelium and its dynamic caveolae for tissue-specific transcytosis *in vivo*: a pathway to overcome cell barriers to drug and gene delivery. *Proc Natl Acad Sci U S A*. 99(4), 1996-2001.

McMahon, H. T. and Boucrot, E. 2011. Molecular mechanism and physiological functions of clathrin-mediated endocytosis. *Nat Rev Mol Cell Biol*. 12(8), 517-533.

Medina-Kauwe, L. K., Xie, J. and Hamm-Alvarez, S. 2005. Intracellular trafficking of nonviral vectors. *Gene Ther*. 12(24), 1734-1751.

Mennesson, E., Erbacher, P., Piller, V., Kieda, C., Midoux, P. and Pichon, C. 2005. Transfection efficiency and uptake process of polyplexes in human lung endothelial cells: a comparative study in non-polarized and polarized cells. *J Gene Med*. 7(6), 729-738.

Minati, L., Edginton, T., Bruzzone, M. G. and Giaccone, G. 2009. Current concepts in Alzheimer's disease: a multidisciplinary review. *Am J Alzheimers Dis Other Demen*. 24(2), 95-121.

Moghimi, S. M., Symonds, P., Murray, J. C., Hunter, A. C., Debska, G. and Szewczyk, A. 2005. A two-stage poly(ethylenimine)-mediated cytotoxicity: implications for gene transfer/therapy. *Mol Ther*. 11(6), 990-995.

Morra, M. 2001. Water in biomaterials surface science. Chichester ; New York, Wiley.

Moulton, H. M., Hase, M. C., Smith, K. M. and Iversen, P. L. 2003. HIV Tat peptide enhances cellular delivery of antisense morpholino oligomers. *Antisense Nucleic Acid Drug Dev*. 13(1), 31-43.

Nagahara, A. H., Merrill, D. A., Coppola, G., Tsukada, S., Schroeder, B. E., Shaked, G. M., Wang, L., Blesch, A., Kim, A., Conner, J. M., Rockenstein, E., Chao, M. V., Koo, E. H., Geschwind, D., Masliah, E., Chiba, A. A. and Tuszynski, M. H. 2009. Neuroprotective effects of brain-derived neurotrophic factor in rodent and primate models of Alzheimer's disease. *Nat Med*. 15(3), 331-337.

Nayak, S. and Herzog, R. W. 2010. Progress and prospects: immune responses to viral vectors. *Gene Ther*. 17(3), 295-304.

Neuwelt, E. A., Hill, S. A. and Frenkel, E. P. 1984. Osmotic blood-brain barrier modification and combination chemotherapy: concurrent tumor regression in areas of barrier opening and progression in brain regions distant to barrier opening. *Neurosurgery*. 15(3), 362-366.

Nguyen, J., Xie, X., Neu, M., Dumitrascu, R., Reul, R., Sitterberg, J., Bakowsky, U., Schermuly, R., Fink, L., Schmehl, T., Gessler, T., Seeger, W. and Kissel, T. 2008. Effects of cell-penetrating peptides and pegylation on transfection efficiency of polyethylenimine in mouse lungs. *J Gene Med*. 10(11), 1236-1246.

Nie, S. 2010. Understanding and overcoming major barriers in cancer nanomedicine. *Nanomedicine (Lond)*. 5(4), 523-528.

Nilsson, H., Dragomir, A., Ahlander, A., Johannesson, M. and Roomans, G. M. 2007. Effects of hyperosmotic stress on cultured airway epithelial cells. *Cell Tissue Res*. 330(2), 257-269.

Pardridge, W. M. 2006. Molecular Trojan horses for blood-brain barrier drug delivery. *Curr Opin Pharmacol*. 6(5), 494-500.

Pardridge, W. M. 2010. Biopharmaceutical drug targeting to the brain. *J Drug Target*. 18(3), 157-167.

Park, M. R., Han, K. O., Han, I. K., Cho, M. H., Nah, J. W., Choi, Y. J. and Cho, C. S. 2005. Degradable polyethylenimine-alt-poly(ethylene glycol) copolymers as novel gene carriers. *J Control Release*. 105(3), 367-380.

Park, M. R., Kim, H. W., Hwang, C. S., Han, K. O., Choi, Y. J., Song, S. C., Cho, M. H. and Cho, C. S. 2008. Highly efficient gene transfer with degradable poly(ester amine) based on poly(ethylene glycol) diacrylate and polyethylenimine *in vitro* and *in vivo*. *J Gene Med*. 10(2), 198-207.

Park, T. E., Kang, B., Kim, Y. K., Zhang, Q., Lee, W. S., Islam, M. A., Kang, S. K., Cho, M. H., Choi, Y. J. and Cho, C. S. 2012. Selective stimulation of caveolae-mediated endocytosis by an osmotic polymannitol-based gene transporter. *Biomaterials*. 33(29), 7272-7281.

Park, T. G., Jeong, J. H. and Kim, S. W. 2006. Current status of polymeric gene

delivery systems. *Adv Drug Deliv Rev*. 58(4), 467-486.

Parton, R. G. and Simons, K. 2007. The multiple faces of caveolae. *Nat Rev Mol Cell Biol*. 8(3), 185-194.

Patel, H. M. and Russell, N. J. 1988. Liposomes: from membrane model to therapeutic applications. *Biochem Soc Trans*. 16(6), 909-910.

Pelkmans, L. and Helenius, A. 2002. Endocytosis via caveolae. *Traffic*. 3(5), 311-320.

Polo, S. and Di Fiore, P. P. 2006. Endocytosis conducts the cell signaling orchestra. *Cell*. 124(5), 897-900.

Pun, S. H. 2004. Cyclodextrin-modified polyethylenimine polymers for gene delivery. *Bioconjug. Chem.* 15(831-840.

Qin, L. J., Gu, Y. T., Zhang, H. and Xue, Y. X. 2009. Bradykinin-induced blood-tumor barrier opening is mediated by tumor necrosis factor-alpha. *Neurosci Lett*. 450(2), 172-175.

Qin, Y., Chen, H., Yuan, W., Kuai, R., Zhang, Q., Xie, F., Zhang, L., Zhang, Z., Liu, J. and He, Q. 2011. Liposome formulated with TAT-modified cholesterol for enhancing the brain delivery. *Int J Pharm*. 419(1-2), 85-95.

Querfurth, H. W. and LaFerla, F. M. 2010. Alzheimer's disease. *N Engl J Med*. 362(4), 329-344.

Rafii, M. S., Baumann, T. L., Bakay, R. A., Ostrove, J. M., Siffert, J., Fleisher, A. S., Herzog, C. D., Barba, D., Pay, M., Salmon, D. P., Chu, Y., Kordower, J. H., Bishop, K., Keator, D., Potkin, S. and Bartus, R. T. 2014. A phase1 study of stereotactic gene delivery of AAV2-NGF for Alzheimer's disease. *Alzheimers Dement*. 10(5), 571-581.

Ragnaill, M. N., Brown, M., Ye, D., Bramini, M., Callanan, S., Lynch, I. and Dawson, K. A. 2011. Internal benchmarking of a human blood-brain barrier cell model for screening of nanoparticle uptake and transcytosis. *Eur J Pharm Biopharm*. 77(3), 360-367.

Ram, Z., Culver, K. W., Oshiro, E. M., Viola, J. J., DeVroom, H. L., Otto, E., Long, Z., Chiang, Y., McGarrity, G. J., Muul, L. M., Katz, D., Blaese, R. M. and Oldfield, E. H. 1997. Therapy of malignant brain tumors by intratumoral implantation of retroviral vector-producing cells. *Nat Med*. 3(12), 1354-1361.

Ramaswamy, S., McBride, J. L., Han, I., Berry-Kravis, E. M., Zhou, L., Herzog, C. D., Gasmi, M., Bartus, R. T. and Kordower, J. H. 2009. Intrastriatal CERE-120 (AAV-Neurturin) protects striatal and cortical neurons and delays motor deficits in a transgenic mouse model of Huntington's disease. *Neurobiol Dis*. 34(1), 40-50.

Rejman, J., Bragonzi, A. and Conese, M. 2005. Role of clathrin- and caveolae-mediated endocytosis in gene transfer mediated by lipo- and polyplexes. *Mol Ther*. 12(3), 468-474.

Rejman, J., Conese, M. and Hoekstra, D. 2006. Gene transfer by means of lipo- and polyplexes: role of clathrin and caveolae-mediated endocytosis. *J Liposome Res*. 16(3), 237-247.

Rejman, J., Oberle, V., Zuhorn, I. S. and Hoekstra, D. 2004. Size-dependent internalization of particles via the pathways of clathrin- and caveolae-mediated endocytosis. *Biochem J*. 377(Pt 1), 159-169.

Ren, W.-h., Chang, J., Yan, C.-h., Qian, X.-m., Long, L.-x., He, B., Yuan, X.-b., Kang, C.-s., Betbeder, D. and Sheng, J. 2010. Development of transferrin functionalized poly (ethylene glycol)/poly (lactic acid) amphiphilic block copolymeric micelles as a potential delivery system targeting brain glioma. *Journal of Materials Science: Materials in Medicine*. 21(9), 2673-2681.

Safinya, C. R. and Ewert, K. K. 2012. Materials chemistry: Liposomes derived from molecular vases. *Nature*. 489(7416), 372-374.

Salahuddin, T. S., Johansson, B. B., Kalimo, H. and Olsson, Y. 1988. Structural changes in the rat brain after carotid infusions of hyperosmolar solutions: a light microscopic and immunohistochemical study. *Neuropathol Appl Neurobiol*. 14(6), 467-482.

Schnitzer, J. E. 2001. Caveolae: from basic trafficking mechanisms to targeting transcytosis for tissue-specific drug and gene delivery *in vivo*. *Adv Drug Deliv Rev*. 49(3), 265-280.

Sens, P. and Turner, M. S. 2006. Budded membrane microdomains as tension regulators. *Phys Rev E Stat Nonlin Soft Matter Phys*. 73(3 Pt 1), 031918.

Simonato, M., Bennett, J., Boulis, N. M., Castro, M. G., Fink, D. J., Goins, W. F., Gray, S. J., Lowenstein, P. R., Vandenberghe, L. H., Wilson, T. J., Wolfe,

J. H. and Glorioso, J. C. 2013. Progress in gene therapy for neurological disorders. *Nat Rev Neurol*. 9(5), 277-291.

Singer, O., Marr, R. A., Rockenstein, E., Crews, L., Coufal, N. G., Gage, F. H., Verma, I. M. and Masliah, E. 2005. Targeting BACE1 with siRNAs ameliorates Alzheimer disease neuropathology in a transgenic model. *Nat Neurosci*. 8(10), 1343-1349.

Smith, R. A., Miller, T. M., Yamanaka, K., Monia, B. P., Condon, T. P., Hung, G., Lobsiger, C. S., Ward, C. M., McAlonis-Downes, M., Wei, H., Wancewicz, E. V., Bennett, C. F. and Cleveland, D. W. 2006. Antisense oligonucleotide therapy for neurodegenerative disease. *J Clin Invest*. 116(8), 2290-2296.

Son, S., Hwang do, W., Singha, K., Jeong, J. H., Park, T. G., Lee, D. S. and Kim, W. J. 2011. RVG peptide tethered bioreducible polyethylenimine for gene delivery to brain. *J Control Release*. 155(1), 18-25.

Stamatovic, S. M., Keep, R. F. and Andjelkovic, A. V. 2008. Brain endothelial cell-cell junctions: how to "open" the blood brain barrier. *Curr Neuropharmacol*. 6(3), 179-192.

Stolberg, S. G. 1999. The biotech death of Jesse Gelsinger. *N Y Times Mag*, 136-140, 149-150.

Sukumaran, S. K., Quon, M. J. and Prasadarao, N. V. 2002. Escherichia coli K1 internalization via caveolae requires caveolin-1 and protein kinase Calpha interaction in human brain microvascular endothelial cells. *J Biol Chem*. 277(52), 50716-50724.

Suzuki, M., McHugh, J., Tork, C., Shelley, B., Klein, S. M., Aebischer, P. and Svendsen, C. N. 2007. GDNF secreting human neural progenitor cells protect dying motor neurons, but not their projection to muscle, in a rat model of familial ALS. *PLoS One*. 2(8), e689.

Sverdlov, M., Shajahan, A. N. and Minshall, R. D. 2007. Tyrosine phosphorylation-dependence of caveolae-mediated endocytosis. *J Cell Mol Med*. 11(6), 1239-1250.

Temin, H. M. 1961. Mixed infection with two types of Rous sarcoma virus. *Virology*. 13(158-163.

Thomas, C. E., Ehrhardt, A. and Kay, M. A. 2003. Progress and problems with the use of viral vectors for gene therapy. *Nat Rev Genet.* 4(5), 346-358.

Thomas, M. and Klibanov, A. M. 2003. Non-viral gene therapy: polycation-mediated DNA delivery. *Appl Microbiol Biotechnol*. 62(1), 27-34.

Tseng, H. R., Wang, H., Wang, S., Su, H., Radu, C. G. and Czernin, J. (2010). A supramolecular approach for preparation of size controllable nanoparticles, Google Patents.

Ulbrich, K., Hekmatara, T., Herbert, E. and Kreuter, J. 2009. Transferrin-and transferrin-receptor-antibody-modified nanoparticles enable drug delivery across the blood–brain barrier (BBB). *European Journal of Pharmaceutics and Biopharmaceutics*. 71(2), 251-256.

van Meer, G. and Simons, K. 1986. The function of tight junctions in maintaining differences in lipid composition between the apical and the basolateral cell surface domains of MDCK cells. *EMBO J*. 5(7), 1455-1464.

Vassar, R. 2002. Beta-secretase (BACE) as a drug target for Alzheimer's disease. *Adv Drug Deliv Rev*. 54(12), 1589-1602.

Vaysse, L., Burgelin, I., Merlio, J. P. and Arveiler, B. 2000. Improved transfection using epithelial cell line-selected ligands and fusogenic peptides. *Biochim. Biophys. Acta*. 1475(369-376.

Visser, C. C., Stevanović, S., Voorwinden, L. H., Bloois, L. v., Gaillard, P. J., Danhof, M., Crommelin, D. J. and Boer, A. G. d. 2005. Targeting liposomes with protein drugs to the blood–brain barrier *in vitro* . *European journal of pharmaceutical sciences*. 25(2), 299-305.

Volonte, D., Galbiati, F., Pestell, R. G. and Lisanti, M. P. 2001. Cellular stress induces the tyrosine phosphorylation of caveolin-1 (Tyr(14)) via activation of p38 mitogen-activated protein kinase and c-Src kinase. Evidence for caveolae, the actin cytoskeleton, and focal adhesions as mechanical sensors of osmotic stress. *J Biol Chem*. 276(11), 8094-8103.

Walker, G. F., Fella, C., Pelisek, J., Fahrmeir, J., Boeckle, S., Ogris, M. and Wagner, E. 2005. Toward synthetic viruses: endosomal pH-triggered deshielding of targeted polyplexes greatly enhances gene transfer *in vitro* and *in vivo*. *Mol Ther*. 11(3), 418-425.

Wang, S., Singh, R. D., Godin, L., Pagano, R. E. and Hubmayr, R. D. 2011. Endocytic response of type I alveolar epithelial cells to hypertonic stress. *Am*

J Physiol Lung Cell Mol Physiol. 300(4), L560-568.

Werth, S., Urban-Klein, B., Dai, L., Hobel, S., Grzelinski, M., Bakowsky, U., Czubayko, F. and Aigner, A. 2006. A low molecular weight fraction of polyethylenimine (PEI) displays increased transfection efficiency of DNA and siRNA in fresh or lyophilized complexes. *J Control Release*. 112(2), 257-270.

Whitehead, K. A., Dorkin, J. R., Vegas, A. J., Chang, P. H., Veiseh, O., Matthews, J., Fenton, O. S., Zhang, Y., Olejnik, K. T., Yesilyurt, V., Chen, D., Barros, S., Klebanov, B., Novobrantseva, T., Langer, R. and Anderson, D. G. 2014. Degradable lipid nanoparticles with predictable *in vivo* siRNA delivery activity. *Nat Commun*. 5(4277.

Wirdefeldt, K., Adami, H. O., Cole, P., Trichopoulos, D. and Mandel, J. 2011. Epidemiology and etiology of Parkinson's disease: a review of the evidence. *Eur J Epidemiol*. 26 Suppl 1(S1-58.

Wirth, T., Parker, N. and Yla-Herttuala, S. 2013. History of gene therapy. *Gene*. 525(2), 162-169.

Wong, H. L., Wu, X. Y. and Bendayan, R. 2012. Nanotechnological advances for the delivery of CNS therapeutics. *Adv Drug Deliv Rev*. 64(7), 686-700.

Xie, F. L., Yao, N., Qin, Y., Zhang, Q. Y., Chen, H. L., Yuan, M. Q., Tang, J., Li, X. K., Fan, W., Zhang, Q., Wu, Y., Hai, L. and He, Q. 2012. Investigation of glucose-modified liposomes using polyethylene glycols with different chain lengths as the linkers for brain targeting. *International Journal of Nanomedicine*. 7(163-175.

Yeo, Y. 2013. Nanoparticulate drug delivery systems : strategies, technologies, and applications. Hoboken, New Jersey, Wiley.

Yin, H., Kanasty, R. L., Eltoukhy, A. A., Vegas, A. J., Dorkin, J. R. and Anderson, D. G. 2014. Non-viral vectors for gene-based therapy. *Nat Rev Genet*. 15(8), 541-555.

Yla-Herttuala, S. 2012. Endgame: glybera finally recommended for approval as the first gene therapy drug in the European union. *Mol Ther*. 20(10), 1831-1832.

Zeier, Z., Aguilar, J. S., Lopez, C. M., Devi-Rao, G. B., Watson, Z. L., Baker, H. V., Wagner, E. K. and Bloom, D. C. 2009. A limited innate immune response is induced by a replication-defective herpes simplex virus vector following delivery to the murine central nervous system. *J Neurovirol.* 15(5-6), 411-424.

Zhi, D., Zhang, S., Wang, B., Zhao, Y., Yang, B. and Yu, S. 2010. Transfection efficiency of cationic lipids with different hydrophobic domains in gene delivery. *Bioconjug Chem*. 21(4), 563-577.

Ziello, J. E., Huang, Y. and Jovin, I. S. 2010. Cellular endocytosis and gene delivery. *Mol Med*. 16(5-6), 222-229.

Summary in Korean

알츠하이머 질병은 가장 흔한 형태의 퇴행성 뇌질환 중 하나로서, 전세계적으로 커다란 문제점으로 부상하고 있음에도 확실한 치료제가 거의 없는 상황이다. 이에 대한 대안으로 각광받고 있는 것이 바로 유전자 치료이다. 유전자 치료는 질병의 원인이 되는 유전자를 직접적으로 조절함으로써 질병의 근원에 접근할 수 있어, 기존에 증상완화에 그쳤던 치료방법의 한계점에 대한 해결방법이 될 수 있다. 특히 RNA 간섭 연구의 발전과 더불어 바이러스 벡터를 이용한 알츠하이머 원인 유전자(예: BACE1)의 억제가 지속적으로 시도되어 왔으며, 새로운 치료법으로서의 잠재력을 인정받고 있다. 그러나 바이러스 벡터는 제조과정이 복잡할 뿐만 아니라 면역원성, 감염 가능성, 염증 유발 등 안전성 문제로 인체에 적용하기에 한계가 많다. 이에 안정성이 높은 비바이러스성 벡터들이 각광을 받고 있으며 나노기술의 발전에 따라 다양한 방식으로 유전자 전달 효율을 극대화 시키는 연구들이 많이 진행되고 있다.

비바이러스성 벡터는 진화적으로 발전해 온 바이러스성 벡터보다 생물학적 장벽을 극복하는 능력이 현저히 떨어지기 때문에 생체 내 조건에서 유전자 전달 효율이 심각하게 저해된다. 일단, 비바이러스성 벡터가 체내에 주입되어 표적 세포 즉, 뇌세포에 도달하기까지 혈청 분해, 면역세포에 의한 제거, 비특이적 세포결합 및 뇌혈장벽 등 세포 외 장벽을 극복해야 한다. 비바이러스성 벡터가 표적 세포 내 들어가더라도 독성 문제, 엔도좀 탈출 및 라이소좀에 의한 분해 등 세포 내 장벽이 치료용 유전자의 RNA 간섭 효과를 방해한다. 따라서 관건은 세포 내부 및 세포 외부 장벽을 효과적으로 극복하는 것이다. 이 연구에서는 생체 내 장벽을 극복하여 알츠하이머 RNA 간섭 치료 효과를 나타내기 위한 비바이러스성

유전자 전달체를 개발하는 것을 목적으로 하고 있다. 첫 번째 연구에서는 세포 내 장벽을 극복하기 위한 비바이러스성 벡터의 개발을, 두 번째 연구에서는 세포 외 장벽 극복을 위해 앞서 개발한 비바이러스성 벡터의 표면 수식을, 마지막으로 세 번째 연구에서는 개발된 벡터의 알츠하이머 RNA 간섭 치료 효과를 생체 내에서 규명하였다.

연구 1에서는 세포 내 장벽을 극복하기 위한 전략으로서 엔도시토시스 기전 조절하고 그 효과를 증명하였다. 엔도시토시스 기전이 세포 내 이입된 유전자의 운명을 결정짓는다는 사실은 수많은 연구를 통해 확실해지고 있다. 여러 엔도시토시스 기전 중 카비올레 엔도시토시스 기전은 라이소좀 소포와 융합되지 않고 이입된 물질들을 골지체나 소포체에 전달하기 때문에 약물전달 경로로 크게 각광받고 있다. 카비올레 소포들은 보통 세포막에서 움직이지 않지만, 리간스-수용체 결합 또는 삼투 스트레스 등 특정한 자극에 의해 세포 내로 이입된다. 카비올레 기전 촉진 방법 중 하나로서 삼투 특성을 지닌 유전자 전달체인 분해성의 만니톨계 유전자 전달체(PMT)를 개발하였다. PMT는 기존 비바이러성 벡터로 가장 광범위하게 연구되고 있는 작은 분자량의 폴리에틸렌이민과 삼투물질인 만니톨을 연결한 일종의 PEI 유도체이다. 여러 세포주에 처리하였을 때, PMT의 에스테르 가수분해와 만니톨의 음이온성 전하에 의한 PEI 양이온 보호 효과로 인해 세포 독성이 유의적으로 감소했다. 또한 라이소좀 분해 회피 방법 중 하나로서, PEI의 양전자 스폰지 효과가 PMT에 의한 유전자 전달에 부분적으로 기여함을 확인하였다. 더욱 중요하게는, PMT/DNA 복합체의 엔도시토시스가 선택적으로 카비올레 매개의 세포 내 섭취로 변화하면서 복합체의 라이소좀 분해 회피에 의해 유전자 전달 효율이 현저히 향상됨을 증명하였다. 관련 메커니즘을 카베올린-1 인산화의 웨스턴 블랏팅 방법으로 확인함으로써 만니톨이

Src 인산화 효소를 활성화 시키는 것과 관련 있음을 밝혔다.

연구 2에서 세포 외 장벽 극복을 위해 PMT에 리간드를 도입하였다. 뇌혈장벽은 뇌에 필요한 일부 물질들만 선택적으로 통과시키기 때문에 뇌혈장벽을 효과적으로 통과하는 유전자 전달체를 만드는 것이 뇌 유전자 치료에 있어 가장 큰 과제이다. 본 연구에서는 '트로이 목마' 전략을 통해 PMT/siRNA 복합체에 뇌혈장벽 통과 능력을 부여하고자 PEG를 매개로 하여 광견병 바이러스 유래의 당단백질(RVG)을 도입하였다(R-PEG-PMT). 가교체로 이용된 폴리에틸렌글리콜(PEG)은 RVG 리간드 간의 입체구조 방해현상을 예방할 뿐만 아니라 생체 내에서 면역세포에 의한 제거를 방지할 것으로 기대하였다. R-PEG-PMT/siRNA 복합체의 뇌혈장벽 통과능력을 평가하기 위해 bEnd.3 세포주와 B23 세포주의 트렌스웰 공배양으로 구축된 시험관내 뇌혈장벽을 이용하여 통과 효율을 측정하였다. 그 결과, RVG 수식이 뇌혈장벽 통과율을 2.2배 증가시켰으며 PMT 또한 PEI에 비해 1.26배 향상시킴을 확인하였다. 관련 기전을 증명하기 위해 엔도시토시스 저해 약물을 처리한 후 R-PEG-PMT/siRNA 복합체의 뇌혈장벽 통과 효율을 측정하고 카베올레 소포의 움직임을 관찰하였다. 그 결과 R-PEG-PMT/siRNA 복합체의 뇌혈장벽 통과가 카베올레 매개 트렌스시토시스에 의존적이며, 연구 1의 결과와 마찬가지로 PMT의 만니톨 부분이 카베올레 소포의 움직임을 자극시키는 것으로 밝혀냈다.

연구 3에서는 연구 1과 2로부터 구축한 뇌 세포 표적형 유전자 전달체를 이용하여 생체 내에 BACE1 siRNA를 전달함으로써 알츠하이머 치료 가능성을 확인하였다. BACE1는 알츠하이머의 원인 유전자 중 하나로서 병리학적 증상인 아밀로이드 베타 생성의 율속인자인 효소이므로

BACE1 발현 억제를 통한 치료 효과를 기대할 수 있다. R-PEG-PMT/siRNA 복합체를 정맥주사 했을 때 다른 유전자 전달체에 비해 뇌에 축적되는 효율이 높았으며 다른 장기에 더 적게 분포하였다. 또한 R-PEG-PMT/siBACE1을 2주 동안 세 번 정맥 주사했을 때 심각한 독성 문제 없이 뇌 특이적으로 유전자 발현 억제 효과를 나타냈다. 알츠하이머 질병의 병리학적 현상이 강하게 나타나는 해마와 대뇌 피질 부위의 BACE1 발현을 RNA와 단백질 수준에서 유의적으로 감소시켰고, 더 나아가 신경독성이 있는 아밀로이드 베타 생성도 억제하는 것을 확인하였다.

연구결과들을 종합적으로 고찰해볼 때, R-PEG-PMT는 알츠하이머 RNA 간섭 치료에 효과적인 유전자 전달체로 이용될 수 있음이 입증되었다. 세포 내 장벽 극복의 측면에서, PMT의 에스테르 결합 부분이 세포 독성을 낮추었으며, 일부 PEI에 의한 엔도좀 탈출 효과 및 만니톨 부분에 의한 카비올레 엔토시토시스 기전이 라이소좀에 의한 유전자 분해를 효과적으로 방지하였다. 또한 세포 외 장벽 극복 측면에서 RVG에 의한 뇌세포 표적 효과 및 뇌혈장벽에 대한 수용체 매개 트렌스시토시스 기능을 확인하였고, PMT에 의한 카비올레 소포 움직임 활성화가 뇌혈장벽 통과 효율을 향상시킴을 입증하였다. 또한 PMT와 RVG의 가교체로 이용된 PEG의 이용이 생체 내에서 면역 세포에 의한 제거를 줄이는 것을 확인하였다. 생체 내에서 R-PEG-PMT를 이용하여 치료 유전자인 siBACE1을 전달한 결과 BACE1의 발현이 억제되고 이에 따라 아밀로이드 베타 생성이 감소되는 것을 확인함으로써 뇌 표적형 유전자 전달체로서 뇌질환 치료에 가능성이 있음을 확인하였다. R-PEG-PMT는 생체 장벽을 극복할 수 있는 뇌 표적형 유전자 전달체로서, 알츠하이머 질병뿐만 아니라 다른 뇌질환 유전자 치료에도 이용될 것으로 기대된다.

Appendix. Mitochondria targeting of siRNA by a novel architectural modification of siRNA

1. Introduction.

Application of RNAi technology, a great tool for functional genomics and development of therapy with high degree of efficiency and specificity, on mitochondria genome had received little attention. With the recent progress of studies on cross-talk between nuclear and mitochondrial genome via microRNA (miRNA), a potential post-transcriptional gene regulation of mitochondrial DNA (mtDNA) has become deserved to be investigated (Barrey, E. *et al.*, 2011;Das, S. *et al.*, 2012). Argonaut 2 (AGO2) protein, a core component of RNAi-induced silencing complex (RISC) which can catalyze the cleavage of targeted transcript was reported to be localized in mitochondria and functioned to mitochondrial mRNA (mtRNA) (Das, S. *et al.*, 2012). Although mitochondria genome encodes only 13 proteins involved in electron transport and ATP synthesis, the maintenance of its circular genome is under necessity of independent regulation of mitochondrial gene expression for metabolic control. In that line, the existence of pre-miRNA, miRNA and RNAi machineries in mitochondria implies the possibility of delicate manipulation of core genes of oxidative phosphorylation (OXPHOS) using RNAi. Based on recent studies, we undertook a development of mitochondria targeted small RNA delivery system as a powerful tool to investigate mitochondrial physiology and dysfunction via RNAi mechanism.

Canonical short interfering RNA (siRNA) molecules are double-stranded RNA (dsRNA) duplexes that typically contain 19-21 nt and 2-nt 3' overhangs. In spite of their immense attractiveness of gene knockdown as therapeutic strategy, they are not enough optimal drug molecules because of their low serum stability and non-targeting specificity. To address the issues, various strategies of chemical modification of siRNA have been proposed including modification of sugar, base, phosphate linkages and duplex architecture (Barrey, E. *et al.*, 2011). In specific, siRNA-mediated mitochondrial RNAi is quite limited since mitochondrial double membranes strongly protect from transfection by conventional transfection technique (Seibel, P. *et al.*, 1995). Therefore, much efforts have been directed toward investigation on the mitochondria permeable gene delivery system for specific localization of nucleic acids into mitochondrial matrix. For example, RNA import complex (RIC)-mediated delivery of antisense RNA was reported to induce specific degradation of targeted mitochondrial mRNA (Mukherjee, J. *et al.*, 2014). Also, peptide nucleic acids (PNAs) have been investigated to inhibit the mitochondrial replication although they cannot cross over the highly impermeable inner membrane (Muratovska, A. *et al.*, 2001).

In this study, we approached a novel system for mitochondrial targeted delivery of siRNA by modification of duplex architecture as shown in Fig. 1. Mitochondrial targeting stem-loop siRNAs (MTS)s were designed for aiming i) to confer the mitochondrial targeting ability and ii) stability to siRNA duplexes, and iii) to facilitate the chemical synthesis via *in vitro* transcription.

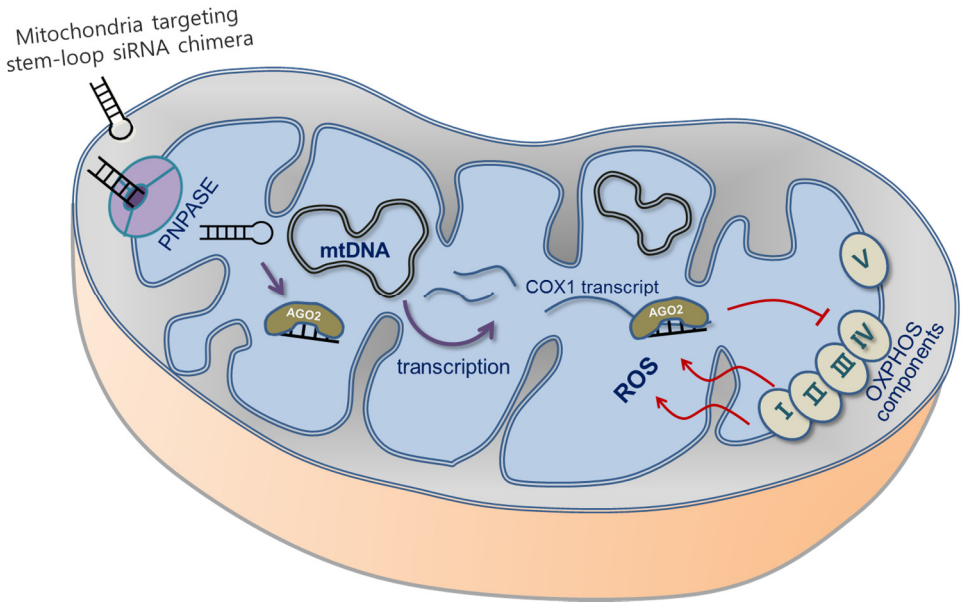

Fig. 1. Schematic illustration of mitochondria targeting siRNA delivery system

2. Materials and methods

1) Generation of mitochondrial targeting stemloop-siRNA

Double-stranded oligonucleotides containing T7 promoter used as templates for *in vitro* transcription were synthesized by Bioneer Co. Ltd.

CR
(5'TAATACGACTCACTATAGCCCATGCATTTGTAATAAGGCAGGGCC
CCCCGCTCCCTTATTACAAATGCATGGGCTT)

MRP1
(5'TAATACGACTCACTATAGCCCATGCATTTGTAATAAAGCGTATCCC
GCTTATTACAAATGCATGGGCTT)

MRP2
(5'TAATACGACTCACTATAGCCCATGCATTTGTAATAACGCCAAGAA
GCGTATCCCGCTGAGCGTTATTACAAATGCATGGGCTT)

RP
(5'TAATACGACTCACTATAGCCCATGCATTTGTAATAACTCCCTGAGC
TTCAGGGAGTTATTACAAATGCATGGGCTT)

All the MTSs were generated using MEGAshortscript T7 Kit following manufacture's protocol and extracted by TRIzol reagent. The qualities and concentrations of MTSs were measured by Nanodrop spectrophotometer.

2) Localization of rhodamine-labled MTSs

The MTSs and siRNA duplexes were rhodamine labled using Label IT®

siRNA Tracker Intracellular Localization Kit according to the manufacture's protocol. HeLa cells were seeded at $10X10^4$ cells/ml and grown to 60% confluence on coverslips inside a dish. The prepared rhodamine-labled MTSs or siRNA duplexes/Lipofectamine RNAimax lipoplexes were treated to the cells. At 5 h post-transfection, the media from the dish was removed and 100 nM of staining solution containing MitoTracker probe was treated and incubated for 45 min under growth condition. After staining, the cells were fixed by 4% paraformaldehyde at room temperature for 10 min and observed under confocal laser scanning microscopy (CLSM) immediately. Colocalization of MTSs and siRNAs in mitochondrial was quantified using ImageJ program (NIH Image, Bethesda, MD).

3) Quantification of mitochondrial RNA

The MTSs and siRNA duplexes/Lipofectamine RNAimax complexes were treated to the HeLa cells seeded on 6-well plates and incubated for 24 h or 48 h without replacing media. For construction of *in vitro* model, complexes were treated every two day for a week. After total RNAs were extracted from the cells using TRizol reagent (Invitrogen, U.S.A.) and the purified RNAs (1 μg) were reversely transcribed into cDNA using AccuPower®CycleScript RT PreMix (dN20) (Bioneer, Korea). The relative levels of MTCO1, MTCO2, MTCO3 and mtTFA were determined by qRT-PCR with SYBR green (Enzynomics, Korea). The amplification was conducted in 95 ^{0}C for 10 min for initial denaturation and 45 cycles of 95 ^{0}C for 10 s and 50 ^{0}C for 15 s and 72 ^{0}C for 15 s.

4) Measurement of mitochondria complex IV activity

The activity of mitochondria complex IV was measured at 24 h or 48 h post-transfection using mitochondria complex IV activity assay kit (Millipore, U.S.A.) according to the manufacture's protocol. Briefly, the cell membrane was lysed using detergent and the mitochondria complex IV was immune-captured within the 96-well plates. The activity of mitochondrial complex IV was determined colorimetrically by measuring change of the absorbance at 550 nm for 120 min when oxidation of cytochrome c occurs.

5) Reactive oxygen species (ROS) staining assay

Intracellular ROS was stained using Image-IT Live green ROS detection kit (Invitrogen, U.S.A) according to the manufacture's protocol. Briefly, HeLa cells were seeded at $20X10^4$ cells on coverslip and 200 nM of MTSs or siRNAs were treated to the cells at 60% confluency. After incubation for 24 h or 48 h, H2-DCFDA solution was treated to the cells protected from light for 30 min at 37 ^{0}C and the Hoechst staining was conducted for last 5 min at 37 ^{0}C. Added staining solution was washed with warm HBSS and fixed with PFA 4%. ROS stained cells were observed under CLSM immediately.

3. Results and discussion

1). Design and synthesis of MTSs

We modified siRNA architectecturally to be continuous with mitochondrial targeting stem-loop signals for mimicking the endogenous miRNA precursors (pre-miRNA) structure (Dassie, J.P. *et al.*, 2009). Some mitochondrial importable RNA sequences from nuclear encoded RNAs, such as tRNAs, RNase P RNA and mitochondrial RNA processing (MRP) RNA required for transcription and translation of mtDNA, were previously reported. In a previous study, licensed import of human RP and MRP RNA stem-loop structure into mitochondrial matrix through PNPASE was demonstrated (Barrey, E. *et al.*, 2011). They employed mitochondrial targeting of stem-loop signals within RNase P RNA to 5'-terminus of tRNA and mRNAs for carrying them to mitochondrial matrix. The mitochondrial targeting RNA sequences in MTS, RP (19 nt) from RNase P and MRP1 (13 nt) and MRP2 (26 nt) from MRP RNA were based on the same study. Non-specific random sequence CR (20 nt) was used as a control stem-loop (Fig. 2).

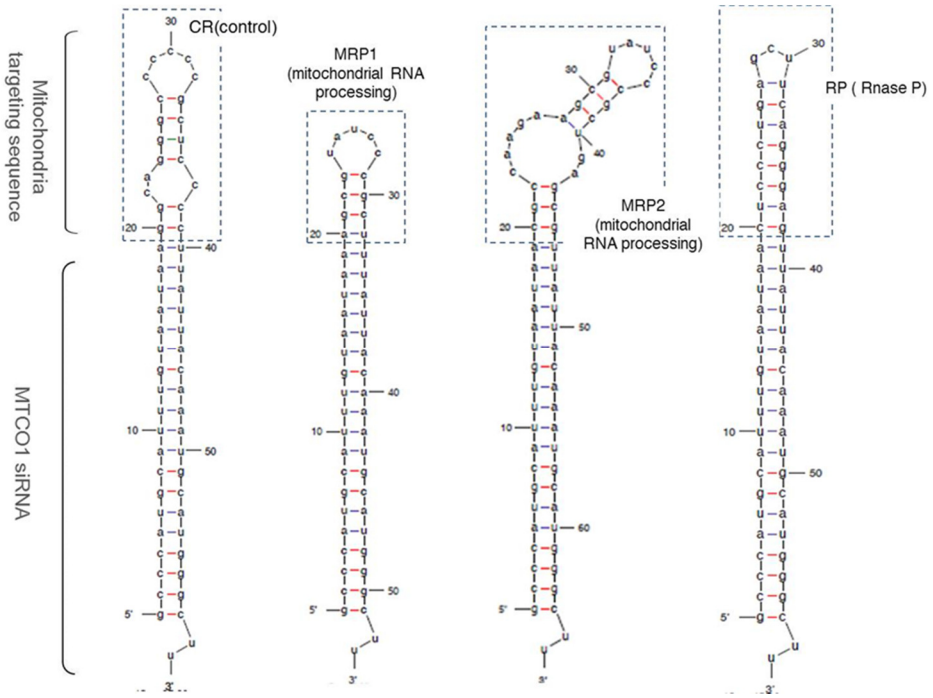

Fig. 2. The suggested secondary structures of MTS. MTCO1 siRNA duplexes which are continuous with a) control stem-loop, b) mitochondria permeable stem-loop from, c) mitochondrial RNA processing and d) RNase P RNA.

As my approach depends on mtDNA regulating-siRNA that includes mitochondria permeable moiety, siRNA was also designed to target one of the mtDNA-encoded subunits of respiratory complex IV, mitochondrial cytochrome c oxidase 1 (MTCO1) using siSearch software tool. Altered expression of MTCO1 transcripts was demonstrated to be involved in various diseases such as gastric cancer, prostate cancer and kinds of neurodegenerative diseases. We hypothesized that the modified siRNA would efficiently target mitochondrial matrix compared to canonical siRNA and finally lead to pathophysiological effect following down-regulation of MTCO1. To produce the MTCO1 targeting MTSs, double stranded oligonucleotides containing T7 promoter were synthesized and used as templates for T7 polymerase-based *in vitro* transcription. The transcribed MTSs were purified using TRizol and the sizes of them were analyzed using polyacrylamide gel electrophoresis (Fig. 3).

Since MTSs mimic endogenous pre-miRNA, the enzymatic process of RNase III on MTSs is required to cleave the targeting sequence leaving mature 21 nt double-stranded RNA. The recombinant dicer was treated to MTSs for insufficient incubation time (8 h) to observe both RNA substrates and cleavage products. The MTSs and cleavage products were separated using 15% polyacrylamide gel. The sizes of cleaved MTSs (CR, MRP1, MRP2 and RP) were similar with that of chemically synthesized siRNA (21 nt), indicating that MTSs are potent substrates of RNase III at the early step of RNAi (Fig. 3).

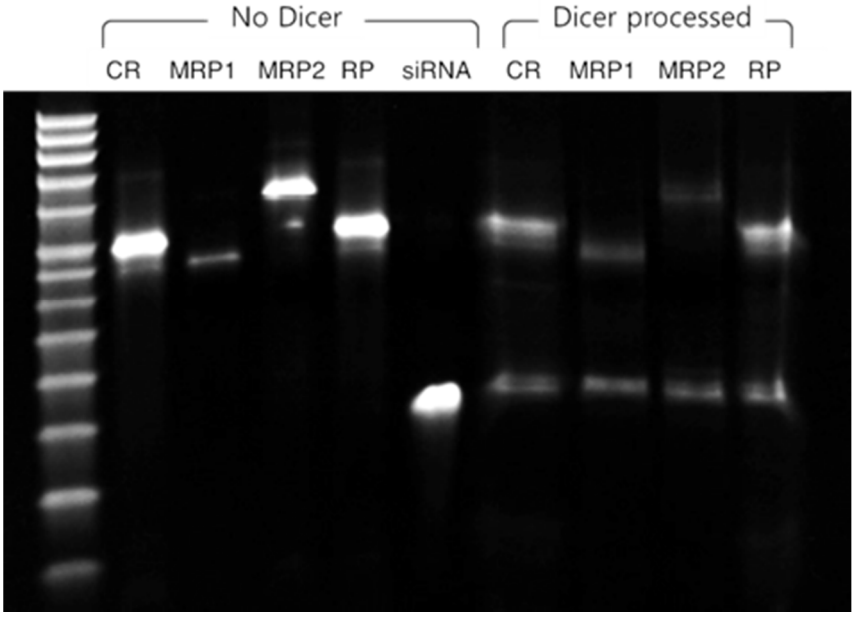

Fig. 3. *In vitro* dicer assay. The MTSs (1 μg) were incubated with 1 unit of recombinant dicer enzyme for 8 h at 37 0C. The RNA cleavage by dicer was analyzed by denaturing 15% polyacrylamide gel electrophoresis followed by EtBr staining.

2) Co-localization of MTSs in mitochondria

The co-localization of rhodamine labled-MTSs and siRNA in mitochondria were analyzed using CLSM and ImageJ program. HeLa cells were transfected with rhodamine-labled MTSs and the mitochondria were stained with Mitotracker staining solution. Compared to canonical siRNA, the MTSs designed to possess mitochondrial targeting sequence-MRP1, MRP2 and RP showed higher yellow signal, indication of co-localization signals of RNAs and mitochondria. On the other hand, CR including random stem-loop sequence was mainly localized in cytoplasm rather than in the mitochondria (Fig. 4A-E). The overlay coefficient analyzed using ImageJ program "colocalization finder" plug-in showed that targeting efficiency of MRP1, MRP2 and RP were approximately two-fold higher than those of canonical siRNA and CR (Fig. 4F). The results indicates that my mitochondria targeting approach works appropriately by conventional liposome-mediated transfection method.

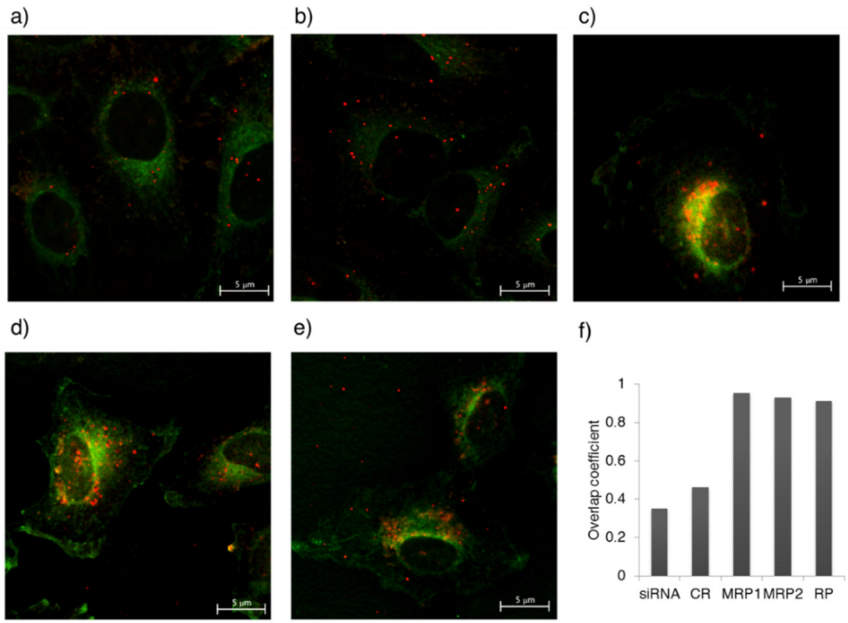

Fig. 4. The co-localization assay of rhodamine-labled siRNA (a) and MTSs (red) (b-e) with green stained-mitochondria. At 5 h post-transfection with rhodamine-labled siRNA or MTSs/Lipofectamine lipoplexes, the HeLa cells were fixed and observed under confocal laser scanning microscopy. The overlay coefficient was analyzed using ImageJ program (f). Scale bar=5µm

3) RNA interference effect of MTSs

We then examined the RNA interference effects of MTSs at 24 h and 48 h post-transfection. The relative levels of mtDNA-encoded subunits of respiratory complex IV transcripts were determined by quantitative RT-PCR (qRT-PCR). For normalization of quantitation of mtRNA transcripts, 16S rRNA was used as a mitochondrial control gene. As shown in Fig. 5, at 24 h post-transfection in HeLa cells, MTCO1 mtRNA transcript was significantly down-regulated by MRP1, MRP2 and RP whereas chemically synthesized siRNA and CR did not show RNAi effect on mtRNA. This result indicates that translocation of siRNA into mitochondrial matrix plays critical roles in RNAi effect on mitochondria. Because mitochondria encoded-OXPHOS genes are transcribed in polycistronic unit before processed by endonuclease cleavage, we were concerned about possible off-target effects of MTSs. To evaluate the off-target effect, the amount of MTCO2 and MTCO3 transcripts which are directly after MTCO1 in precursor RNA were also analyzed. Compared to MTCO1, expression of MTCO2 and MTCO3 were not affected by transfection of MTSs, which is consistent with previous report about RNAi effect of miR-181c on MTCO1 without off-target effect. For quantitative evaluation of inhibitory effect of MTSs on target gene translation, enzyme-linked immunosorbent assay (ELISA) was performed on MTCO1 and GAPDH proteins as internal controls. The MTSs containing mitochondria targeting sequences-MRP1, MRP2 and RP induced a significant down-regulation of MTCO1. Although change in protein level is not perfectly correlated with RNA

level, it was demonstrated that degradation of MTCO1 transcript by MTSs induced knock-down of target protein (Fig. 6). Thus, the results suggest mitochondrial gene targeted RNAi approach is useful for down regulation of mitochondria encoded-OXPHOS components individually in RNA and protein levels with low off-target effect.

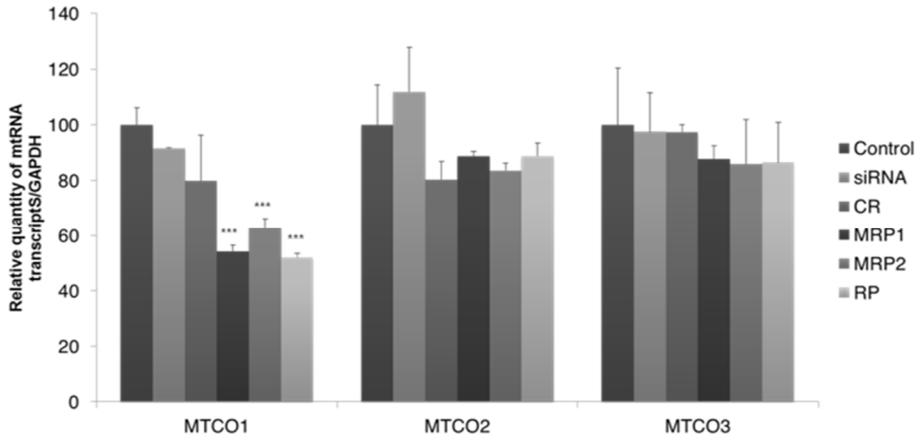

Fig. 5. The physiological effects of MTSs in mitochondria as well as cells. a) The relative quantity of MTCO1, MTCO2 and MTCO3 transcripts measured by qRT-PCR at 24 h post-transfection.

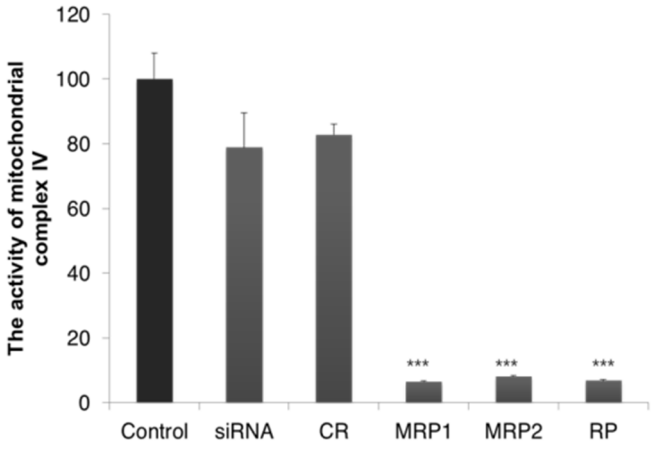

Fig. 6. The percentage of MTCO1 expression normalized by GAPDH expression using ELISA method.

In electron transport chain, cytochrome c oxidase in complex IV catalyzes the electron transfer from cytochrome c to oxygen to form water. To determine the effect of MTSs on mitochondrial function compared to canonical siRNA, the activity of mitochondrial complex IV was measured by detecting oxidation of cytochrome c with colorimetrical method. As shown in Fig. 7, the MTSs having targeting sequence-MRP1, MRP2 and RP significantly reduced the occurrence of cytochrome c oxidation while canonical siRNA and CR did not affect the activity of complex IV in accordance with the above knock-down data. To further evaluate the regulation of mitochondrial function via MTSs, we monitored the formation of reactive oxygen species (ROS) after transfection because the ROS mainly produce from electron transport chain to a number of pathological process including aging, apoptosis, cell injury and cancer, and the rate of ROS production from mitochondria increases in a variety of pathological

condition including inhibition of mitochondrial respiration. Also,when oxidation through cytochrome c oxidase in the myocardial ischema was inhibited, ROS production was facilitated from complex I or III and oxidative damage increased. At 24 h and 48 h post-transfection, H2-DCFDA solution was treated to the HeLa cells to observe the ROS in fluorometric method. The MTSs including mitochondrial targeting sequence generated much higher level of ROS compared to canonical siRNA and CR at 48 h post-transfection (Fig. 8). This result indicate that although knock-down of cytochrome c oxidase occur in 24 h post-transfection, intensive ROS is generated after induced dysfunction of mitochondria complex IV. MTT assay was also conducted to observe the ROS-induced cytotoxicity. In accordance with ROS data, the viability of HeLa cells is decreased significantly at 48 h post-transfection with MTSs compare to siRNA and CR (Fig. 7C-D). These data suggest that MTSs system can induce the pathological condition via RNAi in mitochondria.

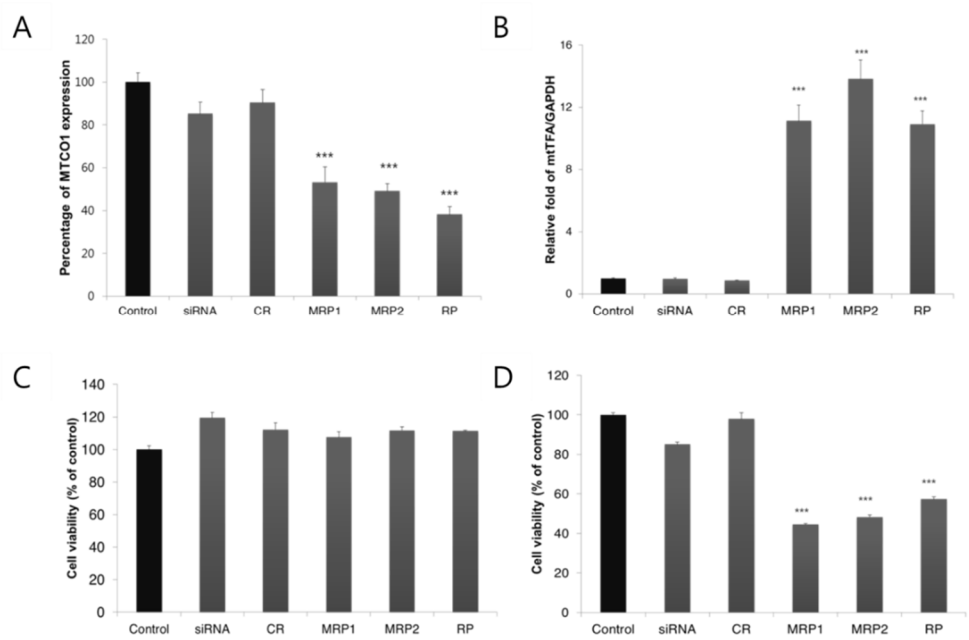

Fig. 7. The physiological effects of MTSs on cells. A. The activity of mitochondrial complex IV by colorimetrical detection of cytochrome c oxidation. B. The relative folds of the amount of mtTFA transcripts normalized by GAPDH to quantify the change of mtDNA copy number. The effect of MTSs on cell viability at 24 h (C)and 48 h (D) post-transfection was measured by MTT assay.

The elevated copy number of mtDNA acts as a compensatory mechanism for reduced mitochondrial respiratory function. To examine the possibility of chronic oxidative stress in *in vitro* model using MTSs, HeLa cells were transfected with 50 nM of MTSs every second day for a week and the mitochondria biogenesis-related nuclear gene as a mitochondrial transcription factor A (mtTFA) was quantified. The long-term transfection with MRP1, MRP2 and RP induced up to 16-fold increase in mtTFA expression normalized by GAPDH while canonical siRNA and CR could not alter the amount of mtTFA (Fig. 7B). As copy number of mtDNA is proportional to mtTFA, this result shows that long-term exposure to HeLa cells induce the chronic dysfunction of mitochondria *in vitro* .

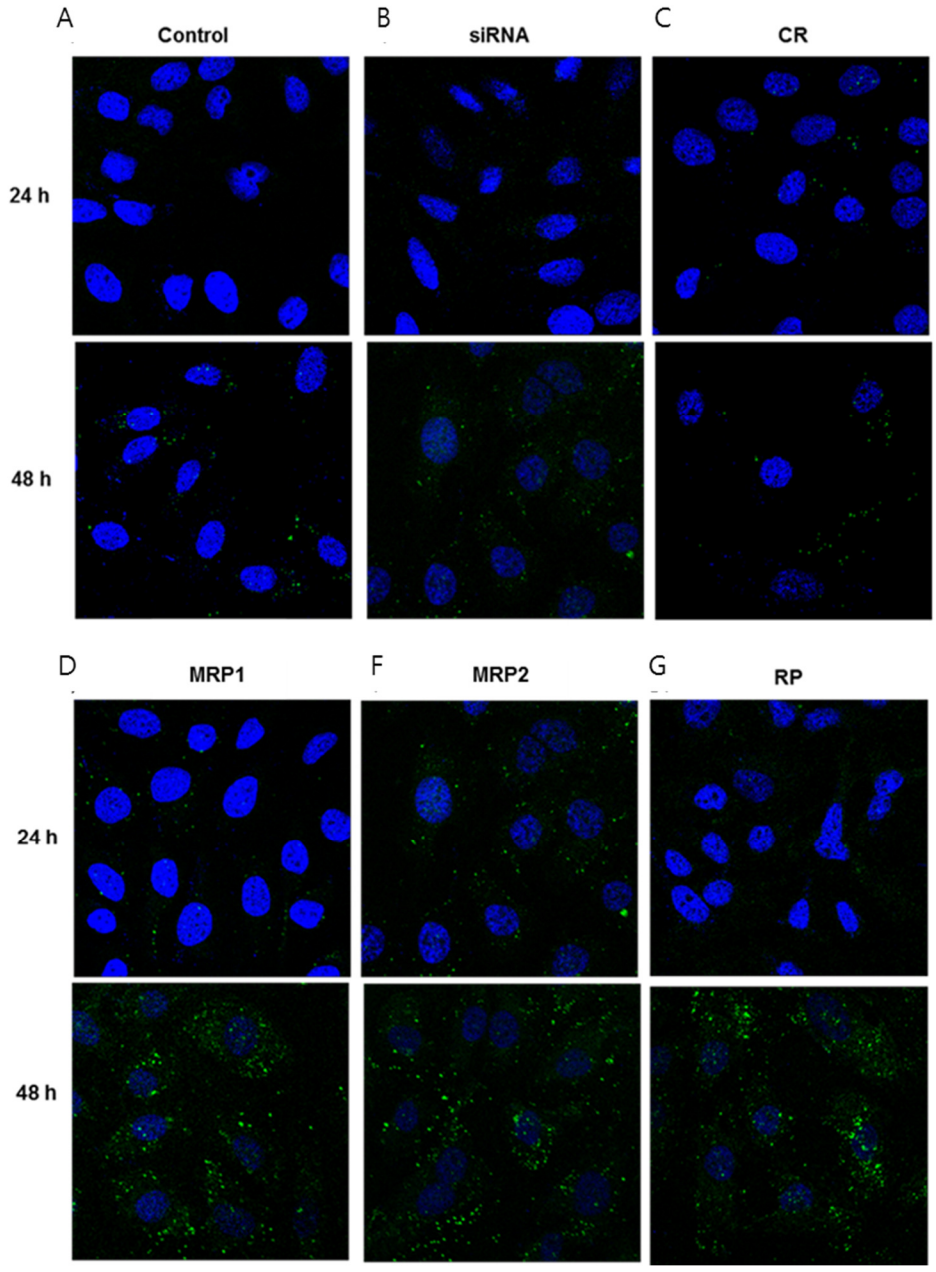

Fig. 8. Intracellular ROS produced after transfection with A) canonical siRNA duplexes B) CR, C) MRP1, E) MRP2 and F) RP. At 24 h or 48 h post-transfection, the ROS was stained using H2-DCFDA solution (green) followed by Hoescht staining (blue).

Recent studies strongly indicated that translocation of pre-miRNA and miRNA to mitochondria played an important role in function of mitochondria. The pattern of mitochondrial resident miRNAs was demonstrated to be altered in pathophysiological condition such as thyroid carcinoma, myeloid leukemia and type-1 diabetes. These findings imply the possibility of regulation of the mitochondrial functions as well as several other cellular processes by delivery of miRNA or siRNA into mitochondria. In that sense, we first developed and characterized mtRNA transcript-targeting siRNA i) available for mtRNA knock-down using RNAi machineries in mitochondria without off-target effect and ii) targeting mitochondria using endogenous RNA stem-loop sequences. For them, we modified the canonical siRNA mimicking miRNA precursor to be continuous with mitochondrial permeable stem-loop sequence (13-26 nt). Synthesized MTSs was found to be substrates of RNase III and down-regulate the mitochondrial gene in RNA and protein levels by conventional liposome-mediated transfection method through degradation of target mtRNA transcripts. We further examined the mitochondrial pathophysiological disorders following down-regulation of cytochrome c oxidase via MTSs such as activity complex IV, ROS production, cell viability and change of mtDNA number.

4. Conclusion

We demonstrated that MTS system is very useful for functional analysis of mitochondrial gene involved in OXPHOS and construction of *in vitro* model via RNAi technique which had been used only for nuclear genome regulation before. As mitochondrial gene regulation remains largely unanswered, mechanism of RNAi in mitochondria needs more explorations with development of mitochondria targeted siRNA delivery system. A novel mitochondria targeted siRNA delivery system will provide improved application and investigation on functions of RNAi in mitochondria.

Literature Cited

Barrey, E., Saint-Auret, G., Bonnamy, B., Damas, D., Boyer, O. and Gidrol, X. 2011. Pre-microRNA and mature microRNA in human mitochondria. PloS one. 6(5), e20220.

Das, S., Ferlito, M., Kent, O. A., Fox-Talbot, K., Wang, R., Liu, D., Raghavachari, N., Yang, Y., Wheelan, S. J. and Murphy, E. 2012. Nuclear miRNA regulates the mitochondrial genome in the heart. Circulation research. 110(12), 1596-1603.

Dassie, J. P., Liu, X. Y., Thomas, G. S., Whitaker, R. M., Thiel, K. W., Stockdale, K. R., Meyerholz, D. K., McCaffrey, A. P., McNamara, J. O., 2nd and Giangrande, P. H. 2009. Systemic administration of optimized aptamer-siRNA chimeras promotes regression of PSMA-expressing tumors. Nat Biotechnol. 27(9), 839-849.

Mukherjee, J., Mahato, B. and Adhya, S. 2014. Vesicular transport of a ribonucleoprotein to mitochondria. Biol Open. 3(11), 1083-1091.

Muratovska, A., Lightowlers, R. N., Taylor, R. W., Turnbull, D. M., Smith, R. A., Wilce, J. A., Martin, S. W. and Murphy, M. P. 2001. Targeting peptide nucleic acid (PNA) oligomers to mitochondria within cells by conjugation to lipophilic cations: implications for mitochondrial DNA replication, expression and disease. Nucleic Acids Res. 29(9), 1852-1863.

Seibel, P., Trappe, J., Villani, G., Klopstock, T., Papa, S. and Reichmann, H. 1995. Transfection of mitochondria: strategy towards a gene therapy of mitochondrial DNA diseases. Nucleic Acids Res. 23(1), 10-17.